Characterization of Membrane Proteins: From a gated plant aquaporin to animal ion channel receptors

Survery, Sabeen

2015

Characterization of Membrane Proteins

From a gated plant aquaporin to animal ion channel receptors

SABEEN SURVERY | FACULTY OF SCIENCE | LUND UNIVERSITY 2015

SABEEN SURVERY

Characterization of Membrane Proteins - From a gated plant aquaporin to animal ion channel receptors

Printed by Media-Tryck, Lund University 2015

LUND UNIVERSITY
Faculty of Science
Department of Biochemistry and Structural Biology
Center for Molecular Protein Science

ISBN 978-91-7422-403-0

Characterization of Membrane Proteins

From a gated plant aquaporin to animal ion channel receptors

Sabeen Survery

LUND
UNIVERSITY

DOCTORAL DISSERTATION

Academic thesis which, by due permission of the Faculty of Science, Lund University, Sweden, will be defended on Friday 12 June, 2015, at 1015 in lecture hall B at the Centre of Chemistry and Chemical Engineering, Getingevagen 60, Lund.

Faculty opponent: Professor Dr. Eric Beitz, Pharmaceutical and Medicinal Chemistry University of Kiel, Germany

Organization:

Lund University

Biochemistry and Structural Biology Center for Molecular Protein Science, PO Box 124, 221 00 Lund, Sweden

Author: Sabeen Survery

Document name: Doctoral dissertation

Date of issue

Sponsoring organization

Title and subtitle: Characterization of Membrane Proteins: from a gated aquaporin to animal ion channel receptors

Abstract

Membrane proteins play several important roles in a cell. Among these proteins are aquaporins (AQPs) and transient receptor potential (TRP) ion channels that mediate water transport, temperature and noxious chemical sensation, respectively. The function of some AQPs, for example the spinach isoform SoPIP2;1 is regulated by pH, phosphorylation and heavy metals such as mercury. However, the mechanisms by which mercury activate or inhibits AQPs are poorly understood. We suggest that mercury binds to SoPIP2;1 close to the C-terminal end and that the binding of mercury results in destabilization of the C-terminal region. This may affect its interaction with the residues forming the gate and therefore lead to an increase of the water permeability of SoPIP2;1 (Paper II). SoPIP2;1 is a highly selective water channel and can be produced as a functional protein in high yield in a heterologous system which suggest that SoPIP2;1 is a good choice for insertion in biomimetic membranes to be used for water purification. However, the stability of SoPIP2;1 in artificial membranes needed to be demonstrated. Thus we determined the stability of SoPIP2;1 in different lipids and identified *E. coli* polar lipids as the best system for reconstitution of SoPIP2;1. The results will contribute towards the effort to use SoPIP2;1 in biomimetic water filtration technology (Paper I).

The animal TRP ion channel subtype A1 (TRPA1) from fruit fly, snake and mosquito has been implicated in warm temperature sensation. However, the threshold temperature which activates human TRPA1 (hTRPA1) is controversial. We addressed this issue by reconstituting the purified hTRPA1 in artificial lipid membranes. The purified hTRPA1 was found to be activated by cold temperatures and electrophilic chemicals. The results resolve the controversy surrounding the threshold temperature for the activation of hTRPA1 (Paper IV). The *Anopheles gambiae* TRPA1 (AgTRPA1) was found to be activated by heat and electrophilic compounds when reconstituted in artificial membranes after purification. The temperature activation as well as the binding of electrophilic ligands to AgTRPA1 resulted in the quenching of fluorescence suggesting that thermal and chemical activation brought about similar conformational changes of the protein and perhaps reflect the dynamic change in the conformation of residues involved in the gating process (Paper III). We also demonstrated that the N-terminal domain of both human and mosquito TRPA1 is not essential for thermal/chemical sensation (Paper III and Paper IV) as opposed to previous reports.

Key words: MIPs, AQPs, TRP ion channels, water transport, electrophilic compounds, themo sensor.

Classification system and/or index terms (if any)

Supplementary bibliographical information

Language: English

ISSN and key title

ISBN 978-91-7422-403-0

Recipient's notes

Number of pages 156

Price

Security classification

Characterization of Membrane Proteins

From a gated plant aquaporin to animal ion channel receptors

Sabeen Survery

LUND
UNIVERSITY

Back cover Malaria mosquito (Anopheles) photo credit to
Centers for disease control and prevention (CDC).

Faculty of Science
Department of Biochemistry and Structural Biology

ISBN 978-91-7422-403-0

Printed in Sweden by Media-Tryck, Lund University
Lund 2015

To My Parents

Abstract

Membrane proteins play several important roles in a cell. Among these proteins are aquaporins (AQPs) and transient receptor potential (TRP) ion channels that mediate water transport, temperature and noxious chemical sensation, respectively. The function of some AQPs, for example the spinach isoform SoPIP2;1 is regulated by pH, phosphorylation and heavy metals such as mercury. However, the mechanisms by which mercury activate or inhibits AQPs are poorly understood. We suggest that mercury binds to SoPIP2;1 close to the C-terminal end and that the binding of mercury results in destabilization of the C-terminal region. This may affect its interaction with the residues forming the gate and therefore lead to an increase of the water permeability of SoPIP2;1 (Paper II). SoPIP2;1 is a highly selective water channel and can be produced as a functional protein in high yield in a heterologous system which suggest that SoPIP2;1 is a good choice for insertion in biomimetic membranes to be used for water purification. However, the stability of SoPIP2;1 in artificial membranes needed to be demonstrated. Thus we determined the stability of SoPIP2;1 in different lipids and identified *E. coli* polar lipids as the best system for reconstitution of SoPIP2;1. The results will contribute towards the effort to use SoPIP2;1 in biomimetic water filtration technology (Paper I).

The animal TRP ion channel subtype A1 (TRPA1) from fruit fly, snake and mosquito has been implicated in warm temperature sensation. However, the threshold temperature which activates human TRPA1 (hTRPA1) is controversial. We addressed this issue by reconstituting the purified hTRPA1 in artificial lipid membranes. The purified hTRPA1 was found to be activated by cold temperatures and electrophilic chemicals. The results resolve the controversy surrounding the threshold temperature for the activation of hTRPA1 (Paper IV). The *Anopheles gambiae* TRPA1 (AgTRPA1) was found to be activated by heat and electrophilic compounds when reconstituted in artificial membranes after purification. The temperature activation as well as the binding of electrophilic ligands to AgTRPA1 resulted in the quenching of fluorescence suggesting that thermal and chemical activation brought about similar conformational changes of the protein and perhaps reflect the dynamic change in the conformation of residues involved in the gating process (Paper III). We also demonstrated that the N-terminal domain of both human and mosquito TRPA1 is not essential for thermal/chemical sensation (Paper III and Paper IV) as opposed to previous reports.

The thesis is based on following papers

I. **Structure and stability of the Spinach Aquaporin *So*PIP2;1 in detergent micelles and lipid membranes**

Plasencia I, Survery S, Ibragimova S, Hansen JS, Kjellbom P, Helix-Nielsen C, Johanson U, Mouritsen OG

PLoS ONE. 2011 | Volume 6 | Issue 2 |

SS took part in the protein expression and purification, performed some of the CD experiment, performed electrophoresis of temperature denatured protein samples and participated in writing of related parts of the paper.

II. **Increased permeability of *So*PIP2;1 by mercury and mutations of cysteine in loop A**

Survery S*, Kirscht A*, Kjellbom P, and Johanson U

*Contributed equally

Manuscript

SS was involved in the design of the study, performed site directed mutagenesis, protein expression and purification of the wild type and mutant proteins, carried out protein stability experiment by CD and data analysis. SS drafted the manuscript together with the co-authors.

III. **The Malaria mosquito *Anopheles gambiae* TRPA1 is an inherent heat- and chemosensitive ion channel irrespective of its N-terminal ankyrin repeat domain**

Survery S, Moparthi L, Kjellbom P, Högestätt ED, Zygmunt PM and Johanson U

Manuscript

SS was involved in the design of the study. SS performed all the experiments and data analyses except the electrophysiological characterizations. SS drafted the manuscript together with the co-authors.

IV. **The human TRPA1 is intrinsically cold- and chemo-sensitive with and without its N-terminal ankyrin repeat domain**

Moparthi L, Survery S, Kreir M, Simonsen C, Kjellbom P, Högestätt, ED Johanson U and Zygmunt PM

Proc Natl Acas Sci U S A, 111(47): 16901-6, 2014

SS was involved in the planning and in pilot experiments for the expression and purification of TRPA1s. SS performed CD experiments and data analyses. SS took part in the writing of related parts of the paper.

Abbreviations

AQP	Aquaporin
AR	Ankyrin repeat
ar	Aromatic
ARD	Ankyrin repeat domain
CD	Circular Dichroism
GLP	GlpF-like protein/Aquaglyceroporin
GIP	GlpF-like intrinsic protein
HIP	Hybrid intrinsic protein
MIP	Major intrinsic protein
NIP	NOD-26 like intrinsic protein
PIP	Plasma membrane intrinsic protein
SIP	Small intrinsic protein
TM	Transmembrane
TIP	Tonoplast intrinsic protein
TRP	Transient receptor potential
TRPA	Transient receptor potential ankyrin
TRPC	Transient receptor potential canonical
TRPM	Transient receptor potential melastatin
TRPML	Transient receptor potential mucolipin
TRPN	Transient receptor potential NOMP-C
TRPP	Transient receptor potential polycystin
TRPV	Transient receptor potential vanniloid
XIP	X-intrinsic protein

Contents

Introduction

The plasma membrane shields the interior of the cells from the outside environment and essentially forms the barrier to the transport of several molecules and ions across the membrane. This barrier function of the plasma membrane is essential to maintain the homeostasis of the cell. However, the survival of organisms equally depends on their response to the changing environmental cues. The plasma membrane of the cell forms the interface that primarily communicates with the environment. It is therefore expected that the membrane will relay the information from the outside environment to the interior of the cells to constitute the cells response to the changing milieu. However, the bland bilayer, which has characteristic composition and properties, is limited in its capacity to integrate the great diversity of the stimuli that organisms encounter during their life time. Therefore, cell membrane harbors an array of specialized proteins involved in the reception of environmental signals and in transport of molecules across the lipid bilayer. Several different types of proteins are found attached to the lipid bilayer and together these are termed membrane proteins. The proteins that are attached loosely to the plasma membrane are called as peripheral proteins. These proteins are attached to the lipid bilayer by either covalent linkage such as palmitoylation or myristoylation or non-covalently to the surface of the membrane. The regulatory subunits of several enzymes and channels are present as peripheral membrane proteins and play important roles in cellular signaling. The proteins that span the membranes are called as integral membrane proteins. The importance of these proteins to the cells can be judged by their involvement in vital functions such as in light sensation, insulin binding, and growth factor reception. Some integral membrane proteins act as channels and transporters for the transport of nutrients and ions across the lipid bilayers. Despite the importance of water homeostasis in cellular function, water cannot readily pass through the membrane and therefore require special channels to be transported across the cell membrane. The water channels in the membranes are formed by a type of integral membrane proteins known as aquaporins (AQPs). Temperature influences several functions in living organsisms including growth, reproduction and metabolism. Temperature sensation is therefore essential for animal survival and is mediated by a group of integral membrane proteins called Transient Receptor Potential ion channels (TRP). The TRPs are also important for anticipation of noxious and harmful tissue damaging chemicals. The TRPs are abundant in animals where they constitute cell response against temperature and noxious chemicals.

However, they are not found in land plants. TRPs are also expressed in taste buds where they help the animals in sensing the pungent chemicals found in food. For example, in humans, TRPs are known to bind electrophilic compounds found in wasabi, thyme, oregano, garlic etc. TRPs transport divalent cations such as Ca^{2+} across the lipid bilayer, upon activation by heat and/or chemicals. Altered expression and function of TRPs has been linked to several diseases.

I have chosen to work with these two integral membrane proteins to understand the basic mechanism that relate the structure of these proteins to their function. In the subsequent paragraph, I will discuss more about the evolution, structure and importance of their role in living organisms.

Chapter 1

Aquaporins

Before the discovery of water channel proteins, it was assumed that water enter into the cells through the lipid bilayer without the need of specialized channels. The work by Paganelli and Solomon in 1957 provided the first evidence for the existence of water conducting pores in human red blood cell membrane (1). The identity of the protein responsible for water conduction in red blood cell was discovered in 1992 by the group of Peter Agre (2). These proteins are now called as aquaporins (3) and recognized as a large family of transmembrane protein ubiquitously present in all kingdoms of life. Later on, several proteins sharing the same overall fold as aquaporin were discovered, and found to transport water, and in some cases small uncharged solutes in addition to water (4, 5, 6, 7). It was soon recognized that they belong to a superfamily of proteins called Major Intrinsic Protein (MIPs) (9) named after AQP0, which is the major intrinsic protein (60%) in eye lens fiber cells. The gene for a glycerol facilitator was identified as early as 1972 (10), however, it was not known that this protein GlpF, belonged to the aquaporin family. Now, more than 1500 sequences belonging to MIPs (also addressed as by the generic term aquaporin in this thesis) have been identified in the publicly available databases reflecting the vastness and diversity of this protein family (8).

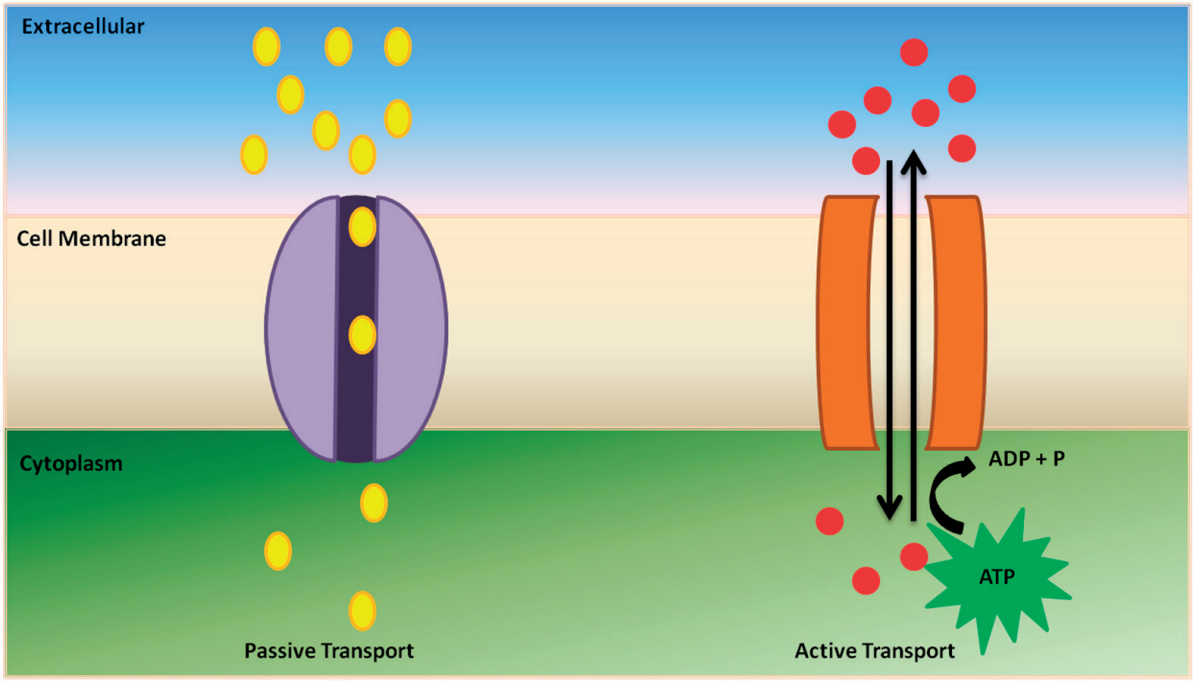

Figure 1: An schematice representation of active and passive transport. Primary active transport can be driven against a concentration gradient e.g. by the hydrolysis of ATP to ADP and inorganic phosphate (P). The passive transport depends on a concentration gradient.

The MIPs function as channels for the passive transport of water and small solutes such as glycerol, urea, hydrogen peroxide, ammonia, carbon dioxide and metalloids, depend on the concentration gradient (11, 12, 13, 14, 15, 16, 17). Some members of the MIP superfamily have been identified that so far not have been shown to display any channel activity (18). The primary sequence, i.e the sequence of amino acids of the MIPs suggest that an early gene duplication gave rise to the overall sequence of MIPs (19). The sequence identity between individual members of the family can be 30% or less but the overall topology is the same with six transmembrane helices and two half helices forming a seven transmembrane domain (8). The pore contains a conserved region called the aromatic/arginine (ar/R) region which is the narrowest part of the pore and plays an important part in the substrate selectivity of the channel. The MIPs are also characterized by the conserved NPA (aspergine, proline, alanine) motifs present at the N-termini of the two half helices. Together they form the NPA domain which restricts the passage of protons through the pore. In water specific aquaporins and in glycerol and water transporting aquaporins (aquaglyceroporins) the NPA boxes are fairly conserved although different between the two groups. In some other aquaporins like SIPs and AQP11 and AQP12 there is some sequences variation in the NPA boxes (8). Several high resolution structures of aquaporins have been reported over the years (20, 21, 22, 23, 24, 25, 26) which has led to the confirmation of the general topology and the mechanism of water and solute transport in AQPs.

Aquaporin function in animals and plants

The aquaporins (AQPs) are essential for water homeostasis and solute transport and thus are important for the proper functioning of cells and tissues in living organisms. The altered function or expression of some animal AQPs have been associated with the diseased states. For example, mice lacking AQP2, AQP3 and AQP4 have defects in urine concentration (27, 28). AQP3 overexpression has been linked to skin cancers (29). The mice lacking AQP5 have defects in saliva secretion (30). Mice with altered AQP0 (missense mutation R33C) have congenital cataracts (31).

AQP4 is involved in water transport across the blood brain barrier (32). It has been proposed that AQP4 inhibition may slow the brain swelling in mouse models of brain edema. Down regulation of AQP7 has been linked to obesity (33). AQP9 is involved in glycerol metabolism and could potentially be important in treating diabetes and obesity (33). Similarly, plant AQPs are essential for survival and response to salt, water and metal stress (33, 36). For example cucumber plant PIP1;2 and PIP2;4 are down regulated by salt stress and polyethylene glycol (PEG) resulting in reduced leaf water conductivity. However, the root hydraulic conductivity decreased only due to PEG stress suggesting that the regulation of water conductivity by AQPs are stress and tissue dependent (34, 35).

The redistribution of AQPs is also one of the responses to salt stress as seen in common bean plant (37). Rice responds to cold stress by altering the expression of AQPs (38). Plant AQPs are also implicated in CO_2 transport (39, 40) which is an important substrate for the synthesis of sugar. For example, decreased NtAQP1 was associated with decreased photosynthesis, which in turn is dependent on CO_2 availability (41). The plant AQPs are also involved in responses heavy metals which are manifested in reduced transport of water through aquaporins (42). Arsenic (43) and aluminum (44) are two metalloids known to be transported by specific AQP isoforms. Other metals such as mercury, cadium, lead and zinc are particularly involved in gating of plant and animal AQP channels and thus contribute to the regulation of AQP activity. (45, 46, 47, 48, 49). Boron and silicon are also transported by specific AQP isoforms (50, 51). Moreover, AQP are also involved in nitrogen metabolism owing to their role as urea transporters (52). Reactive oxygen species (ROS) like H_2O_2 which act as signaling molecules are also known to be transported by specific AQPs (53). Thus AQPs are central to plant water homeostasis and in stress responses against drought, salinity and toxic metalloids and AQPs contribute towards plant growth and signaling through their role in nitrogen acquisition and CO_2 and H_2O_2 transport.

General topology of AQPs

AQPs are small membrane intrinsic proteins with a molecular weight of 25-35 kDa. The AQPs are composed of six transmembrane helices named as TM1, TM2, TM3, TM4, TM5, TM6 and two half helices HB and HE.

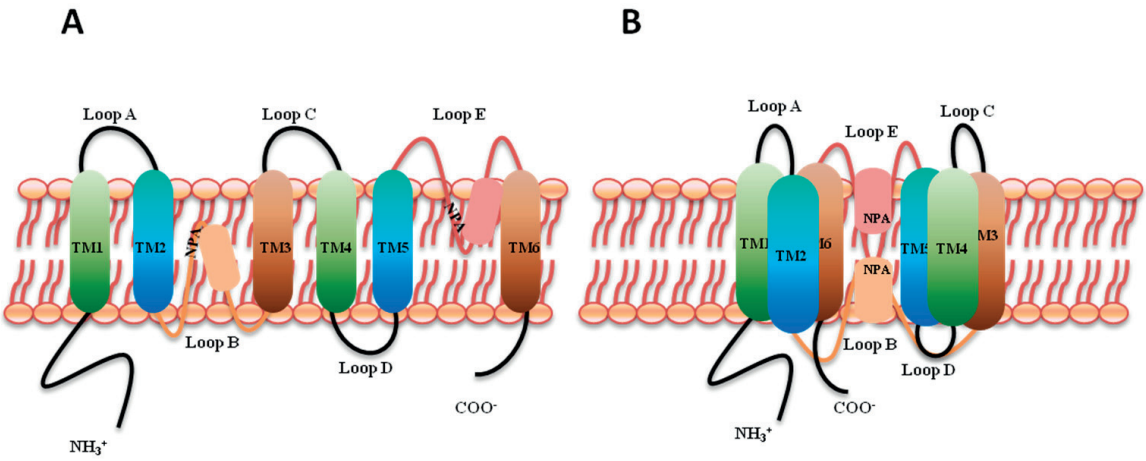

Figure 2: General toplogy of aquaporins. (A) Showing six transmembrane helices connecting with five loops (three extracellular loops: Loop A, C and E and two are the cytosolic side of the membrane: Loop B and D), both N and C termini are in the cytoplasm. (B) Represent the folding of helices. The half helices of Loop B and E dip into the membrane from opposite sides and form a seven transmembrane domain.

These transmembrane helices are joined together by five loops which are named as loop A, loop B, loop C, loop D and loop E. The N-terminal and C-terminal domains are found in the cytoplasm. AQP monomers interact with each other to form a functional homotetrameric unit in which each monomer possess a transporting water pore which is around 20-25 Å in length and is composed of an amphipathic pore lining (54). The carbonyl groups from the backbone forms the hydrophilic surfaces that together with NPA motifs in HB and HE provides the framework for hydrogen bonding which is required for the transport of water or glycerol. The positive charges at the center of the pore, generated by the dipoles of the two half helices HB and HE, represent a barrier to protons. Molecular dynamics simulation suggest that the NPA motives prevents the passage of protons through the pore by reorienting the water molecules thus breaking hydrogen bonds between neighboring water molecules in the single file of water permeating the pore (55). In AQP1 the residues opposite to asparagine of NPA motifs are leucine and phenylalanine compared to two leucine residues at similar positions in GlpF, thus providing the extra space for accommodating the bigger glycerol molecule in GlpF (56). The constriction region towards the extracellular side of the membrane, represented by the ar/R filter, determines the size and type of solute that can pass through the channel. For example, in water specific aquaporins the diameter of the

constriction formed by ar/R filter is approximately 2.8 Å (AQP1) compared to 3.4 Å in aquaglyceroporins (GlpF).

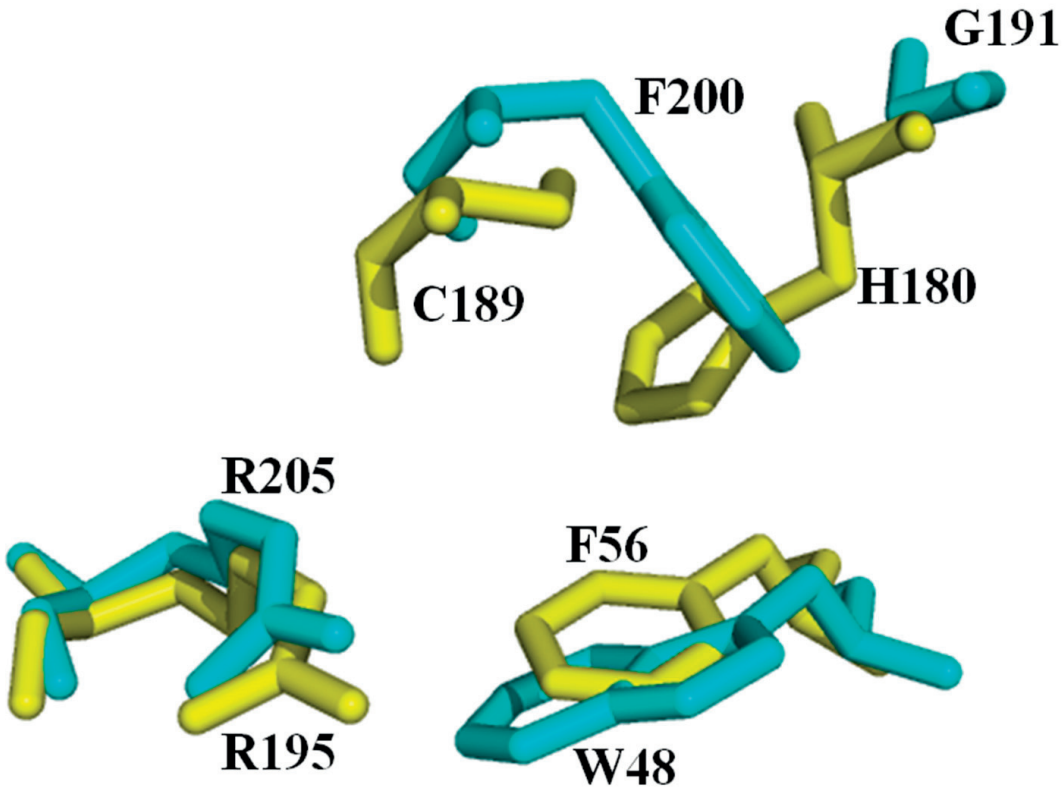

Figure 3: Selectivity filter of AQP1 (PBD ID 1J4N in yellow) and GlpF (PBD ID 1FX8 in cyan).

The ar/R motif is formed by 4 residues, two of which are present in TM2 and TM5, while the invariant arginine and another residue is contributed by loop E. In AQP1, these residues are F 56, H 180, C 189 and R 195. Corresponding residues in GlpF are W 48, G 191, F 200 and R 205. The histidine residue provides the hydrophilic surface to facilitate water permeation in water specific AQPs. The histidine residue is replaced by a glycine residue in glycerol channels. The C 189 provides the site of attachment for mercury which inhibits AQP1 function. The GlpF is by comparison more hydrophobic owing to the presence of two aromatic residues (W 48 and F 200) in the selectivity filter and therefore is more suited to the transport of glycerol than water. Furthermore, it was shown that removal of positive charge by the mutation of arginine and histidine induced a pH dependent proton current in AQP1 which suggests a role also of the ar/R region in proton exclusion through the pore (57, 58). There is a potential central pore at the interface where the four individual monomers meets however, this region is not believed to be involved in the water transport (59).

Conduction of water through AQPs

Water enter the extracellular vestibule in AQP1 and makes contact with the hydrophilic residues K 36 and S 123 in loop A and moves further towards the ar/R filter to hydrogen bond to the residues lining the filter (60).

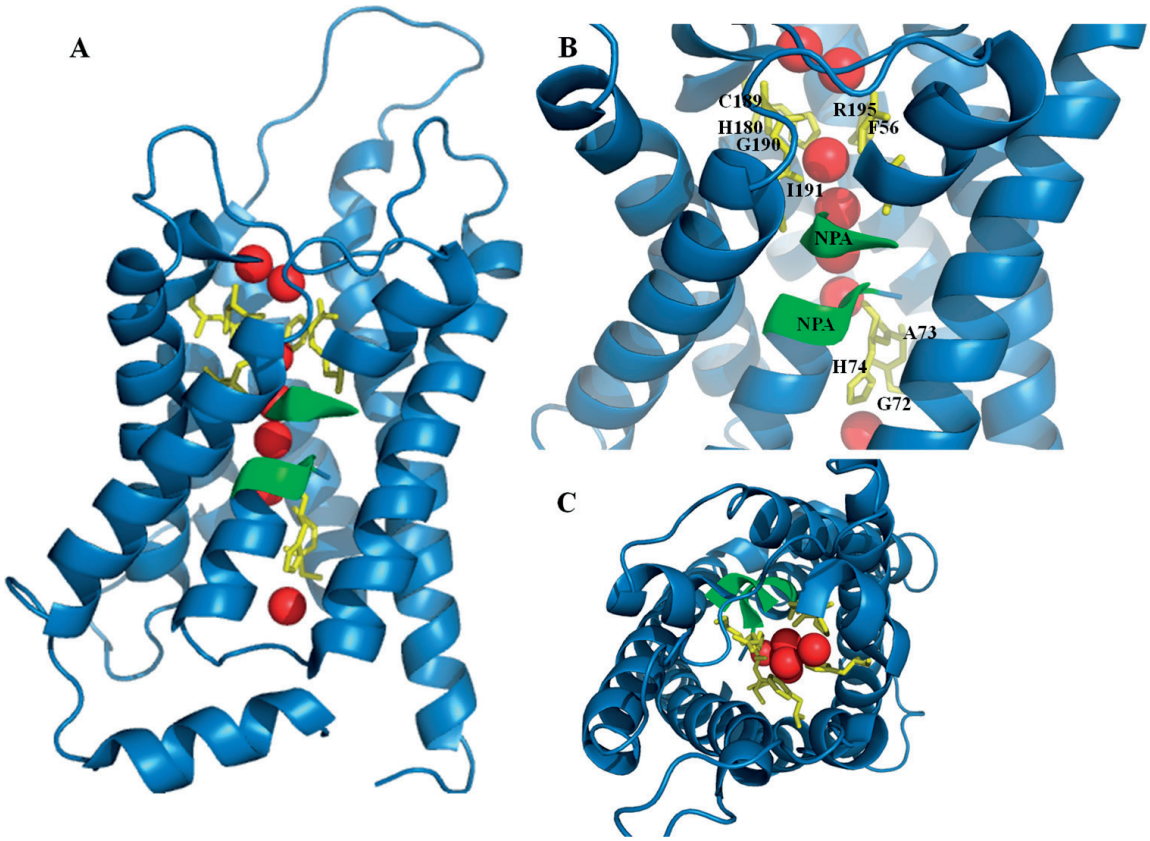

Figure 4: The movment of water molecules and their interaction with residue in AQP1 (PBD ID 1J4N) (A) side view (B) Closer view of the pore region. Residues involed in hydrogen bonding with water molecules (red) are shown in yellow sticks (C) Top view.

The water molecules orient themselves so as to avoid the hydrophobic side chain of F56 and make hydrogen bond interaction with R195 and H180.

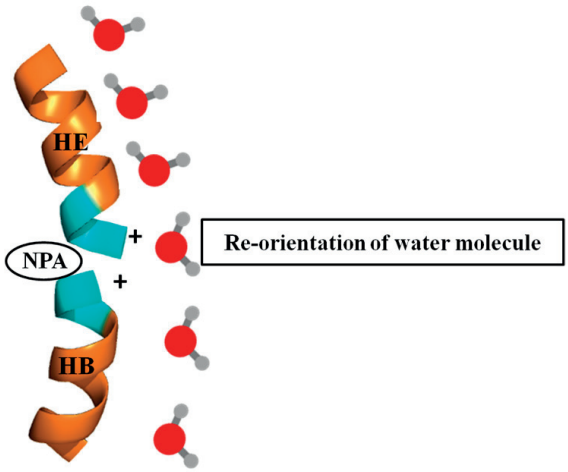

Figure 5: Helix B (HB) and helix E (HE) create strong dipoles, that are focused on the asparagines of the NPA boxes, that repel protons. The re-orientation of water molecules at the NPA box motifs is also shown.

The water moves forward by making hydrogen bond interaction with carbonyl oxygene of C 189, G 190 and I 191 and reaches the NPA boxes. The water molecule interacts with the asparagine residues of the NPA motives and reorients due to the strong electric field generated by the dipoles of the half helices HB and HE. The water molecules then proceed by interacting with the carbonyl of the backbone residues of G 72 and A 73 and the side chain of H 74. Finally the pore widens and the water molecules can enter the cell (53). The movement of water occurs both ways depending upon the concentration gradient. The pore lining, and specially the ar/R and NPA regions, determines the selectivity and permeability of the channel while the surrounding residues and are important for the overall structure of the AQP and for the regulation of channel function, for example by pH, metal ions and phosphorylation.

Classification of AQPs

The true understanding of the AQP family structure and functional diversity can only be appreciated in terms of an evolutionary perspective. Several AQP classes have been identified based on evolutionary relationships (61, 62, 8). The earliest split in the family has been traced to the separation of aquaglyceroporins from the water specific channel aquaporins, here termed water specific AQPs as phylogenetic group. The water specific AQPs are greatly diversified in comparison to aquaglyceroporins, which show only some degree of diversification in vertebrates, for example AQP3, AQP7, AQP9 and AQP10. In comparison, the diversity in the water specific group is prevalent across all

eukaryotes. Most bacteria have only one aquaglyceroporin and only one water specific AQP and archaea have either AQPs or aquaglyceroporin/glycerol transporter (GlpF-Like Proteins; GLPs). The fungi and unicellular eukaryotes do possess varied numbers of GLPs and AQPs. Vertebrates and plants have a great diversity and number of AQP genes reflecting their critical function in higher order organisms. GLPs are absent from vascular plants but present in lower plants such as green algae and mosses where they are grouped together with bacterial GLPs suggesting horizontal gene transfer (63). Higher plants might have lost GLPs due to functional overlap since another subfamily in plants, Nod26-like Intrinsic Proteins (NIPs) transport glycerol in addition of water (63). The diversification of plant and animal AQPs is proposed to have arisen from the gene duplication followed by functional and sequence variance. Based on phylogenetic relationship, the plant and animal AQPs are clustered together into three major groups which include i) Plant small and basic intrinsic proteins (SIPs) and AQP11 and AQP12. (ii) Plant tonoplast intrinsic proteins (TIPs), X-intrinsic proteins (XIPs), hybrid intrinsic proteins (HIPs) and AQP8. (iii) Plant plasma membrane intrinsic proteins (PIPs) and AQP0, AQP1, AQP2, AQP4, AQP5 and AQP6. This grouping of animal and plant AQPs in a phylogenetic tree may invoke a deep orthology scenario in which the diversity was achieved early in the ancestor genes (8). However, this scenario is improbable, since the absence of homologs of fungi and invertebrates in these groupings would require assuming many independent gene losses. Alternatively, it is suggested that plant and animals AQPs have independent origin and their sequences converged over the course of evolution in to these groupings, owing to the similar function of these proteins in animals and plants (64). The C-terminal of SIPs are composed of basic residues and they are found in intracellular membranes similar to the mammalian AQP11 and AQP12. Many SIP members have been identified in plants and green algae (61). Since, algal SIPs are basal to the plant SIPs it is suggested that this family has an ancient origin in plants with independent losses of some family members along the lineage or they might have been the result of horizontal gene transfer. SIPs do not share the conserved residues identified in AQP11 and AQP12, therefore their position in the phylogenetic tree might be due to Long Branch Attraction (LBA) (65). The XIPs, HIPs and TIPs (which are similar to animals AQP8) are found in unicellular eukaryotes, fungi, plants and animals suggesting the ancient origin of this family (8). NIPs are only found in mosses and flowering plants. In the phylogenetic tree, they are grouped together with cyanobacterial and archaeal NIP-like proteins, suggesting horizontal gene transfer (66).

Plant AQPs

The water homeostasis is critical for plant survival, which is indicated by the great number and diversity of AQP family members in plants (67). Most of these AQPs are present in the plasma membrane and tonoplast, two critical barriers to water flux. Based on their location, these aquaporins are named plasma membrane intrinsic protein (PIPs) and tonoplast intrinsic protein (TIPs) as mentioned before. The AQP family in seed plants can be subdivided into five families, a) PIPs (b) TIPs (c) SIPs (d) XIPs (e) NIPs. The mosses contain two additional families name HIPs and GIPs. In addition to PIPs and GIPs, green algae have additional subfamilies (A-E) which are not found in any other plants.

The PIPs are further subdivided into PIP1 and PIP2 isoforms, mainly depending on the length of N and C-termini. The PIP2 have longer C-termini (68) and higher water transport activity compared to PIP1 isoforms. PIP1 isoforms seem to require the co-expression of PIP2 isoforms in order to be targeted to the plasma membrane and in order to show water transport function (69). The PIPs are found in algae to higher plants suggesting that they evolved prior to the embryophyta (68). TIPs are divided into five subfamilies TIP1-5 and they are related to XIPs and HIPs. SIPs are intracellular AQPs that are subdivided into SIP1 and 2 isoforms in seed plants (61). NIPs are also divided into four subgroups (NIP1-4).

Regulation of AQPs

It is remarkable that such a multitude of AQP isoforms are found in plants and for example *Arabidopsis thaliana* and rice have 35 and 39 isoforms respectively. Animals have fewer AQPs, e.g. 13 isoforms in mammalian species (8). The amazing diversity of isoforms within living organisms hints to the importance of AQP function and at the same time suggests that there might be redundency and regulation that fine tune the response of plants and animals to diverse stimuli. Several reports have suggested that plant AQPs are regulated by heteromerization (69), post translational modifications (70), pH (39, 71) and metal binding (42). For example tonoplast intrinsic proteins (TIPs) and plasma membrane intrinsic proteins e.g. (SoPIP2;1) were found to be regulated by phosphorylation (72, 73). Two serine residues of SoPIP2;1 S 274 and S 115, are phosphorylated and found to influence water permeability of the channel when phosphorylated, as shown by mutational studies. The tulip plasma membrane TgPIP2;2 was also found to be regulated by phosphorylation at the corresponding residues (S 116, S 274) (74). Moreover, the regulation of AQP function by Ca^{2+} was suggested by the isolation of plasma membrane vesicles in the presence of chelators.

The same experiments also identified the role of pH in regulation of AQP function (49). Also, the cytosolic pH was found to regulate the root hydraulic conductivity by gating of PIPs (71). Recently, amoeboidal *Dictyostelium* AqpB was found to be gated by phosphorylation at a tyrosine residue in the D-loop (75). Besides water permeability, the phosphorylation may also regulate the subcellular localization of AQPs, as has been established for animal AQP2 and AQP4. For example, S 283 phosphorylation targeted AtPIP2;1 to the plasma membrane (76). Also, a motif was identified in maize PIP2;5 which is essential for directing it to plasma membrane and this motif is highly conserved in plant PIP2s (77). Proteomic analysis of Arabidopsis and rice also identified several phosphorylation sites in aquaporins (78, 79). Later on it was demonstrated that phosphorylation of AtPIP2;1 was necessary for leaf water conductivity in response to circadian cycle (80). Several AQP isoforms have been shown to be phosphorylated, but the kinases and phosphatases that cause the phosphorylation and dephosphorylataion are largely unknown and need to be identified and characterized (81).

Structure of SoPIP2;1

The water transport activity of the spinach PIP2 isform SoPIP2;1 was found to be regulated by the phosphorylation *in vivo* at S 274 in the C-terminal region. In the same study, another serine residue, S 115 in the cytoplasmic B-loop, was identified which was found to be conserved in all 13 PIP1 and PIP2 isoforms. Together with mutational studies in *Xenopus oocytes*, these residues are likely phosphorylation sites that regulate the water channel activity of SoPIP2;1 (6, 82). The structural mechanism behind the phosphorylation dependent effects on the water transport activity of SoPIP2;1 was unknown until the crystal structure of its open and closed forms were reported in 2006 (83). This was the first crystal structure of a plant aquaporin and the first paper which provided a structural mechanism for pH and phosphorylation dependent regulation of an aquaporin. By different crystallization conditions SoPIP2;1 could be crystallized both in an open (3.9 Å) and in a closed conformations (2.1 Å). The overall structure of SoPIP2;1 resembles that of AQP1, with only 0.8 Å root mean square deviation of transmembrane C-alpha atoms. Seven water molecules were found in the structure comprising a continuous unbroken water file along the length of the pore with a distance of 3.4 Å between each molecule. In a molecular dynamic simulation of water permeation, the water molecules displayed a specific orientation near NPA motifes. The structure of SoPIP2;1 was different to other aquaporins in the conformation of the D-loop such that it blocks the pore entrance at the cytosolic side of the pore, in the closed conformation.

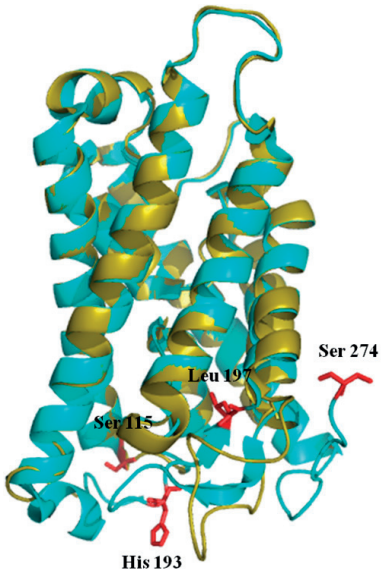

Figure 6: SoPIP2;1 close (PDB ID 1Z98) structure in ice cyan color and in open (PDB ID 2B5F) structure in gold color are superimposed. Residues involved in gating are in stick representation (red).

The hydrophobic D-loop residue leucine 197 which is conserved in PIPs, projects into the pore and narrows it down to 1.4 Å therby preventing water molecules to permeate the pore. The D-loop is displaced 16 Å in the open conformation relative to its position in the closed structure, At the same time helix 5 is extended into the cytoplasm. The projection of helix 5 into the cytoplasm displaces the hydrophobic residues L 197, P 195 and V 194 away from the pore increasing the pore diameter to 4 Å. The open structure resembles AQP1 in this regard. The molecular dynamics simulation also demonstrated the movement of D-loop causing the pore to open in response to the phosphorylation of S 115 and S 274. The AQP0 is suggested to be gated by a T 149, which occupy the same place as L 197 in SoPIP2;1. The structure of SoPIP2;1 also revealed the binding site of a divalent cation Cd^{2+}, which is involved in anchoring the D-loop to the short α-helix in the N-terminal. The Cd^{2+} was interacting with a highly conserved E 31, which makes hydrogen bond with the R 118 of Loop B, which is also highly conserved. The side chain of R 118 in turn is connected with the D-loop residues R 190 and D 191 through a hydrogen bonding network involving three water residues. The phosphorylation of S 115 destabilizes the interaction involving the D-loop, the Cd^{2+} and the short N-terminal helix, thus opening the channel for water transport. The S 274 which is conserved in all PIP2 isforms was found in the non-phosphorylated state to interact with P 199 and L 200 at the end of the D-loop of the neighboring monomer in the homotetramer resulting in a stabilization of the closed conformation of the D-loop of the neighboring monomer. Phosphorylation of S 274 would destabilize these interactions and result in the opening of the pore of the neighboring monomer. The L 197 would move to take up the place previously occupied by S 274 and the helix 5 will

be projected further into the cytoplasm resulting in the opening of the channel. Low pH would facilitate the protonation of H 193. When protonated H 193 forms a salt bridge with D 28, this salt bridge will link the D-loop to the N-terminal, thus causing the channel to close even in the presence of S 115 phosphorylation. The molecular dynamic simulation confirmed the conclusion derived from the structural analysis. In a follow up study the serine residues implicated in gating were mutated to glutamic acid to mimic the phosphorylated state of the serine residues (84). It was expected that these mutations would result in open structures. However, these mutants all crystallized in closed conformations, suggesting that the mutations are not good enough to mimic the actual phosphorylation. However the C-termini are found to be disordered in all closed mutants structures as predicted from the earlier structural studies. The mutation of S115E resulted in the disruption of the interaction with E 31, which act as a ligand for the Cd^{2+}. The E 31 moved away from this site and the binding of Cd^{2+} was affected by the mutation. The helix 5 is projected further into the cytoplasm and the structure looks similar to AQP1 (22) and AQP0 (85). The disruption of the Cd^{2+} binding site destabilized the closed conformation of the channel. It is therefore likely that water transport of PIPs are inhibited by Ca^{2+} and Cd^{2+}. That, loop D remains anchored to loop B suggests that mutating serine residues to glutamates does not fully mimic the phosphorylation state of the protein. Moreover, the water transport activities of the mutants were similar to the wild type suggesting that the closed conformation of the mutants were not the result of crystal packing. In the same study, another serine residue was identified that increased the water transport activity compared to the other mutants suggesting an open conformation of the protein. However, this mutant failed to crystallize so the structural mechanism regulating the opening of channel could not be ascertained.

Effect of mercury on SoPIP2;1

Mercury compounds are known to inhibit the water transport activity of aquaporins in red blood cells (86). The inhibition was attributed to binding of mercury to AQP1(2). In AQP1 the residue responsible for mercury binding was identified as C 189, which is one of the amino acids comprising the ar/R region of the pore (2). The inhibition was suggested to be the steric hindrance caused by the binding of mercury within the pore (87). Not all AQPs are sensitive to mercury inhibition as they lack the critical residue within the pore region responsible for mercury binding. For example, AQP1 and AQP3 (88) are sensitive to mercury while AQP4 is not (89). Like mammalian AQPs, some PIPs are sensitive to mercury while others are insensitive despite having the same cysteine residues. We (paper II) and other groups (48) have determined independently that the water transport activity of SoPIP2;1 increased in the presence

of mercury. The crystal structure demonstrated that mercury binds to three out of four cysteine residues and these structures result in a closed conformation of the protein (48).

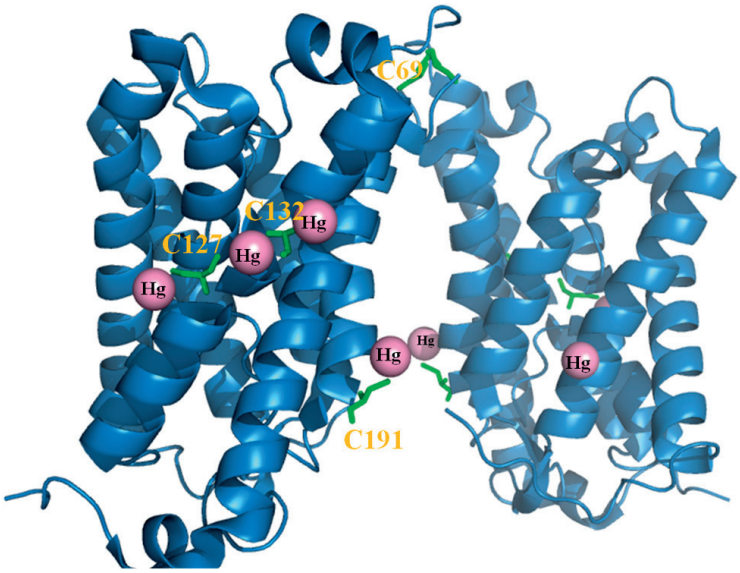

Figure 7: Structure of SoPIP2;1 bound to mercury (PBD ID 4JC6). The cysteines are shown as green sticks , mercury are shown as pink spheres.

However, the water transport activity of mutants lacking these cysteines showed that mercury binding resulted in activation suggesting that these residues do not contribute towards the activation of mercury. The fourth cysteine residue (C 69) participates in disulfide bond formation with the corresponding residue in adjacent protomer (90) and therefore is unavailable for mercury binding.

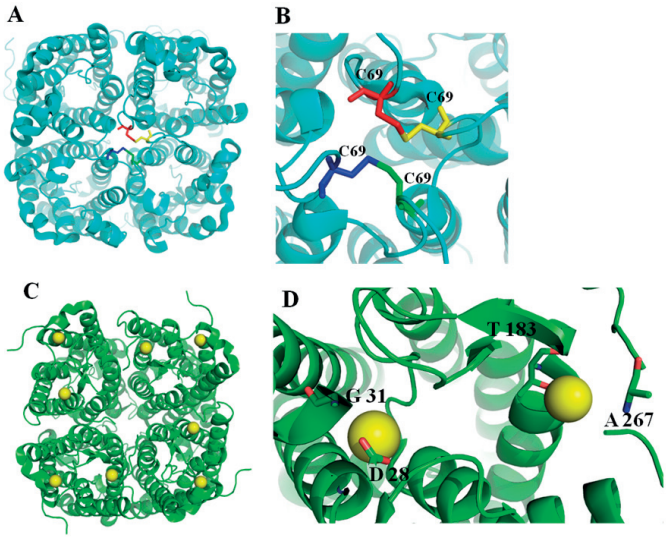

Figure 8: Structure of SoPIP2;1 (PBD ID 1Z98), (A) Cysteine 69 of each protomer are shown as stick. (B) Closer view of C 69 of each proteomer in four different colors are involed in disulphide bond. (C) cytosolic view shows the two Cd^{2+} biding sites (D) Closer view of the Cd^{2+} binding sites. The residues involved in hydrogen bonds with Cd^{2+} are represented as stick.

A detergent molecule was also found in the tetrameric center of the protein. The structure also identified the binding site for a Cd^{2+} in the C-terminal region (48) in addition to the N-terminal site previously identified. The activation of AQPs by mercury is previously reported for AQP6 (91). One of the residues in AQP6 recognized as responsible for the activation of water transport was the same residue that is responsible for the mercury inhibition of AQP1, suggesting that mechanisms for inhibition or activation by mercury is more complex than the simple arrangement of cysteine residues in the protein. For plant AQPs the situation is even more complex since five PIPs in *Populus trichocarpa* were inhibited by mercury (92) despite having the same set of cysteines as SoPIP2;1. An alternate explanation is therefore needed in order to understand the action of mercury on AQP function.

Future perspectives

The AQP field is still young and several challenges are still ahead, foremost among them is to what exact role does each AQP isoform play and what is the overall contribution of several AQP isoforms in animals and plants. To this end, genomics, transcriptomics and proteomics based studies will further our understanding of AQPs. The structure function relationship of one water specific plant AQP isoform has been established. Representative structures from all different AQP subfamilies in plants such as SIP, NIP, XIP and GLPs are needed to better understand their structure and transport function in the evolutionary context. Besides that, AQPs are known to transport water but some

isoforms transport solutes as well and therefore efforts aimed at identifying the solute specificity of different isoforms will increase our appreciation of the role of AQPs in plants. The role of AQPs in signaling as mediated through H_2O_2 and Ca^{2+}, need in depth analysis and more direct studies on plants in their natural settings are desired to better put the role of AQP mediated signaling in perspective. The role of AQPs in gaseous transport is still debated because of the difficulty in direct demonstration of gas transport and therefore methods to directly visualize the transport of gases through the AQP channels are desired.

My contribution to AQP research

In this thesis we have demonstrated the activation of spinach PIP2;1 by mercury and suggested the possible mechanisms by which this activation is achieved (Paper II). We have also characterized the stability of spinach PIP2;1 in the presence of detergents and different lipid systems which ultimately will aid its commercial use in biomimetic membranes for water purification (Paper I).

Chapter 2

TRP ion channels

Responding to various environmental cues is the key to survival in a constantly changing environment. Living organisms especially animals have developed specialized and complex structures and protein to anticipate and respond to the various environmental factors such as light, heat, moisture, chemical and mechanical stress. One of the proteins that have been implicated in sensation of these stimuli are transient receptor potential (TRP) ion channel. TRP channel is an intrinsic membrane protein, which was first discovered in fruit fly *Drosophila melanogaster* in 1989 (93). Since then, several TRP channels have been identified and characterized in animals including vertebrates and invertebrates. The TRP channels are present in plasma membrane of different cells and tissues, where they mediate sensory signaling (94, 95). However there are some TRP family members such as TRPML and TRPP, which are present in subcellular membranes (96). The TRPs found in intracellular membrane are suggested to have role in signal transduction and intracellular trafficking. TRP channels are functionally active as tetramer. Each subunit in a tetramer has six transmembrane spanning helices named S1-S6. The pore region is formed by a reentrant loop region between S5 and S6. Both N and C-terminal regions are located within the cytoplasm. Some TRPs have an several ankyrin repeat domain (ARD) at the N-terminal. Ankyrin repeats are small 33 residues long, characterized by the presence of repeating two anti-parallel helices linked by beta hairpins. The ARD has been linked to thermal and chemical sensation as well as for tetrameric assembly of TRP channels (97, 98). Another feature present in some TRP channel is the presence of TRP box at the C-terminus. This domain is presumably involved in Ca^{2+} binding and found in TRPM, TRPN and TRPC Although, TRPA do not possess a TRP box a recent structure of TRPA1 has been reported which showed an analogous TRP box like helix at the similar position in the structure. TRPs are central to sensory signaling and transport of cations. Mutations in these channels have been shown to result in neurodegeneration, kidney disorder, muscle weakness and hypersensitivity to nociceptive stimuli (99).

TRP classification

The TRP channels are evolutionary conserved and found in fungi, unicellular choanoflagellates, green algae and animals including vertebrates and invertebrates (100). However, land plants seem to have lost the channel over the course of evolution. Fungi have only one representative of the TRP channels, called TRPY1, which is found in vacuolar membrane and activated by mechanosensation and aromatic compounds (101). The yeast TRPY1 has little similarity with TRPs of multicellular organism TRPs and are therefore considered to appear in fungi only after divergence from animals. The TRP channels are now part of a superfamily of protein that has been classified into seven subfamilies based on the sequence similarity. The presence of six out of seven TRP subfamilies in unicellular choanoflagellates, together with the status of these organisms as common ancestor of animals suggest that TRP gene diversity already appeared in a common ancestor of animal and later on gene duplication event have increased the number of channels in the subfamilies further (100). The high sequence similarity exhibited by the member of subfamilies may suggest a conservation of the mechanism of activation, however, this is not the case as the function and mechanism of activation is not conserved within subfamilies. The subfamilies of TRP include TRPA (Ankyrin), TRPC (Canonical), TRPM (Melastatin), TRPN (NOMP-C), TRPV (Vanilloid) and distantly related TRPP (Polycystin) and TRPML (Mucolipin).

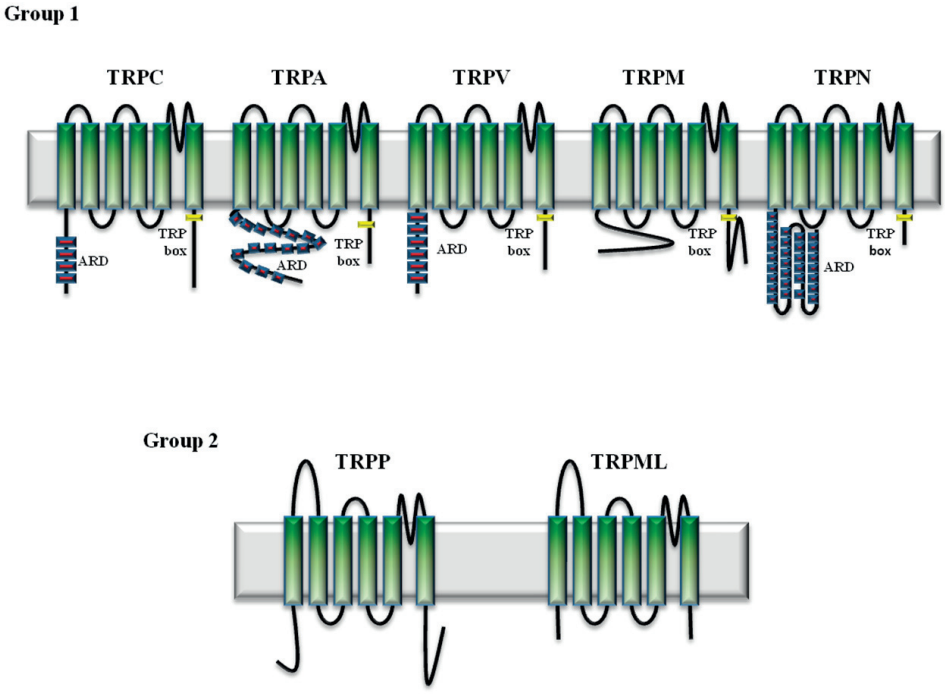

Figure 1: The topology and type of TRPs present in animals. TRPs are divided into two groups (1 and 2) on the basis of sequence similarities. ARD Ankyrin Repeat Domain.

All of the above mentioned TRP subfamilies members are found in mammals except TRPN. The first TRP channel was identified in fruit fly having mutated Transient receptor potential (*trp)* locus. The mutant flies were defective in light response resulted in tenfold decrease in calcium entry, suggesting that TRP protein is Ca^{2+} channel (93). This TRP channel is now recognized in mammals as TRPC. In mammals, TRPCs are further subdivided into seven members. Most TRPC are widely expressed but some of them are highly expressed in nervous system. The activation of TRPC is linked with activation of Phospholipase C (PLC) and production of diacylglycerol (DAG). TRPC1 is suggested to be activated by mechanosensation as well (102). Humans have six different TRPV channels most of which are activated by heat (except TRPV5 and TRPV6), noxious chemicals, pungent compounds and low pH (103) TRPV2 is activated by cell swelling. TRPV3 is activated by spices such as clove, oregano and thyme as well by menthol. There are eight different TRPM channels identified in mammals, which all have TRP box domain at their C-terminal like TRPC. Mammalian TRPM8 is activated by menthol, eucalyptol, icilin and low temperature (23-28 °C). TRPM4 and TRPM5 are unique among TRPs as they are activated by voltage and are selective for monovalent cations. In comparison, TRPM6 and TRPM7 are none selective divalent cations. TRPM2, TRPM6 and TRPM7 also possess enzyme domain at their C-terminal, TRPM2 contain an ADP ribose pyrophosphatase domain and TRPM6 and 7 have a typical protein kinase domain and are therefore called as chanzymes (104). TRPM7 is activated by pH, ATP and also expected be activated by physiological fluid flow (104). The TRPN have no mammalian homologues and are present in worms, flies and fishes. TRPN are characterized by the presence of 29 ankyrin repeats and suggested to be activated by mechanical stimuli (105). The TRPP and TRPML are grouped together as group 2 TRPs, which have little similarity with so called group 1 TRPs (TRPA, TRPC, TRPM, TRPN and TRPV) and are characterized by having a large loop between transmembrane segment one and two. TRPP and TRPML are further subdivided into three members each. TRPP is activated by mechanosensation (106). TRPML has three isoforms in humans and only one among these isoforms (TRPML1) has channel function. TPML1 is localized to the lysosome where it is suggested to work as monovalent cation channel involved in proton flux and regulates intra lysosomal pH (107). Humans have only one type of TRPA channel (108). In comparison, fruit fly *Drosophila* has four TRPA paralogues namely TRPA1, Pyrexia, Painless and Waterwitch. The TRPA encoding gene has ancient origin and it is believed to exist in all animals. A phylogenetic analysis of the TRPA1 gene identified that all electrophile sensitive TRPA1 from insects to vertebrates form a monophyletic TRPA1 clade different from basal TRPAs which are insensitive to electrophiles, suggesting that electrophile sensitivity has been conserved for 500 million years (109).

TRPs and disease

TRPs are important for various sensory signaling and mutation in their gene or modulation of their function have been reported to result in several diseases. Mutation in either TRPP2 or TRPP1 has been implicated in polycystic kidney diseases (PKD). PKD is characterized by the appearance of cysts in several organs, including kidneys resulting in kidney failure. TRPP2 is expressed in cilia-like appendages in most cells where they are proposed be involved in detection of water flow by mechanosenstion (106). Likewise, mutation in TRPC6, which is expressed in the barrier region between kidney and capillaries results in disruption of the barrier. The disruption of the barrier results in proteinuria and end stage renal disorders (110). A gain of function mutation in TRPV4 results in bone growth disorder characterized by short trunk and mild short stature. The channels is also involved in neurodegenerative disorders like scapuloperoneal spinal muscular atrophy characterized by weakened muscles, bone abnormalities and laryngeal palsy. TRPV4 is also implicated in Charcot-Marie-Tooth disease type 2C, which is characterized by impaired vision, hearing, weakened distal limbs (111). Several TRPs of melastatin family have been implicated in diseases. For example, mutation of TRPM1 results in night blindness (112). The mutation of the N-terminal region of TRPM4 results in increased channel concentration at the plasma membrane due to defects in endocytosis, which in turn results in depolarization and lead to blocking of heart contractions due to electrical conductance failure (113). TRPM6 is important for magnesium homeostasis in humans and mutation in this channel results in hypomagnesaemia and secondary hypocalcemia (114). Mutation of TRPML produces lysosomal storage defects which ultimately results in severe neurodegeneration and psychomotor retardation disorder known as Mucolipidosis type IV. TRPA1 channels are involved in sensation of nociceptive and nocifensive stimuli in humans and a gain of function mutation of TRPA1 results in familial episodic pain syndrome characterized by the episodes of pain in upper body induced by physical stress and fasting.

Function/mode of activation of TRPAs

TRP channels are polymodal sensors and are expressed in wide range of tissues and cells, such as sensory neurons, peripheral neurons, inner ear, skin and mucosal membrane etc where they might have role in heat and chemical sensation, mechanosensation, light perception and redox signaling. Noxious heat produces pain and therefore animals use these sensors to seek ambient temperature. So called thermo TRPs includes members from the TRPV, TRPA and TRPM subfamilies. TRPA1 from

rattle snake, fruit fly, frog, lizard and mosquito are activated by heat at characteristic threshold temperature (115, 116, 117).

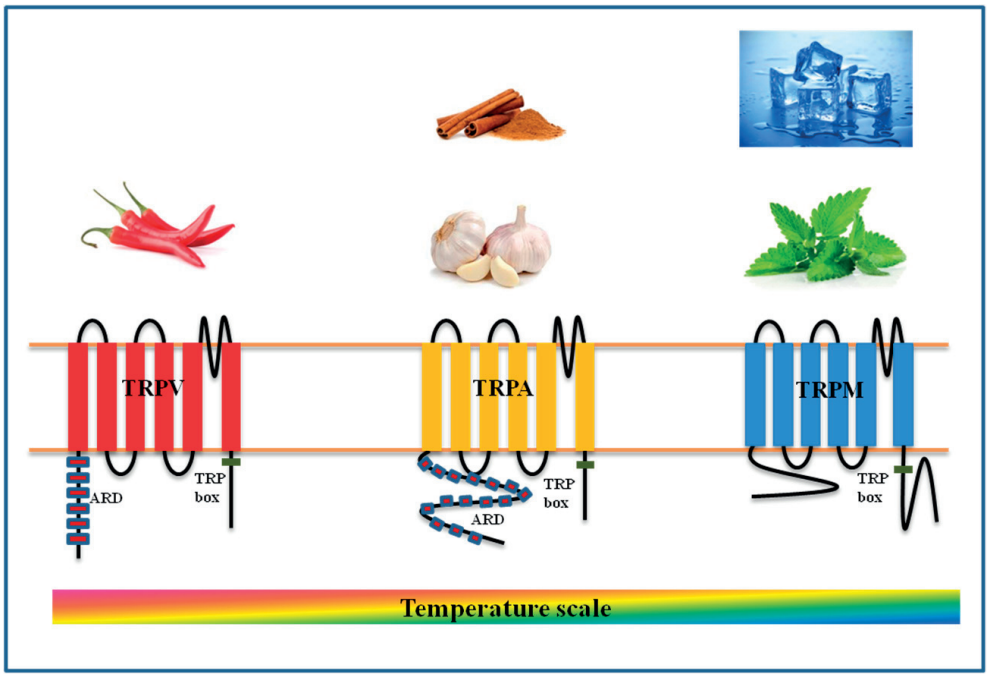

Figure 2: The topology of thermosensor TRP isoforms. The representative chemicals (above) and the temperature range (below) that activate TRP channels. ARD Ankyrin repeat domain. (natural products Images download from the following websites, chilli http://www.qvm.com.au/seasonal-produce/chilli/, cinnamon http://rushnews.rush.edu/2014/07/11/cinnamon-may-help-halt-parkinsons-progression/, garlic http://www.socalpain.com/garlic-pain-relief/, mint https://www.organicfacts.net/health-benefits/herbs-and-spices/health-benefits-of-mint.html, ice https://serenitysecurity.co.uk/team-serenity-take-ice-bucket-challenge/)

In comparison, mouse and human TRPA1s are activated by cold temperature ranging from17-10°C (118, 119). However, the cold activation of human TRPA1 is controversial (120). Out of the four TRPA paralogues in *Drosophila*, three of them are involved in thermal sensation from warm to hot (121). These paralogues include painless, pyrexia and TRPA1. Work on the painless paralogues which is activated by temperature around 42 °C suggests the role of N-terminal ARD in thermal sensation (122). Pyrexia is also involved in heat sensation at temperature close to 40 °C (123). In comparison, the TRPA1 homologue in *Drosophila* is activated in a temperature range of 25-29 °C and is required for seeking ambient temperature (124). Due to alternative splicing there are atleast four isoforms of *Drosophila* TRPA1 which are differ from each other by the length of N-terminal and the presence of 37 residues long region between ARD and the transmembrane helix S1. Presence of this region points towards the role of N-terminal linker region in the thermal sensation the TRPA1 isoforms (125). Studies on chimeric channel from human, snake and fruit fly also suggested a role of

the N-terminal ARD in thermal and chemical sensation (97). However, several other studies have suggested a role of the pore helix and the C-terminal domain in thermal sensation of other thermo TRPs (126, 127, 128). Beside that, TRPM8, which is a cold sensor, do not possess a N-terminal ARD, which have been implicated in thermal sensation (130). The role of N-terminal ARDs in chemical and thermal sensation is controversial and needs to be investigated further. Drosophila TRPA1 and Pyrexia also play their part in circadian rhythms as thermal sensor (131). *Caenorbabditis. elegans* TRPA1 is a cold sensor and play a role in aging by increasing the life span (129). Sensing of cold temperature by TRPA1 in the intestine of the worm resulted in activation of Ca^{2+} sensitive. Protein Kinase C, which in turn activated DAF16/FOXO which play a role in increases of life span. Mosquito TRPA1 expressed in peripheral neurons in the antennae is also activated by heat within the temperature range 25-40 °C (131). The mosquito larvae also used TRPA1 to seek ambient temperature providing a means to control mosquito spreads by targeting TRPA1 (132). Fly and mosquito TRP channels are also involved in detection of volatile and non-volatile chemicals. For example fly TRPA1 is indirectly activated by volatile compound citronellal (133). The same compound potently activate mosquito TRPA1 directly. TRP channels from mammals and flies are also involved in taste sensation. The taste sensation is mediated by TRPA1, Painless and TRPL in flies (109). TRPA1 is also involved in electrophilic compounds detection such as Allyl isothiocyanate (AITC) present in wasabi. Pungent compunds from garlic such as diallyl sulfides and allicin also activates mammalian TRPA1 (131). Other electrophiles such as cinnamaldehyde, acrolein, iodoacetamide are also known to activate the TRPA1 channel (108). These compounds activate the channel by covalent modification of cysteines and lysines in the N-terminal region (134, 135). The cysteines and lysine residues involved in electrophile detection were identified by mutagenesis. As mentioned already the N-terminal region of TRPA1 in flies, mammal and snake is implicated in thermal sensation (97). Other studies have found that these cysteines are involved in disulfide bond formation and therefore are important for structure and assembly and may not be directly involved in electrophile binding and thermal detection (136). TRP channels such as TRPA1 and Painless in worm and flies are also involved in mechanical sensation respectively (137, 138). TRPA homologues, Painless and Waterwitch in flies are involved in hygrosensation and noxious mechanical stimulus (139, 140). The mammalian TRPA1 is involved in O_2 sensing through cysteine modification resulting in activation of the channel (141). Coexpression of TRPA1 with Hypoxia-induceible factor-1α, strongly suggests its role in hypoxia (142). Similarly other ROS, NO and prostaglandins are also sense by TRPA1 through modification of cysteine residues (143). In addition mammalian TRPA1 is also activated by non-electrophilic compounds, such as menthol, which do not modify cysteine residues (144). Menthol

activates the channel at low concentration but inhibits it at higher dose. The menthol sensitivity of mammalian channel is linked with residues within the pore region between S5 and S6 (145). Lidocaine, a local anesthetic also has bimodal effect similar to menthol on TRPA1 activation (146). The Δ(9)-THC found in marijuana is another compound that activates TRPA1 in non-electrophilic manner (147).

Whether thermal sensation and electrophile sensation is mediated by distinct domain in thermosensitive TRP channel is an important pursuit. A few studies have demonstrated that thermal sensation and electrophilic activation exert additive effect on channel activation (148). These studies suggest that the thermal sensing domain is distinct from electrophile binding domain. Moreover, a FRET based approach suggested that binding of ligand did not affects the FRET efficiency, which is however affected by thermal sensation.

Structure of TRPA1

The TRP channels are difficult to crystallize since they are very unstable and conformationally heterogeneous. Structure of ankyrin repeat domains have been published (149, 150) but the X-ray crystal structure of full length TRP channels has not been reported yet. However, several electron microscopic structures of TRP channels with low resolution are available (151, 152). Among these structures, human TRPV1 with and without ligand is reported, close to 4 Å resolution (153, 154). The same group has also reported the structure of human TRPA1 very recently (155). The structure of TRPA1 was possible only in the presence of AITC at 4.24 Å or the antagonist HC030031 with and without additional antagonist A-967079 at 3.9 and 4.7 Å, suggesting the necessity to use agonist and antagonist to reduce the conformational heterogeneity. The structural details was resolved for the proximal cytoplasmic residues and transmembrane region spanning residues from lysine 446 to threonine 1078, which are important in assembly and presumably in ligand binding. The tetrameric assembly of TRPA1 resembles that of TRPV1 and the voltage-gated potassium channel.

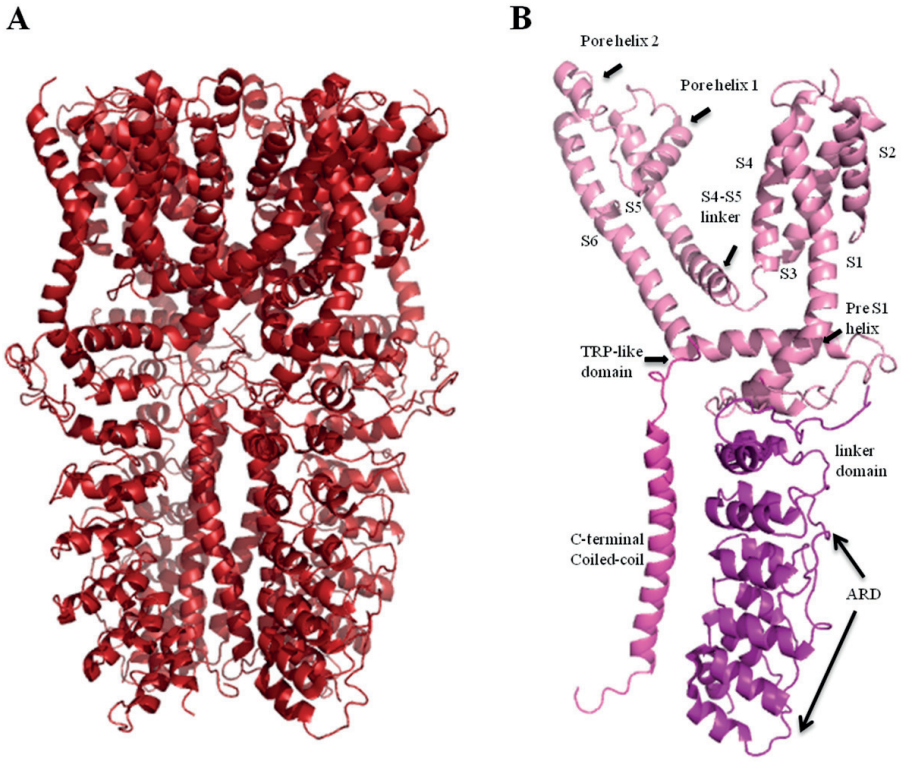

Figure 3: (A) Structure of human TRPA1 (PDB ID: 3J9P), side view . (B) Different structural domains highlighted in the monomer.

Each subunit consists of six transmembrane helices (S1-S6) and a central pore formed by the loop region between S5 and S6. In the structure, the C-terminal domain was found to form an extended coiled-coil region in the center, (156), surrounded by five Ankyrin repeats (ARs) number 12-16. The coiled-coil region of one subunit was shown in the structure to form interaction with the other three subunits, together forming the coiled-coil using the glutamine residues in the heptad repeats at one of the two positions, which are normally occupied by hydrophobic residues in the canonical heptad repeats. This is a novel mechanism by which subunits in TRPA1 are interacting with each other. In comparison, TRPV1 seems to involve ARs on one subunit to interact with three stranded ß-sheets on the adjacent subunit. The glutamine residues in the heptad repeats of the coiled-coil can adopt either destabilizing or stabilizing conformation depending on the suggested binding of inositol hexa phosphate. The four positive charge residues of heptad repeats (K1046, R1050 from one subunit and K1048 and K1052 from another subunit) mediate binding with four negatively charged phosphates from inositol hexa phosphate which in turn promotes the stabilizing conformation of glutamine residues within the coiled-coil providing explanation for the stabilization of channel function by the polyphosphates (157). The TRPA1 does not contain a canonical TRP box still it form an analogous TRP-like helix close to the cytoplasmic part of the pore. The TRP-like domain is proposed to regulate the channel

function through an allosteric mechanism. In the TRPA1 structure, this domain was found to interact with several substructures (pre S1 helix and linker region preceding pre S1 helix) harboring cysteine (C 621, C 641, C 665) and lysine (K 710) residues previously reported to be involved in electrophilic activation of the channel, thus providing the structural basis for allosteric modulation. The authors speculated that binding of electrophile to the cysteines and/or lysine will drive the conformational changes in the TRP-like domain which ultimately relieve the steric hindrance/repulsion resulting in the opening of the channel. However, the structure did not show the binding of AITC (agonist) with any of the cysteine or lysine residues because of the low resolution. Several residues in the transmembrane core and distal N-terminal region are also proposed to bind electrophilic ligands and may therefore contribute toward electrophilic activation. Besides that the TRP-like domain is also connected with the coiled-coil region through a short helix which is proposed by the authors to regulate the channel modulation by the phospholipids. The ARs region showed two distinct regions (a) a stem region formed by the ARs 12-16 and (b) a crescent shaped structure formed by eleven ARs, that were not resolved. The stem interacts with linker region which in turn is in contact with TRP-like domain and therefore transfer of information could take place between ARs and pore. In addition, the AR 12 of the stem makes contact with C-terminal coiled-coil domain which supports the role of ARs in channel assembly. The previous reports of ARs involvement in heat and chemical activation in insect and snake TRPA1s led the authors to speculate that this region might also modulate channel opening. The pore region contain two constrictions one at either end. The TRPV1 has a similar pore structure except that in TRPA1 the extracellular side of the pore region is lined by two short helices (154). Similar arrangement of two outer pore helices is found in bacterial voltage-gated sodium channel. The outer constriction in TRPA1 is slightly narrower (7.0 Å) in comparison to TRPV1 (7.6 Å) and formed by aspartate 915. This residue has been implicated previously in calcium permeability in mouse TRPA1. In comparison, the outer constriction in TRPV1 is formed by glycine 643 and methionine 644. The lower constriction in TRPA1 is formed by isoleucine 957 and valine 961 and measures 6.0 Å which is sufficient to block hydrated calcium. Only one residue isoleucine 679 is required to form the lower constriction in TRPV1. The structure of TRPA1 with antagonists (HC030031 and A-967079) suggests binding of A-967079 in a pocket formed by S5, S6 and the first pore helix. This is the same region predicted by molecular modelling to bind A-967079. Mutation of residue phenylalanine 909 to threonine in the region supposed to bind A-967079 abolished the inhibition of TRPA1 by A-967079 but not by HC030031 suggesting that there are different binding sites for two antagonists. This region is supposed to be mobile in the TRPV1 structure and the restriction of motion in this

region result that the lower gate cannot be opened. This site seems to be unique to A-967079 as the TRPV1 ligands binds in the lower S2-S4 region.

Future perspectives

The electron microscopic structures of TRPA1 provided significant understanding towards mechanisms of inhibition by A-967079 (155). However, it does not resolve the role of N-terminal ARD in electrophilic activation of the TRPA1 channel. Human TRPA1 is activated by cold in comparison with TRPA1s of flies, mosquitoes and snakes which are activated by hot temperatures. How temperature sensation is achieved in TRPA1 or in other so called thermo TRPs is not yet known and therefore, high resolution structures of TRP channels are needed in conjunction with molecular dynamics simulation to solve this puzzle. Other biophysical tools are needed to be developed, to better understand the dynamic nature of TRP channel activation and regulation. The role of signaling molecules such as H_2O_2 and NO in regulation of TRP channel has been recently proposed which need to be investigated in further details. The TRPs are implicated in several human diseases and various nociceptive and nocifensive pathways resulting in pain sensation therefore their inhibitors may find application as pain relief drug or as a tool to study further the structure-function mechanism of TRP channels. The malaria mosquito TRPA1 channel has been implicated in host seeking behavior. The channel is also used by mosquito larvae to seek ambient temperature and therefore compounds that modulate the TRPA1 channel function may represent one of the targets to control mosquitoes and the diseases they spread.

My contribution to TRPA1 research

In this thesis, we have expressed and purified the heat sensing mosquito (*Anopheles gambiae*) TRPA1 and compared it to the cold activated human TRPA1. The functional and biophysical characterization of purified mosquito and human TRPA1 has not been reported before. We investigated the role of TRPA1 with and without its N-terminal ankyrin repeat domain (ARD), which is proposed to play role in thermal sensation and subunit assembly. We found that the ARD are not essential for thermal sensation and subunit assembly. Besides that, electrophilic activation was also not found to depend on ARD (paper III and IV). The study undertaken in this thesis also highlights the fact that thermal and chemical activation is intrinsic to the channel and do not depend on accessory proteins and secondary messengers.

Chapter 3

Methods

A detailed understanding, atomic level, of the structural and functional mechanism at work in proteins can be accomplished by X-ray crystallography and NMR. However, both the techniques are limited in their own capacity. For example, X-ray crystallography required the protein to be studied, to form diffracting crystals of sufficient size and quality. Most membrane proteins do not readily form crystals and therefore, atomic understanding of these proteins might be obtained by NMR. NMR studies, in comparison, are limited by the size of the proteins. Recent development in cryoelectron microscopy has generated structures with near atomic resolution, of proteins, which have eluded crystallization. TRP channels are among the proteins that are difficult to crystallize due to their inherent instability and heterogeneity. TRP field has especially benefited from the development of electron microscopy techniques, the resulting in of the structure of TRPV1 and TRPA1. These studies have increased our knowledge of the TRPs structure but the significant questions such as how thermal sensation is achieved in thermo TRPs and the binding sites for the activating of electrophiles, remain unanswered. The dynamic nature of thermal sensation in thermo TRPs can be studied by low resolution structural techniques such as fluorescence spectroscopy, circular dichroism (CD) spectroscopy, Fourier transform infrared (FTIR) spectroscopy and many more. These techniques can give better information about the dynamic changes in the structure of the protein.

In this section, I will discuss very briefly techniques that we have used for the low resolution structural and functional characterization of the SoPIP2;1 and TRPA1.

* Fluorescence spectroscopy.

* CD spectroscopy.

* Stopped flow spectroscopy of SoPIP2;1 in the reconstituted vesicles.

* Single channel activity measurement of TRPA1 in lipid bilayer.

Fluorescence spectroscopy

Aromatic amino acids in proteins such as tryptophan, tyrosine and phenylalanine act as fluorophore. The intrinsic fluorescence of these amino acids is sensitive towards any change in the molecular environment, which can be monitored by the changes in fluorescence properties such as emission intensity, the shift in excitation and emission maxima. Fluorescence spectroscopy has been used to study the molecular interaction, protein stability and tertiary structural changes in proteins. The fluorescence spectroscopy is based on two processes, absorption and emission of light (Figure 1). When molecules absorb the certain wavelength of light, their electrons get energy to jump from a ground state to an excited state (Figure 2). When these electrons return to their ground state, some of the energy absorbed at excitation is lost due the transition between vibrational energy level (which is also called as internal conversion) therefore the emitted light after transition is released at the longer wavelength and constitutes specific emission spectra of the molecule. It follows that the excitation wavelength is always shorter than the emission wavelength.

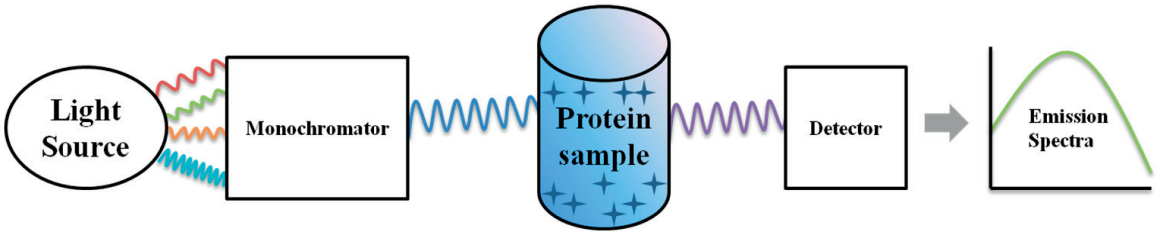

Figure 1: An schematic representation of the fluorescence spectroscopy technique.

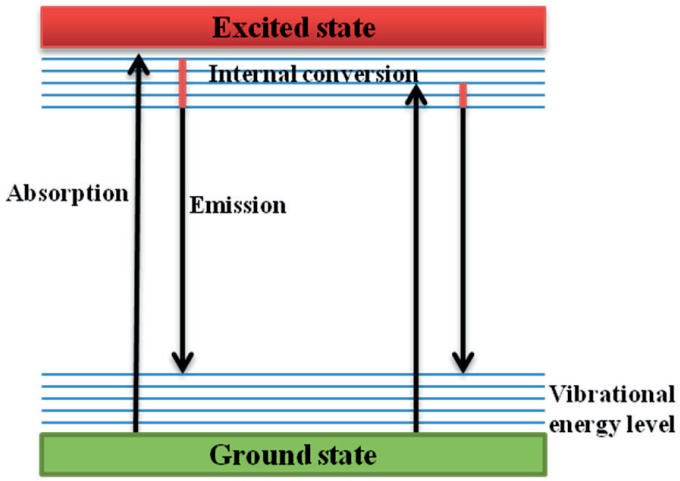

Figure 2: The ground state is shown in green and the red line depicts the excited state. The blue horizontal lines show the vibrational energy level in each state. The vertical arrow shows the energy which is absorbed to jump up to excited state and arrow downward is the emitted light. Due to internal conversion (red line) some energy of the excitation wavelength is lost, so that the emitted light is released at a longer wavelength.

The fluorescence efficiency can be estimated by the quantum yield, which is the ratio of photons emitted to the total photons absorbed. The quantum yield of phenylalanine is very low, therefore, the fluorescence exhibited by the protein is mainly dependent on tyrosine and tryptophan residues. The tryptophans in a protein can be selectively excited at the wavelength of 295 nm (158). Tryptophan is highly sensitive towards the electronic environment of its surrounding (159, 160) (Figure 3) and therefore, any change in the electronic environment near a tryptophan affects its fluorescence properties. For example, decrease in fluorescence intensity (quenching), shift in emission wavelength to the shorter wavelength called as blue shift, which typically indicates the burial of tryptophan residues in the nonpolar interior of a protein or a lipid phase. The emission wavelength may shift to longer wavelength called a red shift, which indicates the exposure of tryptophan residues to a polar environment and mostly accompanied the unfolding/denaturation of the protein (161). These properties of the intrinsic fluorescence can be exploited in order to study the protein-protein interaction, conformational change, ligand binding and protein denaturation etc. In this thesis, we have used the intrinsic fluorescence of the SoPIP2;1 and AgTRPA1to determine their thermal stability and ligand binding parameters.

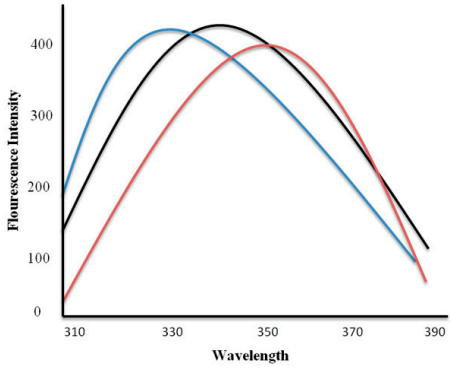

Figure 3: Hand drawn florescence emission spectra of a protein. The black curve represents protein native state, the maximum of the emission move to the lower wavelength when residues are buried into hydrophobic environment (blue curve) or to the longer wavelength when exposed to water (red curve).

Circular dichroism spectroscopy (CD)

The secondary structures of the protein can be inferred by using different types of spectroscopic techniques such as CD and infra red spectroscopy (IR). The principle of CD spectroscopy techniques rely on the absorption of left and right circularly polarized light by the chromophore. In the case of proteins, amino acid are referred to as chromophore because their chirality and therefore all amino acids except glycine have

a tendency to absorb the left and right circularly polarized light to different extents. The Far UV region (175 – 250 nm) in CD spectroscopy is commonly used for the secondary structures determination due its sensitivity towards the peptide bond. Different secondary structures show characteristic pattern on CD spectroscopy (Figure 4) such as α-helices give a positive peak at 190 - 195 nm and two negative peaks at 208 nm and 222 nm. Whereas, β-sheets give a positive peak at 195 - 209 nm and a negative peak at 215 – 220 nm. The random coils exhibit a positive peak at 220 nm and a negative peak at 200 nm. Therefore CD spectroscopy can be used to monitor the protein stability (folding and unfolding of secondary structure of proteins in response to temperature or chemical denaturants) (Paper I).

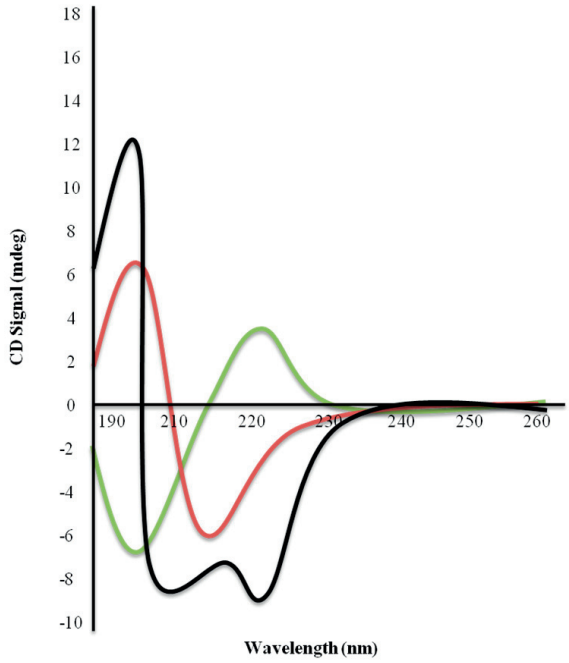

Figure 4: Hand drawnCD spectra of different secondary structure. α-helix (black), β-sheet (red) and random coils (green).

There are different algorithms such as CDSSTR, which can be used to deconvolute the CD data for estimation of different types of secondary structure present in a protein. We have used CD spectroscopy to report on the correct folding and thermal stability of SoPIP2;1 in different lipids system (paper I). We have also used CD spectroscopy to determine the secondary structure content of hTRPA1 and thermal stability of AgTRPA1 protein in a reducing and non-reducing environment (paper III and IV).

Functional characterization

Stopped flow spectrophotometry

Stopped flow spectrophotometry is mainly used to study the kinetics of a reaction in solution. The principle of the technique is very simple as it allows, the rapid mixing of two solutions and therefor to follow the reaction in milliscond up to seconds in time scale. Absorption, fluorescence and light scattering are the detection methods in this technique. We used the stopped flow kinetics to measure the functional activity of SoPIP2;1 reconstituted the lipids vesicles thereby forming proteoliposomes. Different LPRs (lipid to protein ratio) were used to optimize the activity. SoPIP2;1 was inserted into the lipid vesicles, followed by extensive dialysis to remove the detergent. The resulting proteoliposomes (SoPIP2;1 incorporated into lipid vesicles) were mixed with a hypertonic solution and the increase in light scattering was measured due to out flux of water. The presence of functionally active SoPIP2;1 causes the proteoliposomes to shrink faster compared to control liposomes without SoPIP2;1. Below is a representative trace to show water transport activity of SoPIP2;1. Red trace represents the control liposome (empty), purple trace represents the peoteoliposomes in which SoPIP2;1 had been reconstituted using *E. coli* polar lipids.

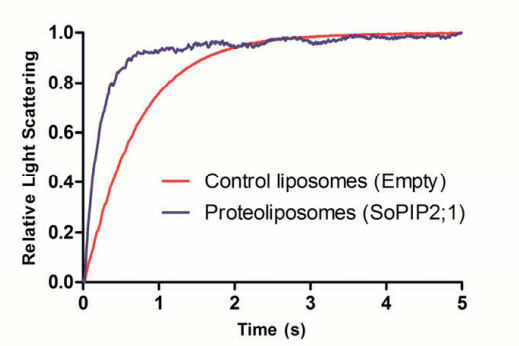

Figure 5: Water transport activity measurement by stopped flow spectrophotometry. The proteoliposomes with an active water channel shrink faster than control liposomes without protein, when challanged with a hypertonic solution.

Single channel patch clamp

Monitoring the functional activity of the purified ion channel is always challenging. Here we have used single channel port-a-patch clamp, a recently modified device where they have replace the patch clamp pipette with the planner-chip based sensor (Nanion Technologies), to characterize the functional activity of the human and mosquito TRPA1 ion channel (Paper III and IV). By using this technique we have measured the flow of current across the lipid bilayer through reconstituted purified ion channel proteins over the time. Port-a-clamp single channel activity studies were carried out using giant unilamellar vesicles (GUVs) which were formed by the electroformation method. In response to applying negative pressure (-20 to -40 mbars), GUVs with size between 1 to 100 µm depending on the lipids concentration will burst and form bilayer with high seal (tens to hundreds of GΩ) directly onto the chip. To prepare proteoliposomes, the purified protein was inserted into GUVs by incubating the GUVs and the detergent purified protein, followed by the removal of detergent with further incubation of GUVs protein mixture with the biobeads. The planar lipid bilayer was obtained after applying the negative pressure. Alternatively, the planar lipid bilayer is first obtained from the GUVs and a much diluted detergent purified protein is later added and was inserted into the planar lipid bilayer under a negative pressure. The measurements were recorded once the good seal was achieved (162).

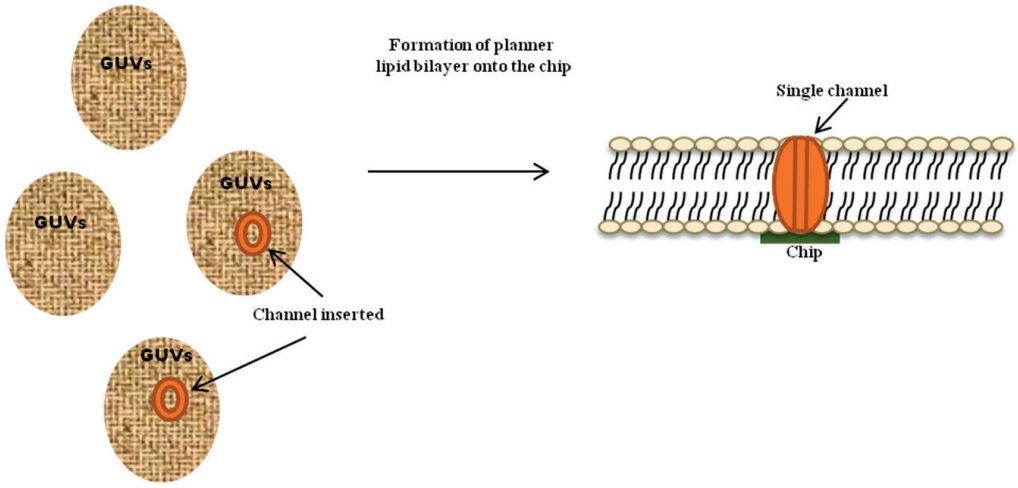

Figure 6: An representation of the formation of lipid bilayer on the chip from gaiant unilamellar vesicles (GUVs).

Patch clamp method records the ion channel activity by measuring the flow of current through the channel. The functionally active ion channel exists in multiple conformation states including close and open forms and it fluctuates between these forms sporadically. The presence of agonist shifts the equilibrium towards open state

by increasing the rate of the transitions from close to open state. To analyze the port-a-patch recording several strategies can be applied. Mainly the open probability (Po) is investigated, which reports the relative time period in the whole recording when the channel is open by measuring the current flow. The second property that can be measured by the port-a-patch is the conductance (Gs). Different ion channel shows characteristic open probability and conductance in response to different agonists. Further analysis of the channel kinetics can be carried out by the identification of the different population of the open and closed states, called as event detection over the time. In this thesis, we have used single channel patch clamp for the characterization of temperature and ligand induced activation of purified human and mosquito TRPA1 channels (Paper IV).

Figure 7: Single channel activity measurement using port-a-patch clamp. (A) bilayer without protein inserted (B) Reconstitued proteoliposome of Δ 1-776 AgTRPA1 activity stimulated with 100 μM AITC, O and C are represented the open and close states. (C) Reconstitued proteoliposome of AgTRPA1 activity stimulated with 100 μM AITC.

Paper summary

Paper I

The hetrologously expressed spinach plasma membrane protein SoPIP2;1 is an ideal protein for biotechnological applications owing to its high yield when expressed in yeast and its selectivity towards water. The water transport activity of this protein is well characterized and high-resolution structures are also available for this protein. However, there is lack of data on the stability of SoPIP2;1 in detergents and different biomimetic membranes, which is necessary for its use in biotechnological application, such as the biomimetic water filtration technology. In this paper, we determined the folding pattern and the thermal stability of secondary and ternary structure of SoPIP2;1 using spectroscopic techniques. To assess the correct folding of SoPIP2;1, we measured the far-UV circular dichorism (CD) spectra in a detergent solution and in different lipid membranes. SoPIP2;1 gives characteristic helical spectra with two negative band at 209 and 222 nm in octyl glucoside (OG) detergent micelles. We tested whether SoPIP2;1 retains its native structure when reconstituted in different lipid membranes. We found that the helical signature of SoPIP2;1 was conserved in different lipid membranes including membranes of *E. coli* lipids, POPE:POPC:POPS:ergosterol and POPE:POPC. The diphytanoylphosphatidylcholine (DPhPC) is known to form stable lipid membranes and has been found to be appropriate for various biotechnological applications. However, SoPIP2;1 lost its native structure in DPhPC as suggested by the far-UV CD spectra. Thus, it is not a suitable lipid for reconstitution of SoPIP2;1. The far-UV CD spectra were also used to obtain the percentage helical content of the protein in detergent and in different lipid membranes. We found that the protein when present in OG micelles had 63% helical content which is consistant with the values obtained from the x-ray structure of SoPIP2;1. The percentage helical content of SoPIP2;1 was also similar when protein was incorporated in proteoliposomes using *E. coli* lipids. Although, the CD Spectra of SoPIP2;1 were similar also in proteoliposome with POPE:POPC:POPS:ergosterol and POPE:POPC, the percentage helical content were significantly lower in these lipids compared to proteoliposomes with *E. coli* lipid. Thus, *E. coli* lipids constitute the best system for SoPIP2;1 reconstitution based on CD spectroscopy. Thermal unfolding experiments were also followed by CD spectroscopy in order to discern the thermal stability of the secondary structure elements of SoPIP2;1 in lipids and in detergents. The SoPIP2;1 followed a two state irreversible unfolding in OG detergent micelles and the midpoint of melting was found to be around 58 °C. This observation was confirmed by the SDS-PAGE analysis where we showed that the

SoPIP2;1 monomers and dimers were present at the temperature below the midpoint but most of the protein aggregated and appeared in the well at temperature above 50 °C. The midpoint of thermal unfolding transition of SoPIP2;1 was higher in lipids (above 70 °C) compared to the detergent micelles (58 °C) suggesting that the lipids increased the thermal stability of SoPIP2;1. Moreover, the different mean residual ellepticity (MRE) values obtained at 20 °C along with the different helical content in various lipid membranes suggest that the protein is interacting differently with membranes of different lipids. The intrinsic tryptophan florescence was used to measure the thermal stability of the tertiary structure of SoPIP2;1. The emission maximum for SoPIP2;1 was found to be 330 nm, which shifted to slightly lower wavelength in *E. coli* lipids suggesting that tryptophans are aligned closely to the edge of the detergent micelles and are relatively easily accessible to the water in detergent micelles as compared to proteoliposomes made of *E. coli* lipids. The intrinsic fluorescence of SoPIP2;1 was quenched at higher temperatures which suggested an increased access of water to the tryptophan residues. This may result from increased fluidity of detergent micelles and lipids at higher temperatures or due to the unfolding or to a local conformational change of tryptophan of protein. The thermal unfolding measured by the tryptophan quenching indicated a two-state unfolding with a midpoint around 58 °C in OG micelles, which corresponds to the analysis obtained from CD spectroscopy. However, the melting curve of SoPIP2;1 did show more than one transition in *E. coli* lipids as opposed to the OG micelles. The first transition might have resulted from the increased fluidity of the lipid membrane at higher temperature. The midpoint of the other transition was more likely caused by the unfolding of SoPIP2;1 above 70 °C, which is similar to the value obtained from the CD spectroscopy. In conclusion, the results of this study identified the suitable lipids system for reconstitution of SoPIP2;1 for biotechnological application.

Paper II

Aquaporins of the PIP subfamily are characterized by the presence of a conserved cysteine residue in loop A (13). The PIPs form functional tetrameric units in which each monomer constitutes a water channel and is capable of transporting water across the membrane. The conserved cysteine residues of adjacent monomers in PIP homotetramers are all aligned at the tetrameric center. The spinach PIP2 isoform (SoPIP2;1) is a well-characterized member of the PIP family and possesses this conserved cysteine residue (C 69) in loop A. In this paper we have determined the nature of the interaction between the conserved cysteine residues and tried to assess the role of cysteine interactions for the function of SoPIP2;1. We observed the dimeric form of SoPIP2;1 during purification, suggesting the presence of at least one disulfide bond. Since C 69 is conserved among plant PIPs it was hypothesized that perhaps this cysteine is important for dimer formation. Site directed mutants C69A and C69S were generated to confirm the role of this cysteine. We used the SDS-PAGE analysis to assess the effect of reducing agents on SoPIP2;1 wild type and cys69 mutants. Compared to wild type SoPIP2;1 the mutants appeared as monomers on SDS-PAGE confirming that C 69 is involved in dimer formation. Thermal denaturation experiments were conducted and followed by CD spectroscopy to determine the influence on the thermodynamic stability by the disulfide bond. We found that the disulfide bond contributed only modestly towards the stability of the protein. To determine the effect of mutations on the function of protein, we reconstituted the wild type and C 69 mutants in liposomes for stopped-flow water transport assays. Remarkably, the mutants were more active compared to the wild type suggesting that perhaps the tetrameric central pore is leaking water. One way to test this hypothesis is to block the four main pores of the homotetramer by the use of mercury, a well-known inhibitor of AQPs. Surprisingly, mercury increased the water transport both in wild type and in the C 69 mutants. The binding of mercury resulted in quenching of tryptophan fluorescence and the effect was reversed by the chelation of mercury by the addition of 2-mercaptoethanol. An independent study carried out by others (48) demonstrated that mercury activation did not depend on the cysteine residues. They identified two binding sites for the metal atom cadium in a crystal structure, wherethe novel second binding site was found to interact with the carbonyl of the C-terminus region. It is known from the closed structure that the S 274 occupies the place in the tetrameric centre of the protein and the C-terminal residues upstream of S 274 are placed between the monomers. Phosphorylated S 274 cannot occupy the same position and the rest of the C-terminal therefore becomes unordered resulting in the opening of the pore. Since, the change in protein conformation upon binding of mercury was time-dependant, we speculated that binding of mercury to the second cadium binding site similarly resulted

in the destabilization of the C-terminal causing the pore to open. Also we found that the effect of mercury on the C 69 mutants was additive. A previous mutational study (13) on another PIP2;1 isoform using transient expression in *Xenopus oocytes*, did not report any enhanced activity of loop A cysteine mutants, although maize PIP2s and SoPIP2;1 are very similar to each other. The major difference between our system, which was based on water transport assay in artificial liposomes, the mutant study in oocytes, was the environment of the protein. In several AQP structures including the one on SoPIP2;1 (89) a detergent molecule has been detected in the centeral pore. We purified the protein in the presence of detergent, but the detergent was subsequently removed by extensive dialysis during the liposome preparation. It is possible that in the native environment a lipid molecule is present, in place of the detergent molecule, and the lipid may prevent water leakage through the central pore. This is further supported by the observation that several other AQP isoforms, which do not possess conserved cysteine residues in loop A, do not leak water through the central pore. The results of this study are discussed in the context of previous structural and functional studies and it was concluded that the activation of SoPIP2;1 brought about by mutation of the conserved C 69 may be due to the heterologous production of the protein. The activation of the protein by mercury was proposed to be due to destabilization of the C-terminal region and opening of the pore.

Paper III

TRP channel subtype, TRPA1 has been involved in chemical and thermal sensation in animals. The TRPA1 isoforms from different animals exhibits distinct threshold temperature for activation. Some insects, such as *Anopheles gambiae* has two TRPA1 isoform; AgTRPA1(A) and AgTRPA1(B), which differ from each other by the presence of additional amino acids at the N-terminal. Both of these isoforms are activated by heat and electrophilic chemicals as demonstrated by heterologous expression studies. Whether, purified AgTRPA1 exhibits thermal and chemical sensation is not known. We have carried out expression of C-terminal c-myc epitope and hexa- histidine tagged AgTRPA1(A) in the methylotrophic yeast *Pichia pastoris*. The TRPA1 isoform has been linked in host seeking and heat avoidance behavior. The TRPA1 is characterized by the presence of N-terminal ankyrin repeat domain (ARD), which has been implicated in thermal and chemical sensation. Therefore we also expressed AgTRPA1 without N-terminal domain (Δ1-776 AgTRPA1) to investigate the role of ARD in thermal and chemical sensation. The membrane fraction from the cells expressing AgTRPA1 and Δ1-776 AgTRPA1 were obtained and subsequently solubilized by the Fos-choline 12

detergent. Nickel affinity chromatography followed by gel filtration chromatography was performed for the purification of the proteins. The proteins were found to be correctly folded as they eluted as tetramer from gel filtration column. The correct folding of AgTRPA1 and Δ1-776 AgTRPA1 was also confirmed by the characteristic alpha helical signature in SRCD spectroscopy. Thermal denaturation of AgTRPA1 and Δ1-776 AgTRPA1 was also carried out, which suggested the complete loss of alpha helical structure at 80 °C. The midpoint of thermal transition was found to be similar for both the protein. However, a minor transition between 30 and 45 °C was also identified in AgTRPA1. The presence of these transitions was not conclusively demonstrated or ruled out in Δ1-776 AgTRPA1 due to variability of the protein samples. The intrinsic tryptophan fluorescence of the protein is sensitive to the changes in local environment and may report on the conformational change exhibited by proteins upon ligand binding and thermal denaturation. We were interested to know whether AgTRPA1 exhibit conformational change upon ligand (AITC) binding or not. The fluorescence spectra at on protein equimolar concentration were found to be similar for both AgTRPA1 and Δ1-776 AgTRPA1, which was quenched upon binding of AITC. It may suggest that the tryptophan residues in the ARD do not contribute to the fluorescence. The EC_{50} values for AITC binding were found to be in similar range for AgTRPA1 and Δ1-776 AgTRPA1. Previously, the EC_{50} value from functional activation was found to be 70.7±12.4 μM, suggesting that some low affinity binding sites required for complete quenching of fluorescence are not essential for activation. We also monitored the intrinsic fluorescence change in AgTRPA1 at different temperatures. Interestingly, the temperature also induced quenching of fluorescence with a midpoint of transition around 38.5 °C. However, temperature failed to completely quench the fluorescence of the proteins, which is consistent with our reasoning that complete quenching of fluorescence is not required for activation. Thus, the intrinsic tryptophan fluorescence can be used to infer the mechanism of AgTRPA1 activation by heat and electrophiles in membrane independent manner. The purified AgTRPA1 with and without ARD was found to be activated by AITC and heat in single channel patch clamp recordings (-100 to +100 mV in 2s). The open probability (Po) was higher and single channel single channel conductance (Gs) was lower at test potential of +60 mV for Δ1-776 AgTRPA1 compared to AgTRPA1. A Q10 value of 28 was calculated for TRPA1 using a simplified equation. The threshold temperature for activation of AgTRPA1 was found to be 25 °C. The Gs was found to be lower for Δ1-776 AgTRPA1 at 30 °C, compared to AgTRPA1 at steady state potential of +60 mV. The opposite behavior was seen at 40 °C, with a Gs increase for Δ1-776 AgTRPA1 and decrease for AgTRPA1. The differences in Gs and Po with and without ARD suggest that N-terminal modulate the temperature and electrophile sensation of AgTRPA1. The single channel activity measurement of AgTRPA1 in response to AITC

was compared with human TRPA1 (hTRPA1) also, which revealed several differences. For example, AgTRPA1 mainly exhibited one single conductance level compared to hTRPA1, which showed several sub conductance level. Also, the Gs of AgTRPA1 with and without ARD were lower compared to hTRPA1. Similarly, Po was found to be lower for Δ1-776 AgTRPA1 compared to human counterpart. These differences might be attributed to the increased number of cysteines present in hTRPA1 (9) compared to AgTRPA1 (4) in the region outside ARD. In conclusion, the results showed that purified AgTRPA1 is intrinsically activated by heat and electrophile, and that N-terminal ARD is not required for this activation, although it may tune the response.

Paper IV

Responding to various chemical and environmental stimuli is important for the survival of any organism. Numerous studies have demonstrated the a role of TRP channel proteins in chemical and thermal sensation. Except for the rat TRPM8 and TRPV1, most of these studies were carried out in heterologous expression system, isolated neuron patches and whole animals. It is therefore needed to establish whether the thermal sensation is intrinsic to these proteins or there is an involvement of secondary messenger(s) and accessory proteins for mediating the thermal sensation. To address its role in intrinsic thermal and chemo sensation, N-terminal deca-histidine tagged human TRPA1 (hTRPA1) with and without its N-terminal Ankyrin repeat domain (ARD) (Δ1-668 hTRPA1) were expressed *Pichia pastoris* expression system. The hTRPA1 and Δ1-668 hTRPA1 were extracted from the membrane using Fos-choline 14. Nickel affinity chromatography was employed to purify the hTRPA1 and Δ1-668 hTRPA1. In order to confirm that deletion of ARD do not affect the folding and tetramerization of Δ1-668 hTRPA1, we carried out size exclusion chromatography and CD spectroscopy. The Δ1-668 hTRPA1 mainly eluted as tetramer and exhibited the characteristic α-helical signature in the CD spectrum. The secondary structure content estimated from CD spectra using Dicroweb software was found to be between 35-45%, which closely matched with the helical content predicted by the transmembrane hidden Markov models and the sequence alignment of Δ1-668 hTRPA1 with the potassium channel (Kv1.2). The purified hTRPA1 and Δ1-668 hTRPA1 were reconstituted in a lipid bilayer and their functionality was confirmed by measuring the ramp current (-100 to +100 mV in 2 s) using Allyl isothiocyanate (AITC) and menthol respectively. Cold sensation has been attributed to TRP family protein TRPM8 and TRPA1 in mammals. However, there are some conflicting reports regarding the role of TRPA1 in cold sensation. We found out in this study that purified hTRPA1 and Δ1-668 hTRPA1 reconstituted in lipid bilayer were inactive at room temperature (22 °C) and become

activated at lower temperature (17-10 °C). The antagonist HC030031 blocked the cold evoked activity of the hTRPA1 and Δ1-668 hTRPA1. The open probability (P_o) increased with the decreasing temperature and the Q10 values were calculated, which showed similar dependence on the temperature as previously found out for the heterologously expressed mouse TRPA1 in cell-attached and in inside-out patches. Single-channel conductance (G_S) of hTRPA1 at 10 °C was also found to be comparable with mouse TRPA1. Electrophilic compounds, AITC, cinnamaldehyde (CA) and N-methylmaleimide (NMM) were also found to activate the purified hTRPA1 and Δ1-668 hTRPA1 suggesting that chemical sensation, like cold sensation, do not essentially require the N-terminal ARD. The activation was reversible and found to be blocked by the antagonist HC030031. The G_S values for all the electrophilic compounds were similar for hTRPA1 and Δ1-668 hTRPA1 at -60 mV but the values differ for both the constructs for AITC and NMM at +60 mV. The P_o values were also different for the hTRPA1 and Δ1-668 hTRPA1. The rectification index for G_S and P_o was also found to deviate for hTRPA1 and Δ1-668 hTRPA1 activated by electrophiles suggesting voltage dependant changes imparted by N-terminal. The orientation of hTRPA1 and Δ1-668 hTRPA1 in the lipid bilayer was demonstrated by application of lipid impermeable compounds MTSEA-biotin and Maleimide-biotin respectively. Both compounds activated the respective constructs only when applied to the external solution suggesting the uniform insertion of protein in the lipid bilayer. The non-electrophilic compounds menthol, C16 and Δ^9THC also activated hTRPA1 and Δ1-668 hTRPA1, supporting direct interaction of these compounds with the proteins, without requiring accessory proteins and secondary messenger. Both the constructs showed differences in rectification index calculated from G_S and P_o for non-electrophilic compounds suggesting the N-terminal alters the response of hTRPA1 towards non-electrophilic compounds in a voltage-dependant manner. We also found out that C16 activated the chimeric menthol insensitive *Drosophila* transmembrane segment 5-hTRPA1 advocating distinct binding sites for C16 and menthol in hTRPA1. Since menthol binds to the transmembrane region of hTRPA1, we use it as an agonist at room temperature to further investigate the role of N-terminal ARDs. We found difference in G_S and P_o value for hTRPA1 and Δ1-668 hTRPA1 at negative and positive potential suggesting voltage dependant modification of hTRPA1 activity by ARD. In conclusion we demonstrated that hTRPA1 is intrinsically active at low temperatures and do not essentially require the N-terminal ARD for cold sensation. Moreover, electrophilic and non-electrophilic compounds activate the channel without the need for ARD and thus seem to binds to the C-terminal and/or transmembrane region. However the N-terminal contributed to the modification of activity in a voltage-dependent manner.

Popular science summary

Cells are the basic unit of life that exhibit dependence on water and ambient temperature to flourish and survive. So it is remarkable that the proteins responsible for the interaction of water and heat with the cell were not discovered until relatively recently. It was assumed for decades that water freely diffuse into and out of the cells without support. The cells are surrounded by a lipid (fat) membrane which forms a barrier to the passage of molecules that are not hydrophobic (fat soluble). Since lipid and water are immiscible, water does not readily pass through the membranes and require assistance in transport across the membranes. The identity of the proteins that form the channel in the membranes for the transport of water molecules was discovered in 1992. These proteins are now called as aquaporins (AQPs). In addition to water, some AQPs also transport other nutrient molecules such as glycerol, urea, ammonia, carbon dioxide and also signaling molecules such as hydrogen peroxide. The AQPs are vital to plant and animal function as exemplified by growth defects and diseases associated with AQP aberrant expression and function and therefore it is essential to study their function. The mechanism of water and nutrient conduction through AQPs is now well established but there are some aspects of the AQP function that are not very well understood. For example, the function of some of these AQPs is known to be inhibited by the mercury a toxic metal found in nature. However, some AQPs are activated by mercury despite sharing the similar structure with the AQPs inhibited by mercury. Although, the activation of AQP by mercury has been recognized for some time, the mechanism of activation is not known. In this thesis, we found out that mercury activate a spinach AQP. The structure of the spinach AQP is known which suggests that some part of the AQP protein act as a gate and open up the channel for water transport upon phosphorylation (a type of modification that is commonly known to regulate the function of large number of proteins). We speculate that mercury activated the spinach AQP by binding close to the gate of the channel and disrupting interactions in the closed form and thereby open it in a similar way as phosphorylation. Toxic heavy metals such as mercury and nickel produced by industrial waste are increasingly incorporated in the food chain and known to modulate the function of AQPs. Our finding shed new light into the mechanism of activation by mercury and will contribute towards a better understanding of AQP function. The spinach AQP is a highly selective water channel and it can be produced in abundance thus making it attractive to use in biotechnological application such as biomimetic water purification

systems. However, this application requires the demonstration of stability of spinach AQP in different biomimetic membranes. We have conducted these studies and we hope that it will contribute towards the efforts to use the spinach AQP in biotechnological application. As mentioned earlier, the heat responsive proteins present in the cell membranes were discovered very recently. These proteins are called transient receptor potential (TRP) ion channels and have several different subtypes with a distinct threshold for temperature activation. Some of these TRPs also lined our taste buds and responsible for the strong taste sensation when activated by chemicals found in food such as wasabi, pepper, chili, oregano, thyme, garlic, onion and compound found in mustard oil, eucalyptus oil, lemon grass and menthol etc. The fruit fly, snake and mosquito TRP type A1 (TRPA1) mediate warm temperature sensation. However, the temperature activation of human TRPA1 is mired in controversy with different researchers reporting disparate threshold temperatures. Moreover, there is no demonstration of TRP activation by temperature in a pure system without presence of accessory proteins and small molecules. We demonstrated the activation of human and mosquito TRPA1 by cold and heat, respectively, in a purified system, thus proving for the first time that temperature sensation is indeed intrinsic to TRPA1, which will eventually resolve the controversy regarding the cold activation of human TRPA1. A large part of the TRPA1 protein is formed by a repetitive unit known as ankyrin repeats. Some researchers have proposed that these repeats are essential for thermal and chemical sensation. We demonstrate in this thesis that TRPA1 still retain the temperature and chemical sensation even after the removal of these repeats. These results will contribute towards a better understanding of TRPA1 function which has been recognized as a target for pain management. Inhibitors of human TRPA1 will have an application as painkillers. Similarly, mosquitos use TRPA1 to identify hosts for sucking blood, thus compounds that modulate the function of TRPA1 may function as mosquito repellants. However, these pursuits will require a better understanding of TRPA1 function. The results of this study may contribute towards these efforts by providing the evidence that ankyrin repeats are not responsible for temperature and chemical sensation and therefore future drug design should target other parts of TRPA1 proteins for selective inhibition of chemical and temperature sensing domain.

Acknowledgments

It is my great pleasure to thanks all the people for their encouragement and support during my PhD studies. There is a list of the people to whom I want to convey my sincere gratitude.

First of all, I want to say special thanks to my supervisors **Urban Johanson** for your guidance, support, excellent supervision and giving me the space to developed myself as an independent researcher. Thank you very much for all your help and encouragement during my research. I also want to say thanks to **Per Kjellbom** for your help and support and sharing your great knowledge about the membrane proteins and especially about aquaporin.

I also want to thanks **Peter Zygmunt, Edward Hogestatt.**

Thanks to collaborators **Ines Plasencia** for introducing me to CD spectroscopy and **Lavanya Moparthi** for electrophysiological studies.

All the past and present members of the aquaporin/TRP group, especially **Maria, Kristina** for being supportive colleagues and good friends and **Jonas** for your help in my beginning time. **Andreas** for being a wonderful person and helping me a lot in my earlier days, I will always miss your conversation. **Anders** and **Yonathan** I always enjoyed talking with you and got a lot of new information. I want to thanks **Hanna, Angelica, Henry, Eva, Michael, Aaron, Sinead** for creating nice environment.

I want to say special thanks to **Adine Karlsson** for all your support and help and small chats we had over coffee.

Thanks **Jeniffer** for the wonderful company, I will miss a lot your baking and sweets.

Thanks to **Gert Carlsson** and **Magnus Alsterfjord** for the technical support.

All the other people at CMPS, making it a nice place to work.

I want to say thanks to all my friends in Sweden, without them it would have been very hard.

Special thanks to my father, mother, my sisters **Rabia** and **Rukhshanda** and my brothers for helping me throughout my journey.

I want to deliver my special thanks to my daughter **Aysha** for being so understanding in such a young age and sacrificing most of her weekends with me in the lab. Your love and antics take all my stress away.

Last but certainly not the least my husband **Raza** for your support not only at home but also at work. This would not have been possible without your support.

References

1. Paganelli CV, Solomon AK. The rate of exchange of tritiated water across the human red cell membrane. The Journal of General physiology. (1957) 41(2):259-277.
2. Preston GM, Carroll TP, Guggino WB, Agre P. Appearance of water channels in Xenopus oocytes expressing red cell CHIP28 protein.
   Science. (1992) 17;256(5055):385-7.
3. Agre P, Sasaki S, Chrispeels MJ. Aquaporins: a family of water channel proteins. Am J Physiol. (1993) 265(3 Pt 2):F461–F461.
4. Fushimi K, Uchida S, Hara Y, Hirata Y, Marumo F, Sasaki S. Cloning and expression of apical membrane water channel of rat kidney collecting tubule. Nature. (1993) 11;361(6412):549–552.
5. Hasegawa H, Ma T, Skach W, Matthay MA, Verkman AS. Molecular cloning of a mercurial-insensitive water channel expressed in selected water-transporting tissues. J Biol Chem. (1994) 25;269(8):5497–5500.
6. Johansson I, Larsson C, Ek B, Kjellbom P. The major integral proteins of spinach leaf plasma membranes are putative aquaporins and are phosphorylated in response to Ca2+ and apoplastic water potential. Plant Cell, 8 (1996) pp. 1181–1191.
7. Sweet G, Gandor C, Voegele R, Wittekindt N, Beuerle J, Truniger V, Lin EC, Boos W. Glycerol facilitator of Escherichia coli: cloning of glpF and identification of the glpF product. J Bacteriol. (1990) 172(1):424-30.
8. Abascal F, Irisarri I, Zardoya R. Diversity and evolution of membrane intrinsic proteins. Biochim Biophys Acta. (2014) 840(5):1468-81.
9. Reizer J, Reizer A, Saier MH Jr. The MIP family of integral membrane channel proteins: sequence comparisons, evolutionary relationships, reconstructed pathway of evolution, and proposed functional differentiation of the two repeated halves of the proteins. Crit Rev Biochem Mol Biol. (1993) 28(3):235-57.
10. Richey DP, Lin EC. Importance of facilitated diffusion for effective utilization of glycerol by Escherichia coli. J Bacteriol. (1972)112(2):784-90.
11. Heller KB, Lin EC, Wilson TH: Substrate specificity and transport properties of the glycerol facilitator of Escherichia coli. J Bacteriol (1980) 144:274-278.
12. Beitz E. Aquaporin water and solute channels from malaria parasites and other pathogenic protozoa. (2006) Chem Med Chem 1:587–592.
13. Holm LM, Klaerke DA, Zeuthen T. Aquaporin 6 is permeable to glycerol and urea. Pflugers ¨Arch. (2004) 448:181–186.

14. Bienert GP, Chaumont F. Aquaporin-facilitated transmembrane diffusion of hydrogen peroxide. Biochim Biophys Acta. (2014) 1840(5):1596-604.
15. Wysocki R, Chéry CC, Wawrzycka D, Van Hulle M, Cornelis R, Thevelein JM, Tamás MJ. The glycerol channel Fps1p mediates the uptake of arsenite and antimonite in Saccharomyces cerevisiae. Mol Microbiol. (2001) 40(6):1391-401.
16. Porquet A, Filella M. Structural evidence of the similarity of Sb(OH)3 and As(OH)3 with glycerol: implications for their uptake. Chem Res Toxicol. (2007) 20:1269–1276.
17. Liu Z, Shen J, Carbrey JM, Mukhopadhyay R, Agre P, Rosen BP. Arsenite transport by mammalian aquaglyceroporins AQP7 and AQP9. Proc Natl Acad Sci USA. (2002) 99:6053–6058.
18. Gonen T, Cheng Y, Kistler J, Walz T. Aquaporin-0 membrane junctions from upon proteolytic cleavage. J Mol Biol. (2004) 342(4) 1337-45.
19. Chrispeels MJ, Agre P. Aquaporins: water channel proteins of plant and animal cells. Trends Biochem Sci. (1994) 19(10):421-5.
20. Tajkhorshid E, Nollert P, Jensen MØ, Miercke LJ, O'Connell J, Stroud RM, Schulten K. Control of the selectivity of the aquaporin water channel family by global orientational tuning. Science. (2002) 19;296(5567):525-30.
21. Tani K, Mitsuma T, Hiroaki Y, Kamegawa A, Nishikawa K, Tanimura Y, Fujiyoshi Y. Mechanism of aquaporin-4's fast and highly selective water conduction and proton exclusion. J Mol Biol. (2009) 19;389(4):694-706.
22. Newby ZE, O'Connell J 3rd, Robles-Colmenares Y, Khademi S, Miercke LJ, Stroud RM.Crystal structure of the aquaglyceroporin PfAQP from the malarial parasite Plasmodium falciparum. Nat Struct Mol Biol. (2008) 15(6):619-25.
23. Savage DF, Egea PF, Robles-Colmenares Y, O'Connell JD 3rd, Stroud RM. Architecture and selectivity in aquaporins: 2.5 a X-ray structure of aquaporin Z. PLoS Biol. (2003) 1(3):E72.
24. Sui H, Han BG, Lee JK, Walian P, Jap BK. Structural basis of water-specific transport through the AQP1 water channel. Nature. (2001) 27;414(6866):872-8.
25. Horsefield R, Nordén K, Fellert M, Backmark A, Törnroth-Horsefield S, Terwisscha van Scheltinga AC, Kvassman J, Kjellbom P, Johanson U, Neutze R. High-resolution x-ray structure of human aquaporin 5. Proc Natl Acad Sci U S A. (2008) 105(36):13327-32.
26. Törnroth-Horsefield S, Wang Y, Hedfalk K, Johanson U, Karlsson M, Tajkhorshid E, Neutze R, Kjellbom P. Structural mechanism of plant aquaporin gating. Nature. (2006) 439(7077):688-94.
27. Ma T, Song Y, Yang B, Gillespie A, Carlson EJ, Epstein CJ, Verkman AS. Nephrogenic diabetes insipidus in mice lacking aquaporin-3 water channels. Proc Natl Acad Sci U S A. (2000) 97(8):4386-91.

28. Yang B, Zhao D, Verkman AS. Hsp90 inhibitor partially corrects nephrogenic diabetes insipidus in a conditional knock-in mouse model of aquaporin-2 mutation. FASEB J. (2009) 23(2):503-12.
29. Hara-Chikuma M, Verkman AS. Prevention of skin tumorigenesis and impairment of epidermal cell proliferation by targeted aquaporin-3 gene disruption. Mol Cell Biol. (2008) (1):326-32.
30. Ma T, Song Y, Gillespie A, Carlson EJ, Epstein CJ, Verkman AS. Defective secretion of saliva in transgenic mice lacking aquaporin-5 water channels. J Biol Chem. (1999) 274(29):20071-4.
31. Kumari SS, Gandhi J, Mustehsan MH, Eren S, Varadaraj K. Functional characterization of an AQP0 missense mutation, R33C, that causes dominant congenital lens cataract, reveals impaired cell-to-cell adhesion. Exp Eye Res. (2013) 116:371-85.
32. Filippidis AS, Kalani MY, Rekate HL. Hydrocephalus and aquaporins: the role of aquaporin-4. Acta Neurochir Suppl. (2012) 113:55-8.
33. Lebeck J. Metabolic impact of the glycerol channels AQP7 and AQP9 in adipose tissue and liver. J Mol Endocrinol. (2014) 52(2):R165-78.
34. Johansson I, Karlsson M, Johanson U, Larsson C, Kjellbom P. The role of aquaporins in cellular and whole plant water balance. Biochim Biophys Acta. (2000) 1465(1-2):324-42.
35. Qian ZJ, Song JJ, Chaumont F, Ye Q. Differential responses of plasma membrane aquaporins in mediating water transport of cucumber seedlings under osmotic and salt stresses. Plant Cell Environ. (2015) 38(3):461-73.
36. Wang LL, Chen AP, Zhong NQ, Liu N, Wu XM, Wang F, Yang CL, Romero MF, Xia GX. The Thellungiella salsuginea tonoplast aquaporin TsTIP1;2 functions in protection against multiple abiotic stresses. Plant Cell Physiol. (2014) 55(1):148-61.
37. Calvo-Polanco M, Sánchez-Romera B1, Aroca R. Mild salt stress conditions induce different responses in root hydraulic conductivity of phaseolus vulgaris over-time. PLoS One. (2014) 9(3):e90631.
38. Ahamed A, Murai-Hatano M, Ishikawa-Sakurai J, Hayashi H, Kawamura Y, Uemura M. Cold stress-induced acclimation in rice is mediated by root-specific aquaporins. Plant Cell Physiol. (2012) 53(8):1445-56.
39. Mori IC, Rhee J, Shibasaka M, Sasano S, Kaneko T, Horie T, Katsuhara M. CO2 transport by PIP2 aquaporins of barley. Plant Cell Physiol. (2014) 55(2):251-7.
40. Uehlein N, Lovisolo C, Siefritz F, Kaldenhoff R. The tobacco aquaporin NtAQP1 is a membrane CO2 pore with physiological functions. Nature. (2003) 425(6959):734-7.
41. Sade N, Gebretsadik M, Seligmann R, Schwartz A, Wallach R, Moshelion M. The role of tobacco Aquaporin1 in improving water use efficiency, hydraulic

conductivity, and yield production under salt stress. Plant Physiol. (2010) 152(1):245-54.

42. Przedpelska-Wasowicz EM, Wierzbicka M. Gating of aquaporins by heavy metals in Allium cepa L. epidermal cells. Protoplasma. (2011) 248(4):663-71.
43. Ma JF, Yamaji N, Mitani N, Xu XY, Su YH, McGrath SP, Zhao FJ. Transporters of arsenite in rice and their role in arsenic accumulation in rice grain. Proc Natl Acad Sci U S A. (2008) 105(29):9931-5.
44. Negishi T, Oshima K, Hattori M, Kanai M, Mano S, Nishimura M, Yoshida K. Tonoplast- and plasma membrane-localized aquaporin-family transporters in blue hydrangea sepals of aluminum hyperaccumulating plant. PLoS One. (2012) 7(8):e43189.
45. Verdoucq L, Grondin A, Maurel C. Structure-function analysis of plant aquaporin AtPIP2;1 gating by divalent cations and protons. Biochem J. (2008) 415(3):409-16.
46. Yukutake Y1, Hirano Y, Suematsu M, Yasui M. Rapid and reversible inhibition of aquaporin-4 by zinc. Biochemistry. (2009) 48(51):12059-61.[
47. Gunnarson E, Zelenina M, Aperia A. Regulation of brain aquaporins. Neuroscience. (2004) 129(4):947-55.
48. Frick A, Järvå M, Ekvall M, Uzdavinys P, Nyblom M, Törnroth-Horsefield S. Mercury increases water permeability of a plant aquaporin through a non-cysteine-related mechanism. Biochem J. (2013) 454(3):491-9.
49. Alleva K, Niemietz CM, Sutka M, Maurel C, Parisi M, Tyerman SD, Amodeo G. Plasma membrane of Beta vulgaris storage root shows high water channel activity regulated by cytoplasmic pH and a dual range of calcium concentrations. J Exp Bot. (2006) ;57(3):609-21.
50. Schnurbusch T, Hayes J, Hrmova M, Baumann U, Ramesh SA, Tyerman SD, Langridge P, Sutton T. Boron toxicity tolerance in barley through reduced expression of the multifunctional aquaporin HvNIP2;1. Plant Physiol. (2010) 153 (4):1706-15.
51. Yamaji N, Ma JF. Spatial distribution and temporal variation of the rice silicon transporter Lsi1. Plant Physiol. (2007) 143(3):1306-13.
52. Li C, Wang W. Urea transport mediated by aquaporin water channel proteins. Subcell Biochem. (2014) 73:227-65.
53. Zhou S, Hu W, Deng X, Ma Z, Chen L, Huang C, Wang C, Wang J, He Y, Yang G, He G. Overexpression of the wheat aquaporin gene, TaAQP7, enhances drought tolerance in transgenic tobacco. PLoS One. (2012) 7(12):e52439.
54. Walz T, Fujiyoshi Y, Engel A. The AQP structure and functional implications. Handb Exp Pharmacol. (2009) 190:31-56.
55. de Groot BL, Grubmüller H. The dynamics and energetics of water permeation and proton exclusion in aquaporins. Curr Opin Struct Biol. (2005) 15(2):176-83.

56. Lee JK, Khademi S, Harries W, Savage D, Miercke L, Stroud RM. Water and glycerol permeation through the glycerol channel GlpF and the aquaporin family. J Synchrotron Radiat. (2004) 11(Pt 1):86-8.

57. Li H, Chen H, Steinbronn C, Wu B, Beitz E, Zeuthen T, Voth GA. Enhancement of proton conductance by mutations of the selectivity filter of aquaporin-1. J Mol Biol. (2011) 407(4):607-20.

58. Beitz E, Wu B, Holm LM, Schultz JE, Zeuthen T. Point mutations in the aromatic/arginine region in aquaporin 1 allow passage of urea, glycerol, ammonia, and protons. Proc Natl Acad Sci U S A. (2006) 103(2):269-74.

59. Anthony TL, Brooks HL, Boassa D, Leonov S, Yanochko GM, Regan JW, Yool AJ. Cloned human aquaporin-1 is a cyclic GMP-gated ion channel. Mol Pharmacol. (2000) 57(3):576-88.

60. Murata K, Mitsuoka K, Hirai T, Walz T, Agre P, Heymann JB, Engel A, Fujiyoshi Y. Structural determinants of water permeation through aquaporin-1. Nature. (2000) 407(6804):599-605.

61. Johanson U, Gustavsson S. A new subfamily of major intrinsic proteins in plants. Mol Biol Evol. (2002) 19(4):456-61.

62. Anderberg HI, Kjellbom P, Johanson U. Annotation of Selaginella moellendorffii Major Intrinsic Proteins and the Evolution of the Protein Family in Terrestrial Plants. Front Plant Sci. (2012) 20;3:33.

63. R. Zardoya, X. Ding, Y. Kitagawa, M.J. Chrispeels. Origin of plant glycerol transporters by horizontal gene transfer and functional recruitment. Proc. Natl. Acad. Sci., 99 (2002), pp. 14893–14896.

64. Perez Di Giorgio J, Soto G, Alleva K, Jozefkowicz C, Amodeo G, Muschietti JP, Ayub ND. Prediction of aquaporin function by integrating evolutionary and functional analyses. J Membr Biol. (2014) 247(2):107-25.

65. G. Soto, K. Alleva, G. Amodeo, J. Muschietti, N.D. Ayub. New insight into the evolution of aquaporins from flowering plants and vertebrates: orthologous identification and functional transfer is possible. Gene, 503 (2012), pp. 165–176.

66. J.H. Danielson, U. Johanson. Phylogeny of major intrinsic proteins. T. Jahn, G. Bienert (Eds.), MIPs and Their Role in the Exchange of Metalloids, vol. 679Springer, New York (2010), pp. 19–31.

67. Kjellbom P, Larsson C, Johansson I I, Karlsson M, Johanson U. Aquaporins and water homeostasis in plants. Trends Plant Sci. 1999 Aug;4(8):308-314.

68. Yaneff A, Sigaut L, Marquez M, Alleva K, Pietrasanta LI, Amodeo G. Heteromerization of PIP aquaporins affects their intrinsic permeability. Proc Natl Acad Sci U S A. (2014) 111(1):231-6.

69. J. Danielson, U. Johanson. Unexpected complexity of the aquaporin gene family in the moss Physcomitrella patens. BMC Plant Biol., 8 (2008), pp. 1–15.

70. di Pietro M, Vialaret J, Li GW, Hem S, Prado K, Rossignol M, Maurel C, Santoni V. Coordinated post-translational responses of aquaporins to abiotic and nutritional stimuli in Arabidopsis roots. Mol Cell Proteomics. (2013) 12(12):3886-97.
71. Tournaire-Roux C, Sutka M, Javot H, Gout E, Gerbeau P, Luu DT, Bligny R, Maurel C. Cytoplasmic pH regulates root water transporting during anoxic stress through gating of aquaporins. Nature. (2003) 25;425(6956):393-7.
72. Johansson I, Karlsson M, Shukla VK, Chrispeels MJ, Larsson C, Kjellbom P.Water transport activity of the plasma membrane aquaporin PM28A is regulated by phosphorylation. Plant Cell. (1998) 10(3):451-9.
73. Daniels MJ, Yeager M. Phosphorylation of aquaporin PvTIP3;1 defined by mass spectrometry and molecular modeling. Biochemistry. (2005) 44(44):14443-54.
74. Azad AK, Katsuhara M, Sawa Y, Ishikawa T, Shibata H. Characterization of four plasma membrane aquaporins in tulip petals: a putative homolog is regulated by phosphorylation. Plant Cell Physiol. (2008) 49(8):1196-208.
75. Von Bülow J, Golldack A, Albers T, Beitz E. The amoeboidal Dictyostelium aquaporin AqpB is gated via Tyr216 and aqpB gene deletion affects random cell motility. Biol Cell. (2015) 107(3):78-88.
76. Prak S, Hem S, Boudet J, Viennois G, Sommerer N, Rossignol M, Maurel C, Santoni V. Multiple phosphorylations in the C-terminal tail of plant plasma membrane aquaporins: role in subcellular trafficking of AtPIP2;1 in response to salt stress. Mol Cell Proteomics. (2008) 6):1019-30.
77. Chevalier AS, Bienert GP, Chaumont F. A new LxxxA motif in the transmembrane Helix3 of maize aquaporins belonging to the plasma membrane intrinsic protein PIP2 group is required for their trafficking to the plasma membrane. Plant Physiol. (2014) 166(1):125-38.
78. Hsu JL, Wang LY, Wang SY, Lin CH, Ho KC, Shi FK, Chang IF. Functional phosphoproteomic profiling of phosphorylation sites in membrane fractions of salt-stressed Arabidopsis thaliana. Proteome Sci. (2009) 10;7:42.
79. Whiteman SA, Nühse TS, Ashford DA, Sanders D, Maathuis FJ. A proteomic and phosphoproteomic analysis of Oryza sativa plasma membrane and vacuolar membrane. Plant J. (2008) 56(1):146-56.
80. Takase T, Ishikawa H, Murakami H, Kikuchi J, Sato-Nara K, Suzuki H. The circadian clock modulates water dynamics and aquaporin expression in Arabidopsis roots. Plant Cell Physiol. (2011) 52(2):373-83.
81. Sjövall-Larsen S, Alexandersson E, Johansson I, Karlsson M, Johanson U, Kjellbom P. Purification and characterization of two protein kinases acting on the aquaporin SoPIP2;1. Biochim Biophys Acta. (2006) 1758(8):1157-64
82. Johansson I, Karlsson M, Shukla VK, Chrispeels MJ, Larsson C, Kjellbom P. Water transport activity of the plasma membrane aquaporin PM28A is regulated by phosphorylation. Plant Cell. (1998) 10(3):451-9.

83. Törnroth-Horsefield S, Wang Y, Hedfalk K, Johanson U, Karlsson M, Tajkhorshid E, Neutze R, Kjellbom P. Structural mechanism of plant aquaporin gating. Nature. (2006) 439(7077):688-94.
84. Nyblom M, Frick A, Wang Y, Ekvall M, Hallgren K, Hedfalk K, Neutze R, Tajkhorshid E, Törnroth-Horsefield S. Structural and functional analysis of SoPIP2;1 mutants adds insight into plant aquaporin gating. J Mol Biol. (2009) 387(3):653-68.
85. Harries WE, Akhavan D, Miercke LJ, Khademi S, Stroud RM. The channel architecture of aquaporin 0 at a 2.2-A resolution. Proc Natl Acad Sci U S A. (2004) 101(39):14045-50.
86. Macey RI. Transport of water and urea in red blood cells. Am J Physiol. (1984) 246(3 Pt 1):C195-203.
87. Savage DF, Stroud RM. Structural basis of aquaporin inhibition by mercury. J Mol Biol. (2007) 368(3):607-17.
88. Kuwahara M, Gu Y, Ishibashi K, Marumo F, Sasaki S. Mercury-sensitive residues and pore site in AQP3 water channel. Biochemistry. (1997) 36(46):13973-8.
89. Nicchia GP, Frigeri A, Liuzzi GM, Santacroce MP, Nico B, Procino G, Quondamatteo F, Herken R, Roncali L, Svelto M. Aquaporin-4-containing astrocytes sustain a temperature- and mercury-insensitive swelling in vitro. Glia. (2000) 31(1):29-38.
90. Bienert GP, Cavez D, Besserer A, Berny MC, Gilis D, Rooman M, Chaumont F. A conserved cysteine residue is involved in disulfide bond formation between plant plasma membrane aquaporin monomers. Biochem J. (2012) 445(1):101-11.
91. Hazama A, Kozono D, Guggino WB, Agre P, Yasui M. Ion permeation of AQP6 water channel protein. Single channel recordings after Hg2+ activation. J Biol Chem. (2002) 277(32):29224-30.
92. Secchi F, MacIver B, Zeidel ML, Zwieniecki MA. Functional analysis of putative genes encoding the PIP2 water channel subfamily in Populus trichocarpa. Tree Physiol. (2009) 29(11):1467-77.
93. Montell C, Rubin GM. Molecular characterization of the Drosophila trp locus: a putative integral membrane protein required for phototransduction. Neuron. (1989) (4):1313-23.
94. Zheng J. Molecular mechanism of TRP channels. Compr Physiol. (2013) (1):221-42.
95. Pedersen SF, Owsianik G, Nilius B. TRP channels: an overview. Cell Calcium. (2005) 38(3-4):233-52.
96. Dong XP, Wang X, Xu H. TRP channels of intracellular membranes. J Neurochem. (2010) 113(2):313-28.

97. Cordero-Morales JF, Gracheva EO, Julius D. Cytoplasmic ankyrin repeats of transient receptor potential A1 (TRPA1) dictate sensitivity to thermal and chemical stimuli. Proc Natl Acad Sci U S A. (2011) 108(46):E1184-91.

98. Phelps CB, Huang RJ, Lishko PV, Wang RR, Gaudet R. Structural analyses of the ankyrin repeat domain of TRPV6 and related TRPV ion channels. Biochemistry. (2008) 47(8):2476-84.

99. Sladek CD, Johnson AK. Integration of thermal and osmotic regulation of water homeostasis: the role of TRPV channels. Am J Physiol Regul Integr Comp Physiol. (2013) 305(7):R669-78.

100. Nilius B, Owsianik G. The transient receptor potential family of ion channels. Genome Biol. (2011) 12(3):218.

101. Chang Y, Schlenstedt G, Flockerzi V, Beck A. Properties of the intracellular transient receptor potential (TRP) channel in yeast, Yvc1. FEBS Lett. (2010) 584(10):2028-32.

102. Freichel M, Vennekens R, Olausson J, Stolz S, Philipp SE, Weissgerber P, Flockerzi V. Functional role of TRPC proteins in native systems: implications from knockout and knock-down studies. J Physiol. (2005) 567(Pt 1):59-66.

103. Jiang LH. Subunit interaction in channel assembly and functional regulation of transient receptor potential melastatin (TRPM) channels. Biochem Soc Trans. (2007) 35(Pt 1):86-8.

104. Xiao R, Zhang B, Dong Y, Gong J, Xu T, Liu J, Xu XZ. A genetic program promotes C. elegans longevity at cold temperatures via a thermosensitive TRP channel. Cell. (2013) 152 (4):806-17.

105. Xiao R, Xu XZ. Function and regulation of TRP family channels in C. elegans. Pflugers Arch. (2009) 458(5):851-60.

106. Retailleau K, Duprat F. Polycystins and partners: proposed role in mechanosensitivity. J Physiol. (2014) 592(Pt 12):2453-71.

107. Kiselyov K, Colletti GA, Terwilliger A, Ketchum K, Lyons CW, Quinn J, Muallem S. TRPML: transporters of metals in lysosomes essential for cell survival? Cell Calcium. (2011) 50(3):288-94.

108. Zygmunt PM, Högestätt ED. TRPA1. Handb Exp Pharmacol. (2014) ;222:583-630.

109. Kang K, Pulver SR, Panzano VC, Chang EC, Griffith LC, Theobald DL, Garrity PA. Analysis of Drosophila TRPA1 reveals an ancient origin for human chemical nociception. Nature. (2010) 464(7288):597-600.

110. Kriz W. TRPC6 - a new podocyte gene involved in focal segmental glomerulosclerosis. Trends Mol Med. (2005) 11(12):527-30.

111. Rock MJ, Prenen J, Funari VA, Funari TL, Merriman B, Nelson SF, Lachman RS, Wilcox WR, Reyno S, Quadrelli R, Vaglio A, Owsianik G, Janssens A, Voets T,

Ikegawa S, Nagai T, Rimoin DL, Nilius B, Cohn DH. Gain-of-function mutations in TRPV4 cause autosomal dominant brachyolmia. Nat Genet. (2008) 40(8):999-1003.

112. Audo I, Kohl S, Leroy BP, Munier FL, Guillonneau X, Mohand-Saïd S, Bujakowska K, Nandrot EF, Lorenz B, Preising M, Kellner U, Renner AB, Bernd A, Antonio A, Moskova-Doumanova V, Lancelot ME, Poloschek CM, Drumare I, Defoort-Dhellemmes S, Wissinger B, Léveillard T, Hamel CP, Schorderet DF, De Baere E, Berger W, Jacobson SG, Zrenner E, Sahel JA, Bhattacharya SS, Zeitz C. TRPM1 is mutated in patients with autosomal-recessive complete congenital stationary night blindness. Am J Hum Genet. (2009) 85(5):720-9.

113. Kruse M, Schulze-Bahr E, Corfield V, Beckmann A, Stallmeyer B, Kurtbay G, Ohmert I, Schulze-Bahr E, Brink P, Pongs O. Impaired endocytosis of the ion channel TRPM4 is associated with human progressive familial heart block type I. J Clin Invest. (2009) 119(9):2737-44.

114. Walder RY, Landau D, Meyer P, Shalev H, Tsolia M, Borochowitz Z, Boettger MB, Beck GE, Englehardt RK, Carmi R, Sheffield VC. Mutation of TRPM6 causes familial hypomagnesemia with secondary hypocalcemia. Nat Genet. (2002) 31(2):171-4.

115. Barbagallo B, Garrity PA. Temperature sensation in Drosophila. Curr Opin Neurobiol. (2015); 34 C: 8-13.

116. Saito S, Nakatsuka K, Takahashi K, Fukuta N, Imagawa T, Ohta T, Tominaga M. Analysis of transient receptor potential ankyrin 1 (TRPA1) in frogs and lizards illuminates both nociceptive heat and chemical sensitivities and coexpression with TRP vanilloid 1 (TRPV1) in ancestral vertebrates. J Biol Chem. 2012 Aug 31;287(36):30743-54.

117. Wang G, Qiu YT, Lu T, Kwon HW, Pitts RJ, Van Loon JJ, Takken W, Zwiebel LJ. Anopheles gambiae TRPA1 is a heat-activated channel expressed in thermosensitive sensilla of female antennae. Eur J Neurosci. (2009) 30(6):967-74.

118. Bandell M, Story GM, Hwang SW, Viswanath V, Eid SR, Petrus MJ, Earley TJ, Patapoutian A. Noxious cold ion channel TRPA1 is activated by pungent compounds and bradykinin. Neuron. (2004) 41(6):849-57.

119. Story GM, Peier AM, Reeve AJ, Eid SR, Mosbacher J, Hricik TR, Earley TJ, Hergarden AC, Andersson DA, Hwang SW, McIntyre P, Jegla T, Bevan S, Patapoutian A. ANKTM1, a TRP-like channel expressed in nociceptive neurons, is activated by cold temperatures. Cell. (2003) 112(6):819-29.

120. Chen J, Kang D, Xu J, Lake M, Hogan JO, Sun C, Walter K, Yao B, Kim D. Species differences and molecular determinant of TRPA1 cold sensitivity. Nat Commun. (2013) ;4:2501.

121. Venkatachalam K, Luo J, Montell C. Evolutionarily conserved, multitasking TRP channels: lessons from worms and flies. Handb Exp Pharmacol. (2014) ;223:937-62.

122. Tracey WD Jr, Wilson RI, Laurent G, Benzer S. painless, a Drosophila gene essential for nociception. Cell. (2003) 113(2):261-73.

123. Lee Y, Lee Y, Lee J, Bang S, Hyun S, Kang J, Hong ST, Bae E, Kaang BK, Kim J. Pyrexia is a new thermal transient receptor potential channel endowing tolerance to high temperatures in Drosophila melanogaster. Nat Genet. (2005) 37(3):305-10.

124. Hamada FN, Rosenzweig M, Kang K, Pulver SR, Ghezzi A, Jegla TJ, Garrity PA. An internal thermal sensor controlling temperature preference in Drosophila. Nature. (2008) 454(7201):217-20.

125. Zhong L, Bellemer A, Yan H, Ken H, Jessica R, Hwang RY, Pitt GS, Tracey WD. Thermosensory and nonthermosensory isoforms of Drosophila melanogaster TRPA1 reveal heat-sensor domains of a thermoTRP Channel. Cell Rep. (2012) 1(1):43-55.

126. Wang, H., Schupp, M., Zurborg, S. & Heppenstall, P. A. Residues in the pore region of Drosophila transient receptor potential A1 dictate sensitivity to thermal stimuli. The Journal of physiology (2013) ; 591, 185-201.

127. Brauchi S, Orta G, Salazar M, Rosenmann E, Latorre R. A hot-sensing cold receptor: C-terminal domain determines thermosensation in transient receptor potential channels. J Neurosci. (2006) 26(18):4835-40.

128. Jabba S, Goyal R, Sosa-Pagán JO, Moldenhauer H, Wu J, Kalmeta B, Bandell M, Latorre R2 Patapoutian A, Grandl J. Directionality of temperature activation in mouse TRPA1 ion channel can be inverted by single-point mutations in ankyrin repeat six. Neuron. (2014) 82(5):1017-31

129. Montell C. The TRP superfamily of cation channels. Sci TKE. (2005); 2005(272):re3.Reviw.

130. Peier AM, Moqrich A, Hergarden AC, Reeve AJ, Andersson DA, Story GM, Earley TJ, Dragoni I, McIntyre P, Bevan S, Patapoutian A. A TRP channel that senses cold stimuli and menthol. Cell. (2002) 108(5):705-15.

131. Lee Y, Montell C. Drosophila TRPA1functions in temperature control of circadian rhythm in pacemaker neurons. J Neurosci. (2013) 33(16):6716-25.

132. Liu C, Zwiebel LJ. Molecular characterization of larval peripheral thermosensory responses of the malaria vector mosquito Anopheles gambiae. PLoS One. (2013) 8(8):e72595.

133. Kwon Y, Kim SH, Ronderos DS, Lee Y, Akitake B, Woodward OM, Guggino WB, Smith DP, Montell C. Drosophila TRPA1 channel is required to avoid the naturally occurring insect repellent citronellal. Curr Biol. 2010 Sep 28;20(18):1672-8.

134. Macpherson LJ, Dubin AE, Evans MJ, Marr F, Schultz PG, Cravatt BF, Patapoutian A. Noxious compounds activate TRPA1 ion channels through covalent modification of cysteines. Nature. (2007) 445(7127):541-5.

135. Hinman A, Chuang HH, Bautista DM, Julius D. TRP channel activation by reversible covalent modification. Proc Natl Acad Sci U S A. (2006) 103(51) 19564-8.

136. Wang L, Cvetkov TL, Chance MR, Moiseenkova-Bell VY. Identification of in vivo disulfide conformation of TRPA1 ion channel. J Biol Chem. (2012) 287(9):6169–6176.

137. Kindt KS, Viswanath V, Macpherson L, Quast K, Hu H, Patapoutian A, Schafer WR. Caenorhabditis elegans TRPA-1 functions in mechanosensation. Nat Neurosci. (2007) 10(5):568-77.

138. Tracey WD, Wilson RI, Laurent G, Benzer S. painless, a Drosophila gene essential for nociception. Cell. (2003) 113:261–273.

139. Liu L, Li Y, Wang R, Yin C, Dong Q, Hing H, Kim C, Welsh MJ. Drosophila hygrosensation requires the TRP channels water witch and nanchung. Nature. (2007) 450:294–298.

140. Johnson WA, Carder JW. Drosophila nociceptors mediate larval aversion to dry surface environments utilizing both the Painless TRP channel and the DEG/ENaC subunit, PPK1. PLoS One. (2012) 7:e32878.

141. Takahashi N, Kuwaki T, Kiyonaka S, Numata T, Kozai D, Mizuno Y, Yamamoto S, Naito S, Knevels E, Carmeliet P, Oga T, Kaneko S, Suga S, Nokami T, Yoshida J, Mori Y. TRPA1 underlies a sensing mechanism for O2. Nat Chem Biol. (2011) 7(10):701-11.

142. Hatano N, Itoh Y, Suzuki H, Muraki Y, Hayashi H, Onozaki K, Wood IC, Beech DJ, Muraki K. Hypoxia-inducible factor-1α (HIF1α) switches on transient receptor potential ankyrin repeat 1 (TRPA1) gene expression via a hypoxia response element-like motif to modulate cytokine release. J Biol Chem. (2012) 287(38):31962-72.

143. Shimizu S, Takahashi N, Mori Y. TRPs as chemosensors (ROS, RNS, RCS, gasotransmitters). Handb Exp Pharmacol. (2014) 223:767-94.

144. Karashima Y, Damann N, Prenen J, Talavera K, Segal A, Voets T, Nilius B. Bimodal action of menthol on the transient receptor potential channel TRPA1. J Neurosci. (2007) 27(37):9874-84.

145. Xiao B, Dubin AE, Bursulaya B, Viswanath V, Jegla TJ, Patapoutian A. Identification of transmembrane domain 5 as a critical molecular determinant of menthol sensitivity in mammalian TRPA1 channels. J Neurosci. (2008) 28(39):9640-51.

146. Leffler A, Lattrell A, Kronewald S, Niedermirtl F, Nau C. Activation of TRPA1 by membrane permeable local anesthetics. Mol Pain. (2011) 7:62.

147. Jordt SE, Bautista DM, Chuang HH, McKemy DD, Zygmunt PM, Högestätt ED, Meng ID, Julius D. Mustard oils and cannabinoids excite sensory nerve fibres through the TRP channel ANKTM1. Nature. (2004) 427(6971):260-5.

148. Yang F1, Cui Y, Wang K, Zheng J. Thermosensitive TRP channel pore turret is part of the temperature activation pathway. Proc Natl Acad Sci U S A. (2010) 107(15):7083-8.

149. Lishko PV, Procko E, Jin X, Phelps CB, Gaudet R. The ankyrin repeats of TRPV1 bind multiple ligands and modulate channel sensitivity. Neuron. (2007) 54(6):905-18.

150. McCleverty CJ, Koesema E, Patapoutian A, Lesley SA, Kreusch A. Crystal structure of the human TRPV2 channel ankyrin repeat domain. Protein Sci. (2006) 15:2201–2206.

151. Moiseenkova-Bell VY1, Stanciu LA, Serysheva II, Tobe BJ, Wensel TG. Structure of TRPV1 channel revealed by electron cryomicroscopy. Proc Natl Acad Sci U S A. (2008) 105(21):7451-5.

152. Moiseenkova-Bell V, Wensel TG. Functional and structural studies of TRP channels heterologously expressed in budding yeast. Adv Exp Med Biol. (2011) 704:25-40.

153. Liao M, Cao E, Julius D, Cheng Y. Structure of the TRPV1 ion channel determined by electron cryo-microscopy. Nature. (2013) 504(7478):107-12.

154. Cao E, Liao M, Cheng Y, Julius D. TRPV1 structures in distinct conformations reveal activation mechanisms. Nature. (2013) 504(7478):113-8.

155. Paulsen CE, Armache JP, Gao Y, Cheng Y, Julius D. Structure of the TRPA1 ion channel suggests regulatory mechanisms. Nature. (2015)

156. Brown JH, Cohen C, Parry DA. Heptad breaks in alpha-helical coiled coils: stutters and stammers. Proteins. (1996) 26(2):134-45.

157. Kim D, Cavanaugh EJ. Requirement of a soluble intracellular factor for activation of transient receptor potential A1 by pungent chemicals: role of inorganic polyphosphates. J Neurosci. (2007) 13;27(24):6500-9.

158. Teale F.W.J, G. Weber. Ultraviolet fluorescence of the aromatic amino acids. Biochem. J. (1957) 65:476–482.

159. Swaminathan R, Krishnamoorthy G, Periasamy N. Similarity of fluorescence lifetime distributions for single tryptophan proteins in the random coil state. Biophys. J. (1994) 67:2013–2023.

160. Gudgin E, Lopez-Delgado R, Ware W.R. The tryptophan fluorescence lifetime puzzle. A study of decay times in aqueous solution as a function of pH and buffer composition. Can. J. Chem. (1981) 59:1037–1044.

161. Matias Moller and Ana Denicola. Protein tryptophan accessibility studied by fluorescence Quenching. Biochemistry and Molecular Biology Education. (2002) Vol. 30 (3) 175–178.

162. Kreir M, Farre C, Beckler M, George M, Fertig N. Rapid screening of membrane protein activity: electrophysiological analysis of OmpF reconstituted in proteoliposomes. Lab Chip (2008) 8(4):587 – 595.

Paper I

OPEN ACCESS Freely available online

PLoS one

Structure and Stability of the Spinach Aquaporin SoPIP2;1 in Detergent Micelles and Lipid Membranes

Inés Plasencia[1]*, Sabeen Survery[2], Sania Ibragimova[3,5], Jesper S. Hansen[4,5], Per Kjellbom[2], Claus Helix-Nielsen[3,5], Urban Johanson[2], Ole G. Mouritsen[1]

1 Department of Physics and Chemistry, MEMPHYS-Center for Biomembrane Physics, University of Southern Denmark, Odense, Denmark, **2** Department of Biochemistry and Structural Biology, Center for Molecular Protein Science, Lund University, Lund, Sweden, **3** DTU Physics, Technical University of Denmark, Lyngby, Denmark, **4** DTU Nanotech, Technical University of Denmark, Lyngby, Denmark, **5** Aquaporin A/S, Copenhagen, Denmark

Abstract

Background: SoPIP2;1 constitutes one of the major integral proteins in spinach leaf plasma membranes and belongs to the aquaporin family. SoPIP2;1 is a highly permeable and selective water channel that has been successfully overexpressed and purified with high yields. In order to optimize reconstitution of the purified protein into biomimetic systems, we have here for the first time characterized the structural stability of SoPIP2;1.

Methodology/Principal Finding: We have characterized the protein structural stability after purification and after reconstitution into detergent micelles and proteoliposomes using circular dichroism and fluorescence spectroscopy techniques. The structure of SoPIP2;1 was analyzed either with the protein solubilized with octyl-β-D-glucopyranoside (OG) or reconstituted into lipid membranes formed by *E. coli* lipids, diphytanoylphosphatidylcholine (DPhPC), or reconstituted into lipid membranes formed from mixtures of 1-palmitoyl-2-oleoyl-phosphatidylcholine (POPE), 1-palmitoyl-2oleoyl-phosphatidylethanolamine (POPE), 1-palmitoyl-2-oleoyl-phosphatidylserine (POPS), and ergosterol. Generally, SoPIP2;1 secondary structure was found to be predominantly α-helical in accordance with crystallographic data. The protein has a high thermal structural stability in detergent solutions, with an irreversible thermal unfolding occurring at a melting temperature of 58°C. Incorporation of the protein into lipid membranes increases the structural stability as evidenced by an increased melting temperature of up to 70°C.

Conclusion/Significance: The results of this study provide insights into SoPIP2;1 stability in various host membranes and suggest suitable choices of detergent and lipid composition for reconstitution of SoPIP2;1 into biomimetic membranes for biotechnological applications.

Citation: Plasencia I, Survery S, Ibragimova S, Hansen JS, Kjellbom P, et al. (2011) Structure and Stability of the Spinach Aquaporin SoPIP2;1 in Detergent Micelles and Lipid Membranes. PLoS ONE 6(2): e14674. doi:10.1371/journal.pone.0014674

Editor: Maria Moran, Hospital 12 Octubre Madrid, Spain

Received July 2, 2010; **Accepted** December 23, 2010; **Published** February 14, 2011

Funding: This study has been undertaken in the MEMBAQ project (Incorporation of Aquaporins in Membranes for Industrial Applications) supported by the Sixth European Research Framework Programme under contract [NMP4-CT-2006-033234] and the Danish National Advanced Technology Foundation (Industrial biomimetic water membranes) under contract [023-2007-1]. MEMPHYS-Center for Biomembrane Physics is supported by the Danish National Research Foundation. Financial support was also provided by Formas and the Swedish Research Council (VR). The funding agencies had no role in study design, data collection and analysis, decision to publish or preparation of the manuscript.

Competing Interests: The authors have declared that no competing interests exist.

* E-mail: miplsen@memphys.sdu.dk

Introduction

MIPs (major intrinsic proteins) are found in eubacteria, archae, fungi, plants and animals [1]. According to substrate specificity, MIPs are mainly classified into AQPs (aquaporins - or water channels) if they are only permeable to water, or GLPs (aquaglyceroporins - or glycerol-uptake facilitators) if they also facilitate passive diffusion of small solutes such as glycerol or urea [2,3]. In addition, a structural role in the formation of cell junctions has been described for some MIPs [4].

Most members of the aquaporin super family have molecular masses, ranging from 25 to 31 kDa. The three-dimensional structures of several MIPs have been determined [5–7], and the quaternary structures of the proteins reveal that they all form homotetramers where each monomer acts as a functional unit [2]. Based on sequence similarity, the functional unit of all members in this family are predicted to have six hydrophobic, membrane-spanning α-helices connected by five loops of variable length that delimit a polar channel with two wide vestibules and a narrow pore [8,9]. Two of the connecting loops, namely B and E, interact with each other from opposite sides through two highly conserved NPA (Asn-Pro-Ala) motifs forming a seventh transmembrane region that contributes to the pore region [10]. Highly conserved residues that stabilize the structure are found in the helices, e.g. the transmembrane helix-helix packing motif GXXXG [11], as well as conserved polar and charged buried residues that have been proposed to form hydrogen bonds and ion pairs [12].

Plants encode a very large and diverse MIP family. They have been classified into at least five subfamilies in higher plants: plasma membranes intrinsic proteins (PIPs), tonoplast intrinsic proteins (TIPs), the small basic intrinsic proteins (SIPs), NOD26-like intrinsic proteins (NIPs), and the recently discovered X intrinsic

protein (XIPs) [13,14]. PIPs form the most highly conserved subfamily in plants and are further divided into two groups named PIP1 and PIP2 [15]. In addition to several single amino acid residue substitutions, PIP2s are characterized by a short N-terminal and a longer C-terminal relative to PIP1s [16]. Moreover, differences are found in the water transport activity in oocytes where PIP2s are more active than PIP1s [16]. It has been suggested that PIP2s are specific for water, whereas PIP1s have been reported to facilitate the transport of solutes such as glycerol, boric acid, urea, and carbon dioxide in addition to water [17–19].

The spinach (*Spinacia oleracea*) genome contains at least three PIP1 and four PIP2 genes [20]. Recently, a new nomenclature which reflects the phylogenetic classification of plants MIP genes and proteins has been adopted [14]. In accordance with this nomenclature, the spinach PIPs PM28A, PM28B and PM28C have been renamed SoPIP2;1, SoPIP1;1 and SoPIP1;2, respectively. SoPIP2;1 can be overexpressed and purified with high yields [21] and its structure has been solved with Angstrom resolution [5,22]. However, the structural stability parameters of SoPIP2;1 have not been examined neither when solubilized by detergents nor after the protein reconstitution into membranes subsequent to the heterologous expression.

Due to the fact that the transport characteristics of SoPIP2;1 is well described (e.g. from protein reconstitution into oocytes and *E. coli* membranes [23]) it is a good candidate for being used in technological applications, and the high selectivity and water permeability of SoPIP2;1 makes it particularly interesting for a biomimetic water filtration technology. AQP mediated water transport is a prominent example of how Nature itself has developed an effective mechanism for purifying water, and many technologies based on biomimetic membrane transport is now attracting considerable interest (for a review see [24]). However, successful reconstitution and stabilization of functional proteins in biomimetic membranes depends on suitable choices of both detergent and host lipid membrane components.

Detergents are commonly used to solubilize membrane proteins, and many membrane proteins have been solubilized with various detergents without the loss of biological activity [25]. Sugar-based detergents and poly(oxyethylen)-based detergents are at presently the most commonly used. In the particular case of SoPIP2;1 different detergents like octyl-β-D-thioglucopyranide (OTG) and octyl-β-D-glucopyranoside (OG) have been used. We encountered problems with protein stability using OTG, presumably related to the low solubility of OTG at low temperatures, leading to aggregation of the protein under these conditions. Consequently we performed our work using OG micelles where no stability problems occurred with any of the preparations used in this work.

One of the major challenges in designing biomimetic systems based on integral membrane proteins is the reconstitution of the proteins into the membrane. A common strategy involves the incorporation of detergent solubilized proteins into vesicles followed by detergent extraction. The detergent-free vesicles are then fused with a receiving membrane. Typical lipid species for fusogenic vesicles are palmitoyl-oleoyl-phosphatidylethanolamine (POPE) -phosphatidylcholine (POPC) and -phosphatidylserine (POPS) lipids supplied with sterols e.g. ergosterol [26]. Other common lipids for biomimetic membranes are *E. coli* lipid extracts and diphytanoylphosphatidylcholine (DPhPC). In this study we examine SoPIP2;1 stability in four different membrane systems: *E. coli* lipids, DPhPC, POPE: POPC: POPS:ergosterol and POPE: POPC mixtures.

In this paper we present results from an extended secondary and ternary structural characterization of the protein in detergent micelles and in lipid membranes using spectroscopic techniques. Specifically we study the thermal secondary structure stability of SoPIP2;1 when reconstituted in detergent micelles or in lipid membranes using a detailed analysis by Circular Dichroism spectroscopy. In addition we performed Emission Fluorescent spectroscopy analysis of the six tryptophan (Trp) amino acids present in the primary sequence of SoPIP2;1 in order to obtain information about the thermal ternary structure stability of the protein.

Results

First we characterize the folding patterns for SoPIP2;1 in detergent and lipid. Then we characterized the thermal stability of SoPIP2;1 secondary and tertiary structure.

SoPIP2;1 α-helical content in different systems

The far-UV CD spectra of SoPIP2;1 dissolved in PBS with 1% OG display the characteristics of a predominantly α-helical protein with negative bands around 209 nm and 222 nm (Figure 1, full line). The deconvolution analysis reported a α-helix content of 63% (Table 1). This value matches perfectly with the one obtained after the analysis of the PDB file 1Z98 from the X-ray diffraction data of this protein [22]. Although light scattering tend to flatten out the CD spectra obtained from protein in lipid vesicles making a direct comparison to micelles difficult, the characteristic α-helical structure for aquaporins is rather well preserved when the SoPIP2;1 is reconstituted in lipid complex membranes of *E. coli* lipids (Figure 1 and Table 1). This is consistent with previous results demonstrating protein activity (water flux) regardless if SoPIP2;1 is purified in OTG [21] or OG (unpublished results, J.S. Hansen). Other aquaporins have also been successfully reconstituted in *E. coli* lipid membranes [27,28].

We then tested whether SoPIP2;1 could be reconstituted in DPhPC membranes as DPhPC is generally recognized as forming stable black lipid membranes [29–31], making this lipid, in principle, suitable for being used in the design of water-filtration systems. However our CD analysis of the SoPIP2;1-DPhPC mixture suggested that this lipid does not preserve the structure of this protein. Although spectra could be obtained (see Figure 1) reproducibility was low for SoPIP2;1-DPhPC mixtures. White precipitate particles were commonly observed during the reconstitution process which may be directly related to the apparition of denatured protein aggregates. The aggregation of the protein in DPhPC could be related to the difficulties encountered in forming liposomes even when extrusion methods were used. Also dynamic light scattering analysis of the DPhPC suspension reported very broad structural features. Specimens with diameters ranging from 51 to 2669 nm (range of the diameters taken from the calculated

Table 1. Summary of the SoPIP2;1 secondary structure results.

	%			
	α-Helix	**β-sheet**	**Turns**	**Random**
OG micelles	63	20	3	15
***E. coli* lipid**	61	17	7	16
POPE:POPC:POPS:Ergosterol	48	25	6	18
POPE:POPC	43	27	9	21
DPhPC	42	30	7	21

doi:10.1371/journal.pone.0014674.t001

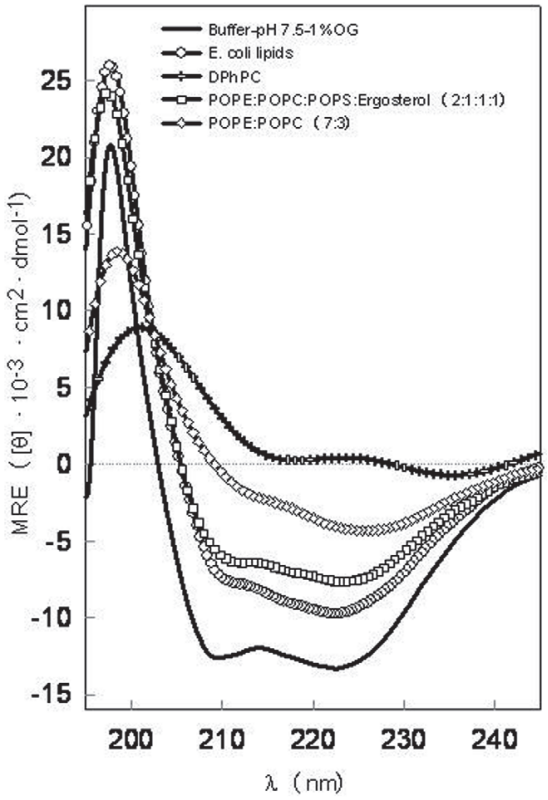

Figure 1. Far-UV CD spectra of SoPIP2;1. The measurements were obtained at 20°C in phosphate buffer, pH 7.5, NaCl 150 mM containing 1% OG and in different lipid membranes.
doi:10.1371/journal.pone.0014674.g001

Gaussian distribution of the sizes between 10% and 90% of the total distribution) were found in the same sample. The polydispersity index was 0.308, confirming a high liposome structural heterogeneity. These results suggest that this lipid does not provide a good membrane environment for a successful and stable SoPIP2;1 membrane incorporation. Hence, we exclude DPhPC bilayers as a host lipid membrane for SoPIP2;1.

We then examined POPE:POPC:POPS:Ergosterol (2:1:1:1 molar ratio) as this mixture has been shown to be as a good fusogenic lipid mixture [32] applicable for the further incorporation of aquaporins into industrial membrane water-filtration systems. The CD spectrum from SoPIP2;1/POPE:POPC:POPS:Ergosterol mixture does not look very different from the one obtained when the protein is reconstituted into *E. coli* lipid membranes (Figure 1). However, the α-helical content reported after the deconvolution analysis is lower (Table 1) and associated with an increase in the β-sheet content and the other analyzed structures. The spectra obtained with another suitable fusogenic lipid mixture, POPE:POPC (7:3 molar ratio), showed even less helical-like spectra although the deconvolution results report values similar to those obtained with the more complex fusogenic mixture (Figure 1 and Table 1).

Taken together we conclude that the best lipid system identified for the reconstitution of SoPIP2;1 is *E. coli* lipid membranes, followed by POPE:POPC:POPS:Ergosterol and POPE:POPC. In contrast DPhPC was found not to be suitable for the SoPIP2;1 membrane reconstitution.

Thermal stability of SoPIP2;1 secondary structure

One method to characterize the unfolding process of a protein is to study the effect of temperature changes on its structure. This provides important information about the conformational stability of protein. The thermal stability of SoPIP2;1 was found to differ between detergent micelles and the different lipid species studied here, as evidenced by CD spectroscopy (Figure 2). The changes in the secondary structure spectra associated with temperature increase was found to be larger for the protein reconstituted into detergent micelles (Figure 2, A) compared to *E. coli* lipids (Figure 2, B), the POPE:POPC:POPS:Ergosterol mixture (Figure 2, C) and the POPE:POPC mixture (Figure 2, D).

A summary of the results can be found in Figure 3 for the thermal stability of the secondary structure where the Mean residue ellipticity (MRE) at 222 nm were plotted as a function of the temperature for all systems studied. The different MRE values at 20°C (initial state) demonstrate that the protein is structured or interacting in different ways with the different detergents or lipids used. Therefore it can be assumed that the protein acquires different structural initial states as quantified by the deconvolution analyses in the different environments tested (Table 1). The SoPIP2;1 structure is more sensitive to the temperature changes when it is reconstituted into detergent micelles than when it is reconstituted into lipid membrane systems. Although the unfolding transition is not reversible, the transition midpoint can be used to quantify the thermal stability of the protein [33].

The variation of MRE 222 nm with increasing temperature shows that the protein in detergent micelles solution has a melting temperature around 58°C. The decreasing temperature ramp measurement failed to report the same initial state (data not shown), indicating an irreversible unfolding of the protein under these conditions. A white precipitate in the sample after incubation at the melting temperature was observed probably caused by the presence of unfolded protein aggregates that precipitated at the bottom of the sample cuvette. Thus the structural stability of the protein can be maintained up to 50°C. The melting temperature value around 58°C was also confirmed by SDS-PAGE (Figure 4). Presence of monomers and dimer bands can be observed at temperatures below 58°C but these bands disappear at higher temperatures and aggregated protein was retained in the well. Bands corresponding to complexes larger than the tetrameric protein are visible between 55 and 60°C.

Protein reconstitution in complex membranes lipid mixtures (*E. coli* or POPE:POPC:POPS:Ergosterol) increases the stability of SoPIP2;1 against temperature changes in the system. The spectra of the protein reconstituted in these membranes exhibited a different behavior in response to the temperature increase compared to the protein reconstituted in detergent-micelles (Figure 2). In this case of reconstitution in membrane lipid mixtures, only minor changes were observed in the spectra and appeared first above 70°C. This is clearly evident in the MRE 222 nm value representation (Figure 3).

Thermal stability of SoPIP2;1 tertiary structure

SoPIP2;1 contains six tryptophan (Trp) residues in the primary sequence. These residues can be used as intrinsic fluorophores for analyzing the protein ternary structure (see the cartoon in Figure 5A) as the Trp fluorescence emission spectrum is sensitive to both the polarity and the dynamics of the environment surrounding the aromatic side chain. Therefore, the variation in the Trp fluorescence emission spectra reports changes in tertiary

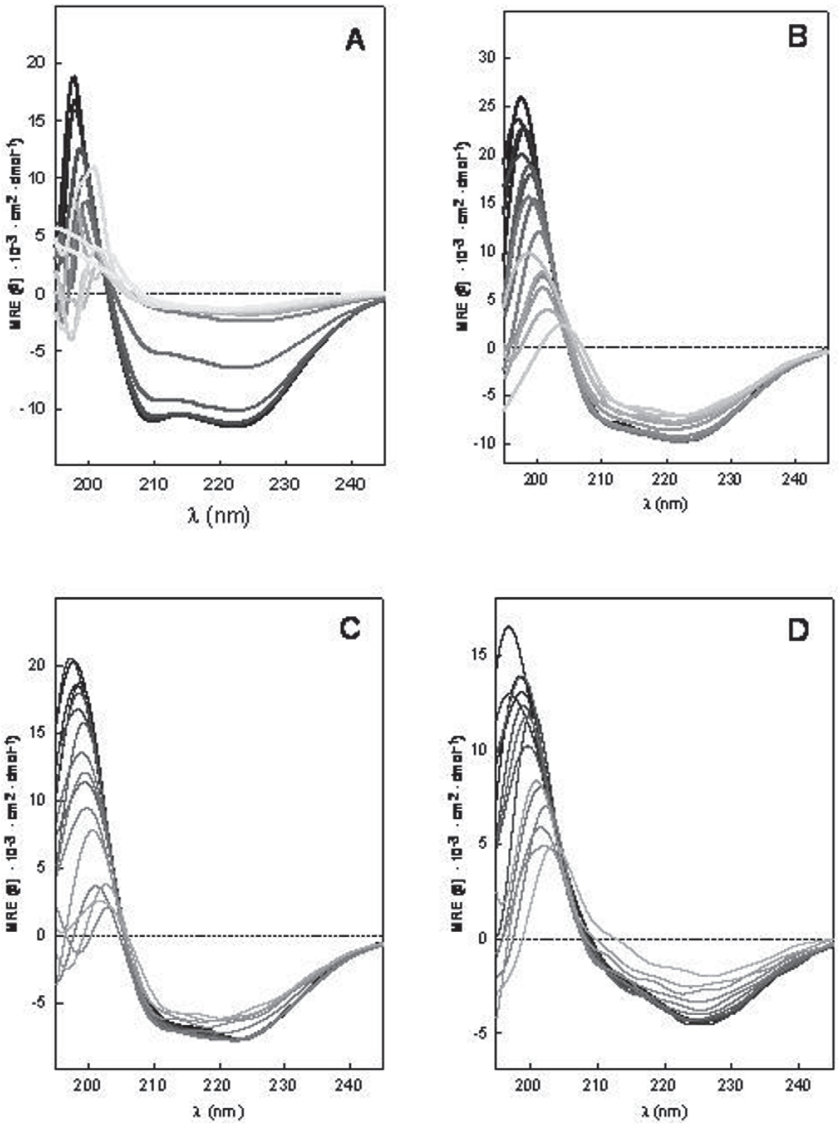

Figure 2. Thermal unfolding of the secondary structure of SoPIP2;1. Protein was reconstituted in A) OG micelles, B) *E. coli* lipid membranes, C) POPE:POPC:POPS:Ergosterol membranes and D) POPE:POPC membranes. Temperatures are represented by the grayscale colors from black, 20°C to very light gray, 95°C.
doi:10.1371/journal.pone.0014674.g002

structure of the protein. Thus the Trp is generally blue-shifted from 350 nm in environments of low polarity such as the hydrophobic interior of a protein or in a lipid membrane environment and Trp fluorescence in proteins has been classified into five classes by Reshetnyak et al. [34]. According to this classification, the dominant fluorescence around 329 nm corresponds to a class of Trp side chains that are in a relatively non-polar environment and H-bonded in an 2:1 exciplex that fluoresces at 331 nm [34]. Inspection of the three-dimensional structure of SoPIP2;1 indicated that the Trps of this protein are positioned close to the surface of the protein (see cartoon i in Figure 5A) [22]. SoPIP2;1 reconstituted into detergent-micelles exhibited a maximum fluorescence at 330 nm indicating that the region of the protein where the Trps are located is positioned at the edge of the detergent micelles thereby facilitating the contacts between Trps and water molecules (see cartoon ii in Figure 5A and experimental results in Figure 5B). The easier accessibility of the water to the Trp environment is due to the loosely packed hydrophobic tails of the detergents interacting with the protein in detergent-micelles. A shift to lower wavelength values was always observed when the protein was reconstituted into lipid membranes (representative spectra showed with the *E. coli* membranes in Figure 5B). It demonstrates that the lipid membrane environment offers a more extensive hydrophobic surface for interaction with

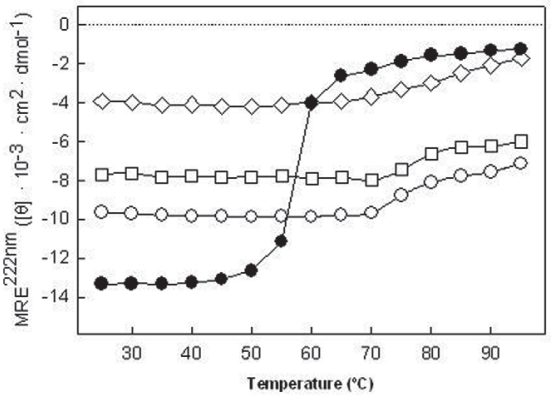

Figure 3. MRE at 222 nm as a function of temperature. SoPIP2;1 in OG micelles (●), *E. coli* lipid membranes (□), POPE:POPC:POPS:Ergosterol (o) and POPE:POPC (◇).
doi:10.1371/journal.pone.0014674.g003

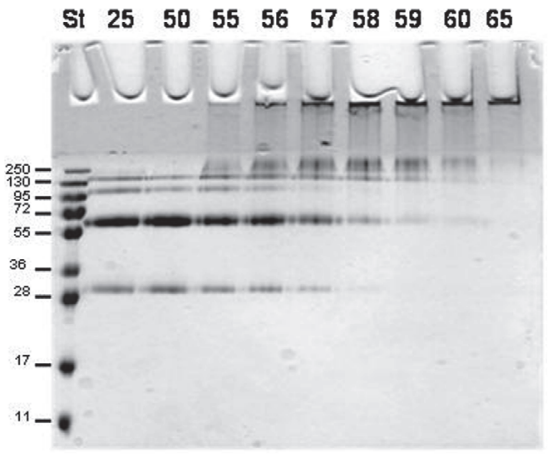

Figure 4. Thermal denaturation of SoPIP2;1. It can be visualized by SDS-PAGE since large aggregates are formed that cannot enter the gel. After incubation at room temperature the normal bands corresponding to monomeric, dimeric, trimeric and tetrameric SoPIP2;1 are evident. No aggregates were found at 50°C whereas at the melting point, 58°C, as determined by CD, part of the protein was aggregated. At 65°C the aggregation was complete. The samples were incubated at the indicated temperatures (25–65°C) for 10 minutes before sample loading buffer was added followed by 10 minutes incubation at room temperature. St, standard with indicated Mw in kDa in the left side of the gel.
doi:10.1371/journal.pone.0014674.g004

the transmembrane protein (cartoon iii in figure 5A). It is also consistent with the higher temperature stability exhibited by the protein in the membrane systems. Thermal stability of the protein was also monitored by following the Trp fluorescence vs. increasing temperature. The Trp fluorescence was quenched at higher temperatures while the wavelength at which maximum emission took place was not affected significantly (Figure 5B and 6).

For transmembrane proteins two components are generally contributing to a higher water access to the Trp location. One is the fluidity of the micelles or membranes and the other is the progressive unfolding of the protein. In case of detergent micelles, the effect of possible micelle fluidity is not very high. The protein reconstituted into micelle solution exhibited a very similar profile to the protein unfolding analyzed by CD. In this situation the principal transition occur around 58°C (Figure 6). When the protein is reconstituted in lipid membranes the profile is more complex with more than one transition indicating the contribution of both components to the final state (Figure 6). The first transition may reflect a change in the lipids that allows water to access the Trp environment without any structural change in the protein. In any case the steeper slope, likely to be related to the protein unfolding, occurs around 70°C correlating well with the data obtained by CD spectroscopy.

Discussion

The structural stability of the protein is important as a precedent for good functionality after reconstitution. Here we used CD spectroscopy as an effective and fast tool for testing the structural properties of SoPIP2;1 and its stability in different environments. CD spectroscopy has already been used with many other proteins and it has been used for determining the melting temperature of proteins [33,35,36].

A high-resolution X-ray structure (PDB data 1Z98) has been published for untagged SoPIP2;1 [22], but the structural stability properties of SoPIP2;1 have never before been studied after overexpression and reconstitution into different membrane or membrane-like environments. A helical content of 60% was reported in the 1Z98 SoPIP2;1 crystallographic structure. However, the helical content determination is not complete as 1Z98 does not report the first 23 and the last 7 residues of the protein. Our CD measurements of His-tagged SoPIP2;1 in OG micelles, the same detergent also used to solubilize the protein for crystalization, showed a 63% helical content, a value that matches well with the high resolution structure of SoPIP2;1 demonstrating that CD spectroscopy is a very useful tool for testing the secondary structure stability of the protein reconstituted in different systems.

Regarding the tetrameric quaternary structure of SoPIP2;1, two mechanisms could explain the results shown in Figure 3: unfolding or dissociation of the tetrameric protein complex. The moderate change in MRE as function of temperature observed when the protein is reconstituted in phospholipid membranes could be related to protein unfolding in a small protein population. Considering that the CD results are giving an average value of the folding pattern this would imply that most of the protein is correctly folded. However, it is also possible that the change in MRE is due to dissociation of the aquaporin tetrameric complexes. In that case also monomers and dimers may occur in the membrane at higher temperatures giving rise to the changes in MRE as observed.

The information obtained by CD was also validated with Trp fluorescence emission. These measurements provided information about the protein tertiary structure and incorporation into the membrane. Our results revealed that POPE:POPC:POPS:Ergosterol, POPE:POPC and *E. coli* lipids all are appropriate lipid systems for reconstitution of SoPIP2;1 as they supported structural and thermal stability of the protein. The results from the latter system is consistent with the work by Karlsson et al. [21] using stop-flow measurements demonstrating water transport functionality for SoPIP2;1 in *E. coli* lipids. In contrast DPhPC does not provide a suitable host lipid membrane for SoPIP2;1.

It have been suggested that aquaporins exhibit greater stability [37–42] compared to the structurally closely related glycerol facilitators (aquaglyceroporins) [28,43–45]. Galka and collabora-

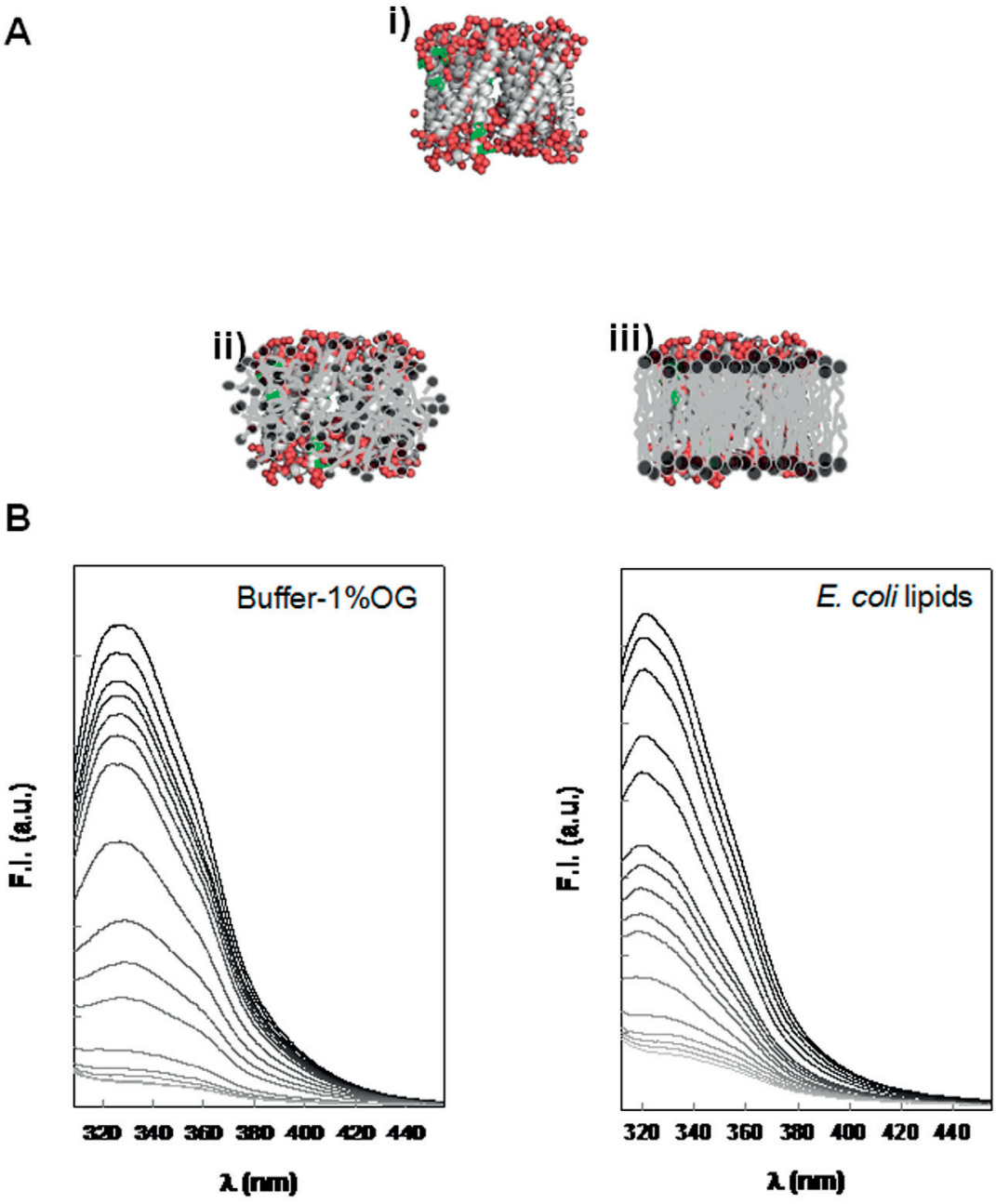

Figure 5. Fluorescence spectroscopy analysis of the protein ternary structure behavior. A) Cartoons illustrating the Trp residues (green) position in the protein ternary structure SoPIP2;1. The structure derives from the PDB file 1Z98 [22] using VMD software is shown in i [50], an illustration of the protein position in detergent micelles in ii and in lipid bilayers in iii. B) Thermal unfolding of SoPIP2;1 monitored by tryptophan fluorescence. To the left, the protein is reconstituted into OG micelles and to the right the protein is reconstituted into *E. coli* lipid membranes. Temperatures are represented by the grayscale colors from black, 20°C to very light gray, 95°C.
doi:10.1371/journal.pone.0014674.g005

tors [36] showed using SDS-PAGE electrophoresis that *E. coli* GlpF aquaglyceroporin has an unfolding temperature of the tetramer around 60°C in detergent solutions of dodecyl β-D-maltoside (DDM). The same temperature was obtained for the tertiary structure monitored by Trp fluorescence [36]. When these authors studied the secondary thermal stability by far-UV CD

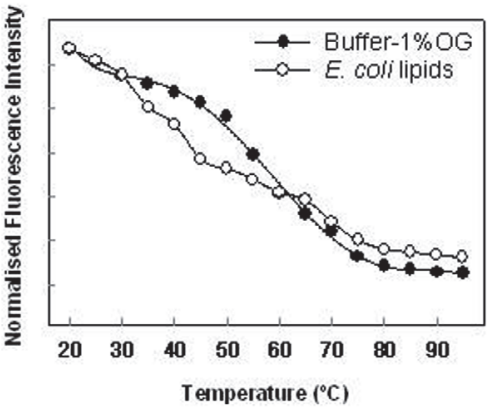

Figure 6. Fluorescence intensity at the maximum of the emission spectra as a function of temperature. The protein reconstituted in detergent micelles show one principal transitions in comparison with the protein reconstituted in lipid membranes where at least three different transitions can be observed. Fluorescence intensity values are normalized to the higher intensity value observed with the protein in micelles suspension at 20°C.
doi:10.1371/journal.pone.0014674.g006

spectroscopy they observed a two-state unfolding transition occurring around 70°C for GlpF in DDM. When GlpF was reconstituted into lysomyristoylphophatidylcholine (LMPC) micelles, the tetramer unfolded around 80°C and the thermal stability of the secondary structure was reported to have a transition temperature of 87°C. Compared with our results obtained for SoPIP2;1, GlpF in LMPC micelles apparently has a higher stability than SoPIP2;1 in OG micelles and phospholipid bilayers. On the other hand SoPIP2;1 reconstituted into the bilayer-forming phospholipid mixtures tested here shows a similar melting temperature as GlpF in DMM. Unfortunately a direct comparison is not possible as we do not have the same GlpF/lipid systems to compare with.

In conclusion we have shown that SoPIP2;1 can exist as a stable folded protein in OG detergent micelles solutions and that the protein can be transferred from detergent micelles solutions and reconstituted into selected phospholipid membranes preserving its structural characteristics. It is likely that more suitable reconstitution systems exist for SoPIP2;1 than those studied in the present work. In order to efficiently test a range of systems, new methods are called for. Presently we are working on developing a new microscopic method that will allow us to test at the same time the incorporation and distribution of the protein in different membrane systems and evaluate the yield of the incorporation and characterize the protein functionality.

Materials and Methods

E. coli lipids total extract, 1,2-Diphytanoyl-sn-Glycero-3-Phosphocholine (DPhPC), 1-palmitoyl-2-oleoyl-*sn*-glycero-3-phosphoethanolamine (POPE), 1-palmitoyl-2-oleoyl-*sn*-glycero-3-phosphocholine (POPC) and 1-palmitoyl-2-oleoyl-*sn*-glycero-3-phospho-L-serine (sodium salt) (POPS) were purchased from Avanti Polar Lipids, Inc. (Alabaster, AL). Octyl-β-D-glucopyranoside (OG) was purchased from Anatrace (Maumee, OH) and Sigma-Aldrich (Brondby, Denmark). Ergosterol and all the other chemicals were obtained from Sigma-Aldrich (Brondby, Denmark).

Heterologous protein overexpression

Functional SoPIP2;1 was overproduced in the methylotrophic yeast *Pichia pastoris* as His-tagged protein with a myc epitope [21]. The fusion protein has 303 amino acid and a molecular weight (Mw) of 32512 Da. The strain was grown in a 3 L fermentor typically resulting in 230 g wet cells/L culture after 24 h of methanol induction. Urea/NaOH washed membranes were prepared as described previously [21] and SoPIP2;1 was solubilised in 5% OG. Solubilized His-tagged material was purified using Ni-affinity chromatography as previously published [21]. The eluted protein was concentrated using a VivaSpin 20 concentrator (cutoff MW 10 kDa, VivaScience) and the buffer was then changed to 10 mM phosphate buffer, pH 7.5, NaCl 150 mM (PBS) supplemented with 10% glycerol and 1% OG using a PD-10 column resulting in a final concentration of 10–15 mg/ml as determined by Bearden [46].

Electrophoresis

Pure protein (5 μg) in 20 μL of phosphate buffer (10 mM potassium phosphate, 150 mM NaCl, 1% OG and 10% glycerol pH 7.5) was incubated for 10 minutes at different temperatures (25°C–65°C). After incubation, sample loading buffer (125 mM Tris-HCl pH 6.8, 20% glycerol, 4% SDS, 10% (v/v) β-mercaptoethanol 0.1% bromophenol blue) was added to the protein and further incubated for 10 minutes at room temperature. SDS- PAGE (12%) of the sample was performed as described by Laemmli [47]. Protein was visualized by staining the gel with Coomassie brilliant blue R250.

Dynamic Light Scattering (DLS)

Multilamellar 4 mg/ml DPhPC vesicles were formed by evaporation of the chloroform solvent by nitrogen gas and drying 30 minutes in the dessicator, followed by resolvation of the lipid film in sterile filtered 0.2 M KCl in double distilled water. The vesicle solution was extruded 11 times through a 100 nm polycarbonate filter. DLS size distribution analyses of 0.1 mg/ml DPhPC vesicles in 0.2 M KCl at 25°C were performed with a Malvern Zetasizer NanoZS instrument courtesy of LiPlasome Pharma A/S. Standard cuvettes (67.740 from Hounisen, Denmark) were used. 3 measurements of 13 runs each were taken and averaged. The analysis was carried out with the software program DTS 5.10, using an in-built general purpose analysis model.

Liposome and Protoliposome reconstitution

Purified SoPIP2;1 was reconstituted into vesicles by mixing with *E. coli* lipids total extract or DPhPC or POPE:POPC:POPS:Ergosterol (2:1:1:1 mol ratio) (complex fusogenic mixture) or POPE:POPC (7:3 mol ratio) (binary fusogenic mixture) solubilized in 1% OG at a lipid-to-protein molar ratio (LPR) of 200 in phosphate buffer 10 mM, NaCl 150 mM, pH 7.5 at a final 0.1 mg/mL concentration of protein. The mixture was dialyzed in Slide-A-Lyzer® Dialysis Cassettes from Thermo Scientific, Pierce Biotechnology, (Rockford, IL) with a molecular cut-off of 10,000 Mw at room temperature for 4 days with two buffer changes per day. Control vesicles were made in the same manner without protein.

Circular Dichroism (CD) and Fluorescence

CD spectra were acquired with a Jasco 815 spectrometer (Jasco UK, Essex, UK). The sample temperature was controlled by a built-in Peltier device. The protein or lipid-protein solutions were placed in a quartz cuvette with a 0.1 cm path length and the spectra were collected at 20 nm/min between 250–190 nm with a

response time of 0.25 s and a data pitch of 0.1 nm. Baselines were collected in the same manner and spectra were baseline corrected. CD spectra for samples without protein, i.e. buffer or buffer with detergent and lipid did not exhibit ellipticity. Mean residue ellipticity (MRE) ($[\theta] \times 10^{-3}$ deg cm^2 dmol^{-1}) as calculated using the equation $[\theta]_M = M\theta/10 \cdot l \cdot c \cdot n$, where M is 32512 g/mol, θ is the measured ellipticity in millidegrees, l is the cell path length, c is the protein concentration in grams per liter, and n = 303 residues. Deconvolution of the CD spectra into pure component spectra was performed using the algorithm CDSSTR [48] accessed through Dichroweb [49]. α-helical changes were followed observing the variation in MRE at 222 nm for the temperature stability measurements between 20°C and 95°C.

Fluorescence spectra were collected in an ISS Chronos fluorometer (ISS Champaign, IL) using a 280 nm diode as excitation source.

Acknowledgments

Adine Karlsson is gratefully acknowledged for technical assistance in providing purified SoPIP2;1. We are grateful for the helpful comments provided by anonymous referees.

Author Contributions

Conceived and designed the experiments: IP. Performed the experiments: IP SS SI. Analyzed the data: IP. Contributed reagents/materials/analysis tools: PK UJ OGM. Wrote the paper: IP JSH CHN UJ OGM.

References

1. Engel A, Stahlberg H (2002) Aquaglyceroporins: channel proteins with a conserved core, multiple functions, and variable surfaces. Int Rev Cytol 215: 75–104.
2. Engel A, Fujiyoshi Y, Agre P (2000) The importance of aquaporin water channel protein structures. Embo J 19: 800–806.
3. Park JH, Saier MH, Jr. (1996) Phylogenetic characterization of the MIP family of transmembrane channel proteins. J Membr Biol 153: 171–180.
4. Engel A, Fujiyoshi Y, Gonen T, Walz T (2008) Junction-forming aquaporins. Curr Opin Struct Biol 18: 229–235.
5. Kukulski W, Schenk AD, Johanson U, Braun T, de Groot BL, et al. (2005) The 5A structure of heterologously expressed plant aquaporin SoPIP2;1. J Mol Biol 350: 611–616.
6. Murata K, Mitsuoka K, Hirai T, Walz T, Agre P, et al. (2000) Structural determinants of water permeation through aquaporin-1. Nature 407: 599–605.
7. Savage DF, Egea PF, Robles-Colmenares Y, O'Connell JD, 3rd, Stroud RM (2003) Architecture and selectivity in aquaporins: 2.5 a X-ray structure of aquaporin Z. PLoS Biol 1: E72.
8. Gorin MB, Yancey SB, Cline J, Revel JP, Horwitz J (1984) The major intrinsic protein (MIP) of the bovine lens fiber membrane: characterization and structure based on cDNA cloning. Cell 39: 49–59.
9. Preston GM, Jung JS, Guggino WB, Agre P (1994) Membrane topology of aquaporin CHIP. Analysis of functional epitope-scanning mutants by vectorial proteolysis. J Biol Chem 269: 1668–1673.
10. Zardoya R (2005) Phylogeny and evolution of the major intrinsic protein family. Biol Cell 97: 397–414.
11. Russ WP, Engelman DM (2000) The GxxxG motif: a framework for transmembrane helix-helix association. J Mol Biol 296: 911–919.
12. Heymann JB, Engel A (2000) Structural clues in the sequences of the aquaporins. J Mol Biol 295: 1039–1053.
13. Danielson JA, Johanson U (2008) Unexpected complexity of the aquaporin gene family in the moss Physcomitrella patens. BMC Plant Biol 8: 45.
14. Johanson U, Karlsson M, Johansson I, Gustavsson S, Sjovall S, et al. (2001) The complete set of genes encoding major intrinsic proteins in Arabidopsis provides a framework for a new nomenclature for major intrinsic proteins in plants. Plant Physiol 126: 1358–1369.
15. Kammerloher W, Fischer U, Piechottka GP, Schaffner AR (1994) Water channels in the plant plasma membrane cloned by immunoselection from a mammalian expression system. Plant J 6: 187–199.
16. Chaumont F, Barrieu F, Jung R, Chrispeels MJ (2000) Plasma membrane intrinsic proteins from maize cluster in two sequence subgroups with differential aquaporin activity. Plant Physiol 122: 1025–1034.
17. Biela A, Grote K, Otto B, Hoth S, Hedrich R, et al. (1999) The Nicotiana tabacum plasma membrane aquaporin NtAQP1 is mercury-insensitive and permeable for glycerol. Plant J 18: 565–570.
18. Dordas C, Chrispeels MJ, Brown PH (2000) Permeability and channel-mediated transport of boric acid across membrane vesicles isolated from squash roots. Plant Physiol 124: 1349–1362.
19. Gaspar M, Bousser A, Sissoëff I, Roche O, Hoarau j, et al. (2003) cloning and characterization of ZmPIP1-5b, and aquaporin transporting water and urea. Plant Sci 165: 21–31.
20. Fraysse LC, Wells B, McCann MC, Kjellbom P (2005) Specific plasma membrane aquaporins of the PIP1 subfamily are expressed in sieve elements and guard cells. Biol Cell 97: 519–534.
21. Karlsson M, Fotiadis D, Sjovall S, Johansson I, Hedfalk K, et al. (2003) Reconstitution of water channel function of an aquaporin overexpressed and purified from Pichia pastoris. FEBS Lett 537: 68–72.
22. Tornroth-Horsefield S, Wang Y, Hedfalk K, Johanson U, Karlsson M, et al. (2006) Structural mechanism of plant aquaporin gating. Nature 439: 688–694.
23. Johansson I, Karlsson M, Shukla VK, Chrispeels MJ, Larsson C, et al. (1998) Water transport activity of the plasma membrane aquaporin PM28A is regulated by phosphorylation. Plant Cell 10: 451–459.
24. Nielsen CH (2009) Biomimetic membranes for sensor and separation applications. Anal Bioanal Chem.
25. Seddon AM, Curnow P, Booth PJ (2004) Membrane proteins, lipids and detergents: not just a soap opera. Biochim Biophys Acta 1666: 105–117.
26. Rand RP, Parsegian VA (1986) Mimicry and mechanism in phospholipid models of membrane fusion. Annu Rev Physiol 48: 201–212.
27. Borgnia MJ, Kozono D, Calamita G, Maloney PC, Agre P (1999) Functional reconstitution and characterization of AqpZ, the E. coli water channel protein. J Mol Biol 291: 1169–1179.
28. Manley DM, McComb ME, Perreault H, Donald LJ, Duckworth HW, et al. (2000) Secondary structure and oligomerization of the E. coli glycerol facilitator. Biochemistry 39: 12303–12311.
29. Baba T, Toshima Y, Minamikawa H, Hato M, Suzuki K, et al. (1999) Formation and characterization of planar lipid bilayer membranes from synthetic phytanyl-chained glycolipids. Biochim Biophys Acta 1421: 91–102.
30. Janko K, Benz R (1977) Properties of lipid bilayer membranes made from lipids containing phytanic acid. Biochim Biophys Acta 470: 8–16.
31. Lindsey H, Petersen NO, Chan SI (1979) Physicochemical characterization of 1,2-diphytanoyl-sn-glycero-3-phosphocholine in model membrane systems. Biochim Biophys Acta 555: 147–167.
32. Woodbury DJ (1999) Nystatin/ergosterol method for reconstituting ion channels into planar lipid bilayers. Methods Enzymol 294: 319–339.
33. Minetti CA, Remeta DP (2006) Energetics of membrane protein folding and stability. Arch Biochem Biophys 453: 32–53.
34. Reshetnyak YK, Burstein EA (2001) Decomposition of protein tryptophan fluorescence spectra into log-normal components. II. The statistical proof of discreteness of tryptophan classes in proteins. Biophys J 81: 1710–1734.
35. Sehgal P, Mogensen JE, Otzen DE (2005) Using micellar mole fractions to assess membrane protein stability in mixed micelles. Biochim Biophys Acta 1716: 59–68.
36. Galka JJ, Baturin SJ, Manley DM, Kehler AJ, O'Neil JD (2008) Stability of the glycerol facilitator in detergent solutions. Biochemistry 47: 3513–3524.
37. Aerts T, Xia JZ, Slegers H, de Block J, Clauwaert J (1990) Hydrodynamic characterization of the major intrinsic protein from the bovine lens fiber membranes. Extraction in n-octyl-beta-D-glucopyranoside and evidence for a tetrameric structure. J Biol Chem 265: 8675–8680.
38. Beuron F, Le Caherec F, Guillam MT, Cavalier A, Garret A, et al. (1995) Structural analysis of a MIP family protein from the digestive tract of Cicadella viridis. J Biol Chem 270: 17414–17422.
39. Konig N, Zampighi GA, Butler PJ (1997) Characterisation of the major intrinsic protein (MIP) from bovine lens fibre membranes by electron microscopy and hydrodynamics. J Mol Biol 265: 590–602.
40. Ringler P, Borgnia MJ, Stahlberg H, Maloney PC, Agre P, et al. (1999) Structure of the water channel AqpZ from Escherichia coli revealed by electron crystallography. J Mol Biol 291: 1181–1190.
41. Smith BL, Agre P (1991) Erythrocyte Mr 28,000 transmembrane protein exists as a multisubunit oligomer similar to channel proteins. J Biol Chem 266: 6407–6415.
42. Verbavatz JM, Brown D, Sabolic I, Valenti G, Ausiello DA, et al. (1993) Tetrameric assembly of CHIP28 water channels in liposomes and cell membranes: a freeze-fracture study. J Cell Biol 123: 605–618.
43. Bron P, Lagree V, Froger A, Rolland JP, Hubert JF, et al. (1999) Oligomerization state of MIP proteins expressed in Xenopus oocytes as revealed by freeze-fracture electron-microscopy analysis. J Struct Biol 128: 287–296.
44. Duchesne L, Deschamps S, Pellerin I, Lagree V, Froger A, et al. (2001) Oligomerization of water and solute channels of the major intrinsic protein (MIP) family. Kidney Int 60: 422–426.
45. Stahlberg H, Braun T, de Groot B, Philippsen A, Borgnia MJ, et al. (2000) The 6.9-A structure of GlpF: a basis for homology modeling of the glycerol channel from Escherichia coli. J Struct Biol 132: 133–141.
46. Bearden JC, Jr. (1978) Quantitation of submicrogram quantities of protein by an improved protein-dye binding assay. Biochim Biophys Acta 533: 525–529.
47. Laemmli UK (1970) Cleavage of structural proteins during the assembly of the head of bacteriophage T4. Nature 227: 680–685.

48. Compton LA, Johnson WC, Jr. (1986) Analysis of protein circular dichroism spectra for secondary structure using a simple matrix multiplication. Anal Biochem 155: 155–167.
49. Whitmore L, Wallace BA (2004) DICHROWEB, an online server for protein secondary structure analyses from circular dichroism spectroscopic data. Nucleic Acids Res 32: W668–673.
50. Humphrey W, Dalke A, Schulten K (1996) VMD: visual molecular dynamics. J Mol Graph 14: 33—3827—38.

Paper IV

Human TRPA1 is intrinsically cold- and chemosensitive with and without its N-terminal ankyrin repeat domain

Lavanya Moparthi[a], Sabeen Survery[a], Mohamed Kreir[b,c], Charlotte Simonsen[d], Per Kjellbom[a], Edward D. Högestätt[d,1], Urban Johanson[a,1], and Peter M. Zygmunt[d]

[a]Department of Biochemistry and Structural Biology, Center for Molecular Protein Science, Lund University, SE-221 00 Lund, Sweden; [b]Nanion Technologies GmbH, D-80636 Munich, Germany; [c]Department of Biophysics, Jacobs University Bremen, D-27857 Bremen, Germany; and [d]Clinical Chemistry and Pharmacology, Department of Laboratory Medicine, Lund University, SE-221 85 Lund, Sweden

Edited* by Lutz Birnbaumer, National Institute of Environmental Health Sciences, Research Triangle Park, NC, and approved October 14, 2014 (received for review July 7, 2014)

We have purified and reconstituted human transient receptor potential (TRP) subtype A1 (hTRPA1) into lipid bilayers and recorded single-channel currents to understand its inherent thermo- and chemosensory properties as well as the role of the ankyrin repeat domain (ARD) of the N terminus in channel behavior. We report that hTRPA1 with and without its N-terminal ARD (Δ1–688 hTRPA1) is intrinsically cold-sensitive, and thus, cold-sensing properties of hTRPA1 reside outside the N-terminal ARD. We show activation of hTRPA1 by the thiol oxidant 2-((biotinoyl)amino)ethyl methanethiosulfonate (MTSEA-biotin) and that electrophilic compounds activate hTRPA1 in the presence and absence of the N-terminal ARD. The nonelectrophilic compounds menthol and the cannabinoid Δ^9-tetrahydrocannabiorcol (C16) directly activate hTRPA1 at different sites independent of the N-terminal ARD. The TRPA1 antagonist HC030031 inhibited cold and chemical activation of hTRPA1 and Δ1–688 hTRPA1, supporting a direct interaction with hTRPA1 outside the N-terminal ARD. These findings show that hTRPA1 is an intrinsically cold- and chemosensitive ion channel. Thus, second messengers, including Ca^{2+}, or accessory proteins are not needed for hTRPA1 responses to cold or chemical activators. We suggest that conformational changes outside the N-terminal ARD by cold, electrophiles, and nonelectrophiles are important in hTRPA1 channel gating and that targeting chemical interaction sites outside the N-terminal ARD provides possibilities to fine tune TRPA1-based drug therapies (e.g., for treatment of pain associated with cold hypersensitivity and cardiovascular disease).

cold sensing | irritants | pain | sensory neuron | TRP channels

A number of vertebrate and invertebrate transient receptor potential (TRP) ion channels have been implicated in temperature sensation (1–3), but only the rat menthol receptor TRP subtype M8 (TRPM8) and the rat capsaicin receptor TRP subtype V1 (TRPV1) have been shown to possess intrinsic thermosensitivity (4, 5). In 2003, Story et al. (6) proposed that the mouse TRPA1 is a noxious cold sensor. Story et al. (6) showed that TRPA1 was present in nociceptive primary sensory neurons and that CHO cells heterologously expressing the mouse TRPA1 displayed cold sensitivity. Most subsequent studies of cold responses in heterologous TRPA1 expression systems, isolated primary sensory neurons, and whole animals have provided evidence in support of mouse and rat TRPA1 being involved in noxious cold transduction (7). Interestingly, a familial episodic pain syndrome triggered by cold is caused by a gain-of-function mutation in the TRPA1 gene, indicating that TRPA1 may have a key role in human noxious cold sensation (8). Thus, human TRPA1 (hTRPA1) may be a relevant drug target for treatment of this condition and other pathological conditions, such as inflammation, nerve injury, and chemotherapy-induced neuropathy, that are characterized by TRPA1-dependent cold allodynia or hypersensitivity (7). However, in vitro studies of the expressed hTRPA1 have generated conflicting findings (8–15), and no study has provided evidence that mammalian TRPA1 channels are, indeed. intrinsically cold-sensitive proteins, which would require examination of the purified protein in a defined membrane environment.

Heterologous expression studies of chimeric or mutated TRPA1 channels have proposed that the N-terminal region plays an important role in thermal and chemical sensitivity of both mammalian and insect TRPA1 (14, 16–19). Initial studies indicated that mammalian TRPA1 is activated by cysteine-reactive electrophilic compounds and oxidants, such as diallyl disulfide in garlic (9, 10, 20, 21). Targeted gene mutations have identified cysteines present in the N terminus of TRPA1 as important for electrophilic and oxidative TRPA1 channel activation (22, 23). Because several of these cysteines are involved in protein disulfide formation (24–26), it is not unlikely that such mutations will have pronounced effects on the overall TRPA1 channel structure and function (7). Electrophilic compounds can also covalently bind to cysteines in the transmembrane segments and the C-terminal domain of mammalian TRPA1 (23, 26), and the electrophiles *p*-benzoquinone, isovelleral, and polygodial robustly activate the heterologously expressed triple mutant hTRPA1-3C (27, 28) that was initially used to identify certain N-terminal cysteine residues in hTRPA1 as key targets for electrophiles (22). However, it is yet to be shown that covalent binding sites outside the N-terminal

Significance

The ability of an organism to detect and avoid noxious temperatures is crucial for survival. It is, therefore, of great interest that several transient receptor potential (TRP) ion channels have been proposed as temperature sensors. However, to date, only the menthol receptor (TRP subtype M8) and the chili pepper receptor (TRP subtype V1) have been shown to be intrinsically temperature-sensitive proteins in mammals. In this study, we show that the purified wasabi receptor (TRP subtype A1) is a cold sensor. Thus, mammals have at least two cold sensors that, together, cover pleasant (TRP subtype M8) and unpleasant (TRP subtype A1) cold temperatures. Our findings add to the understanding of how the temperature sense is organized and its role in pain associated with cold hypersensitivity.

Author contributions: P.K., E.D.H., U.J., and P.M.Z. designed research; L.M., S.S., M.K., C.S., E.D.H., and P.M.Z. performed research; L.M., S.S., M.K., C.S., E.D.H., U.J., and P.M.Z. analyzed data; L.M., E.D.H., and P.M.Z. wrote the paper; L.M. performed and analyzed biochemistry and electrophysiology; S.S. performed and analyzed circular dichroism spectroscopy; M.K. performed and analyzed electrophysiology; C.S. designed, performed, and analyzed calcium imaging; P.K. directed the study; E.D.H. and P.M.Z. conceived, designed, and directed the study; and U.J. designed and directed the study.

Conflict of interest statement: M.K. is employed by Nanion Technologies GmbH.

*This Direct Submission article had a prearranged editor.

Freely available online through the PNAS open access option.

[1]To whom correspondence may be addressed. Email: edward.hogestatt@med.lu.se or urban.johanson@biochemistry.lu.se.

This article contains supporting information online at www.pnas.org/lookup/suppl/doi:10.1073/pnas.1412689111/-/DCSupplemental.

ankyrin repeat domain (ARD) contribute to the regulation of channel gating.

Another key feature of mammalian TRPA1 is the responsiveness to nonelectrophilic compounds with very different chemical structures, such as menthol and the cannabinoids Δ^9-tetrahydrocannabinol (Δ^9-THC) and Δ^9-tetrahydrocannabiorcol (C16) (7). However, if nonelectrophilic compounds activate TRPA1 directly and at the same site on TRPA1 is not known. The site of action of nonelectrophilic TRPA1 activators is important to clarify, because some TRPA1 activators are antinoiceptive (29, 30), and nontissue-damaging TRPA1 activators may be used clinically for pharmacological regulation of TRPA1 channel activity (29).

Here, we have purified and inserted hTRPA1 with and without its N-terminal ARD (Δ1–688 hTRPA1) into lipid bilayers for functional studies using patch-clamp electrophysiology to explore the inherent thermo- and chemosensitivity of hTRPA1. Because of the great potential of TRPA1 as a drug target for treatment of human pain and the existence of mammalian TRPA1 species differences (7), the human variant of TRPA1 was chosen for these studies. We addressed the role of the N-terminal ARD in cold and chemical sensitivity by deleting the N-terminal ARD, something that cannot be studied in cells heterologously expressing TRPA1, because the N-terminal ARD is needed for insertion of the ion channel into the plasma membrane (31). Our findings consolidate hTRPA1 as a multimodal nocisensor responding to cold and chemicals. It is suggested that conformational changes outside the N-terminal ARD by cold, electrophiles, and nonelectrophilic compounds are important in hTRPA1 channel gating. Targeting chemical interaction sites outside the N-terminal ARD may provide possibilities to fine tune TRPA1-based drug therapies [e.g., for treatment of pain associated with cold hypersensitivity (7) and cardiovascular disease (32)].

Results

Purification of Functional hTRPA1. To purify hTRPA1 and Δ1–688 hTRPA1, we used a *Pichia pastoris* expression system previously proven to be successful in the purification of other integral membrane proteins (33, 34). Initial screening of various detergents identified a series of fos-choline detergents as particularly effective for extraction of hTRPA1 and Δ1–688 hTRPA1 from *P. pastoris* cell membranes. Out of this screening, we chose fos-choline-14 for the purification and functional studies of the hTRPA1 channels. Intact hTRPA1 and Δ1–688 hTRPA1 with N-terminal decahistidine tags, which did not compromise the functionality of hTRPA1 when expressed in HEK293 cells (Fig. S1 *A–D*), were purified by Nickel affinity chromatography (Fig. 1); Δ1–688 hTRPA1 was obtained at a higher yield (3 mg/10 g cells) and purity than hTRPA1 (0.3 mg/10 g cells) using a one-step purification procedure. Based on Image Quant analysis, the purities of hTRPA1 and Δ1–688 hTRPA1 were estimated to be 50% and 95%, respectively.

In contrast to the heterologously expressed hTRPA1, there is no information on the functional properties and folding of Δ1–688 hTRPA1. Therefore, gel filtration and circular dichroism (CD) spectroscopy were implemented to evaluate the consequences of the removal of the N terminus on tetramerization and folding of the protein. As shown by the chromatogram, Δ1–688 hTRPA1 eluted mainly as a tetramer (Fig. 1*C*), and the far UV CD spectra showed that Δ1–688 hTRPA1 has the characteristics of a predominately α-helical structure with minima at 208 and 222 nm (Fig. 1*D*). The secondary structure composition was estimated by the Dicroweb software using CDSSTR, SELCON3, and CONTINLL algorithms, suggesting that Δ1–688 hTRPA1 contains 35–45% of α-helices, 15–20% of β-strands, 20–25% of turns, and 20–25% of unordered structure. The expected minima of α-helical content based on prediction of transmembrane domains (transmembrane hidden Markov models) and sequence alignment of Δ1–688 hTRPA1 with the potassium channel (Kv1.2) with known structure were 27% and 36%, respectively, which are in good agreement with the experimental data. Both the CD spectral data and the tetrameric oligomeric state of the purified protein suggest that it is correctly folded and functionally intact. In line with the general view that functional TRP channels are tetrameric protein complexes (2, 24), initial electrophysiological experiments measuring ramp currents (−100 to + 100 mV in 2 s) showed that hTRPA1 and Δ1–688 hTRPA1 reconstituted into planar lipid bilayers are functional proteins, because they responded to allyl isothiocyanate (AITC) and menthol, respectively, with single-channel currents at both negative and positive test potentials (Fig. S1*E*). Because AITC is supposed to activate TRPA1 by binding to the N terminus (22, 23), menthol was used to assess the functionality of Δ1–688 hTRPA1, because this nonelectrophilic compound presumably interacts with the S5 transmembrane domain (35).

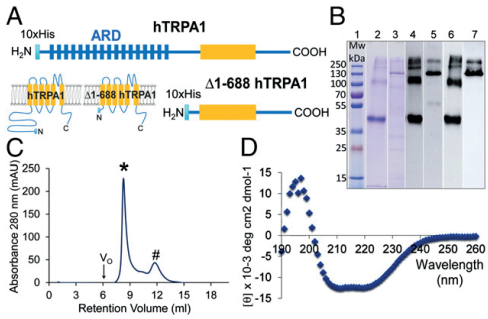

Fig. 1. Purification of hTRPA1 with and without the N-terminal ARD. (*A*) hTRPA1 was expressed either intact (1–1,119 aa) or without the ARD of the N terminus (Δ1–688 hTRPA1; 689–1,119 aa) with N-terminal decahistidine tags (10×His). (*B*) Affinity-purified hTRPA1 (lanes 3, 5, and 7) and Δ1–688 hTRPA1 (lanes 2, 4, and 6) visualized by Coomassie staining (lanes 2 and 3) and Western blotting (lanes 4–7) using either tetrahistidine antibody (lanes 4 and 5) or hTRPA1 antibody (lanes 6 and 7). The amounts of protein were 5 μg for Coomassie staining and 200 ng hTRPA1 and 40 ng Δ1–688 hTRPA1 for Western blotting. (*C*) As shown by the chromatogram, using a Superdex 200 size exclusion column, Δ1–688 hTRPA1 eluted mainly as a tetramer (*). V_o and # indicate void volume and monomer, respectively. (*D*) CD spectroscopy analysis disclosed typical characteristics of Δ1–688 hTRPA1 as a folded protein of high α-helical content. Mw, molecular mass.

Activation of hTRPA1 by Cold. TRPA1 activity was rarely observed at room temperature (22 °C), whereas cooling consistently activated hTRPA1 and Δ1–688 hTRPA1 at both positive and negative test potentials (Fig. 2, Figs. S2*B* and S3 *A* and *D*, and Table S1). Bilayers without proteins did not respond to cooling (Fig. S2*C*). Exposure to the TRPA1 blocker HC030031 inhibited cold-induced activation of hTRPA1 and Δ1–688 hTRPA1 by 71% and 76%, respectively (Fig. 2 *C* and *D*). Cooling from 22 °C to 10 °C dramatically increased single-channel open probability (P_o) (Fig. 2 *A*, *B*, and *E*). Our experimental setup did not allow us to obtain stable temperatures below 10 °C, which is why P_o values between 22 °C and 10 °C were used to calculate Q10 values of 0.025 and 0.018 from Arrhenius plots for hTRPA1 and Δ1–688 hTRPA1, respectively (Fig. 2*E*). A similar temperature dependence of the heterologously expressed mouse TRPA1 was observed in cell-attached and inside-out patches (36, 37) and with single-channel conductance (G_s) values at 10 °C, comparable with what we found for hTRPA1 (G_s = 50 ± 4 pS, n = 4). The G_s values at 10 °C differed between hTRPA1 and Δ1–688 hTRPA1 ($P < 0.05$, one-way ANOVA followed by Bonferroni's multiple comparison test) (Table S1). Notably, the cold-induced activity was reversible, and the G_s, but not P_o, decreased by 49% ± 10% (n = 3;

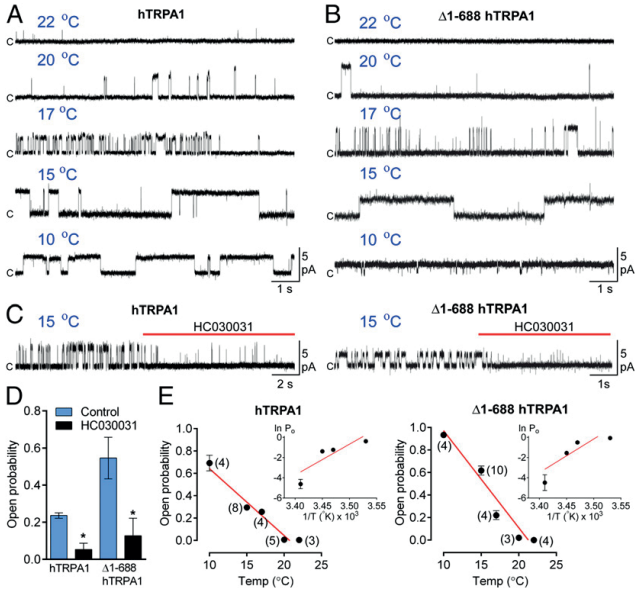

Fig. 2. The hTRPA1 is intrinsically cold-sensitive with and without the N-terminal ARD. Purified hTRPA1 and Δ1–688 hTRPA1 were inserted into planar lipid bilayers. (*A*–*C*) As shown by representative traces, cooling evoked substantial hTRPA1 and Δ1–688 hTRPA1 single-channel activity at a test potential of +60 mV (upward deflection shows open-channel state, and c shows closed-channel state). Amplitude histograms corresponding to each trace are shown in Fig. S2*A*. (*C*) Traces showing inhibition of cold responses of hTRPA1 and Δ1–688 hTRPA1 by the TRPA1 antagonist HC030031 (100 μM). (*D*) Graph with P_o values calculated from a time period of 1 min before and a time period of 1 min after treatment of hTRPA1 ($n = 3$) and Δ1–688 hTRPA1 ($n = 4$) with HC030031 at 15 °C. Complete inhibition was achieved after 1 min. Data are represented as means ± SEMs. $*P < 0.05$ indicates statistically significant differences using the Student's paired *t* test. (*E*) Plots summarize the P_o at various temperatures (number of experiments within parentheses) for (*Left*) hTRPA1and (*Right*) Δ1–688 hTRPA1. *Insets* show Arrhenius plots of the same data, with P_o values as the natural logarithm (ln) and temperature (T) as reciprocal Kelvin. Single-channel currents were recorded with the patch-clamp technique in a symmetrical K^+ solution.

$P < 0.05$, one-sample *t* test) when hTRPA1 was repeatedly exposed to 15 °C (Fig. S3*A*). This decline in G_s may reflect an inherent calcium-independent change in pore size, but it should not affect our analysis of cold-induced responses, because the analysis was based only on a first exposure to the indicated temperatures.

Activation of hTRPA1 by Electrophiles in the Absence of the N-Terminal ARD. Having established that the N-terminal ARD of hTRPA1 is not required for activation by cold, we asked if electrophiles can activate hTRPA1 in the absence of its N-terminal ARD at room temperature. Single-channel currents were rarely observed at test potentials of −60 and +60 mV or in voltage ramp recordings from −100 to +100 mV in the absence of TRPA1 activators (Fig. 2 *A*, *B*, and *E*, and Figs. S1*E* and S3*A*). However, AITC, cinnamaldehyde (CA), and *N*-methylmaleimide (NMM) but not the vehicle (1% ethanol) produced activation of both hTRPA1 and Δ1–688 hTRPA1 at −60 and +60 mV, whereas no activity was observed in the presence of activators on empty bilayers (Fig. 3*A* and Figs. S5, S6*B*, and S7). As shown for cinnamaldehyde, the effect was reversible (Fig. S3*B*). The activities of hTRPA1 and Δ1–688 hTRPA1 were blocked by HC030031 in a reversible manner (Fig. 3*B* and Fig. S3*C*): $P_o = 0.56 \pm 0.09$ and $P_o = 0.03 \pm 0.02$ as calculated for 1 min before and 1 min after the addition of HC030031, respectively, for hTRPA1 ($n = 4$). Whereas the G_s values for hTRPA1 and Δ1–688 hTRPA1 at −60 mV were similar in the presence for all electrophilic compounds, the G_s values at +60 mV differed between hTRPA1 and Δ1–688 hTRPA1 in the presence of AITC and NMM (Fig. 4*A* and Table S1). Comparison of P_o values revealed differences in ligand activation between hTRPA1 and Δ1–688 hTRPA1 at both positive and negative test potentials (Fig. 4*B* and Table S1). Additional calculations of the rectification index (+60/−60 mV) for G_s and P_o showed clear differences between hTRPA1 and Δ1–688 hTRPA1 when exposed to electrophiles (Fig. 4*C*), indicating that the N terminus modified hTRPA1 channel behavior in a voltage-dependent manner.

The ability of the hydrophilic thiol oxidant 2-((biotinoyl) amino)ethyl methanethiosulfonate-biotin (MTSEA-biotin; Fig. S4), which is active on TRPA1 from the intracellular side (23), to activate hTRPA1 ($G_s = 128 \pm 2$ pS and $P_o = 0.71 \pm 0.02$ at +60 mV; $n = 5$) only when applied in the bath solution (Fig. S4) indicates a uniform orientation of the protein in the lipid bilayer. Based on our findings that NMM activated the N-terminal ARD-deleted hTRPA1 and its ability to bind cysteine residues outside the N-terminal ARD (23, 26), we used a hydrophilic maleimide-biotin derivative (Fig. S4) for studies of Δ1–688 hTRPA1. Our data suggest a similar uniform orientation for Δ1–688 hTRPA1 in the lipid bilayer, because maleimide-biotin only activated this protein when applied to the bath solution (Fig. S4). The Gs and P_o values for maleimide-biotin ($G_s = 46 \pm 6$ pS and $P_o = 0.41 \pm 0.03$ at +60 mV, $n = 4$) are similar to those obtained with NMM at a test potential of +60 mV (Fig. 4 *A* and *B* Table S1).

Activation of hTRPA1 by Nonelectrophilic Compounds. In addition to being a chemosensor of thiol-reactive electrophiles and oxidants, TRPA1 is also activated by nonelectrophilic compounds, including Δ^9-THC, C16, menthol, carvacrol, clotrimazole, and dihydropyridines (7). A few heterologous expression studies using site-directed mutagenesis, chimeric channel constructs, or isolated

NEUROSCIENCE

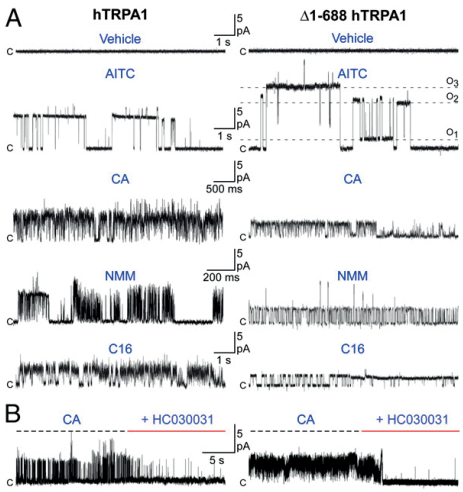

Fig. 3. Electrophilic and nonelectrophilic compounds activate purified hTRPA1 with and without the N-terminal ARD. (*A*) Representative traces show single-channel activity (upward deflection shows open-channel state, and c shows closed-channel state) for (*Left*) hTRPA1 and (*Right*) Δ1–688 hTRPA1 without the N-terminal ARD when inserted into planar lipid bilayers and exposed to the electrophilic compounds AITC (100 μM), cinnamaldehyde (CA; 100 μM), and NMM (100 μM) and the nonelectrophilic compound C16 (100 μM). Multiple distinct open-channel levels (dotted lines) were observed for AITC in Δ1–688 hTRPA1, of which the main level (O_3) was used for calculations of the G_s values presented in Fig. 4 and Table S1 (Fig. S5 presents responses at −60 mV). As shown by representative traces, the vehicle (ethanol at 1%) used for all test compounds evoked no activation of either hTRPA1 variant ($n = 3$). Amplitude histograms corresponding to each trace in *A* are shown in Fig. S7. (*B*) The TRPA1 antagonist HC030031 (100 μM) blocked CA-induced hTRPA1 ($n = 4$) and Δ1–688 hTRPA1 channel activity ($n = 2$). Channel currents were recorded with the patch-clamp technique in a symmetrical K^+ solution at a test potential of +60 mV.

inside-out patches suggest that nonelectrophilic compounds, including menthol and Δ^9-THC, directly interact with TRPA1 (35, 38). In this study using the purified channel, we provide final proof that Δ^9-THC, C16, and menthol directly activate hTRPA1 without the involvement of other cellular proteins or second messengers, including inositol triphosphate and Ca^{2+} (Figs. 3*A*, 4, and 5 and Figs. S1*E* and S5–S7). As with electrophilic compounds, menthol and C16 also activated hTRPA1 without the N-terminal ARD (Figs. 3*A*, 4, and 5 and Figs. S5 and S7). Importantly, the very lipophilic and potent cannabinoid receptor agonist CP55940, which in contrast to Δ^9-THC and C16, does not activate hTRPA1 expressed in HEK293 cells (29), did not trigger hTRPA1 channel activity, whereas Δ^9-THC produced activation when subsequently applied to the same bilayer (Fig. S6*A*); G_s for Δ^9-THC at +60 mV was 87 ± 7 pS ($n = 5$). This pharmacological profile together with our finding that electrophilic and nonelectrophilic TRPA1 activators are without effect on lipid bilayers in the absence of protein (Fig. S6*B*) support a specific interaction with hTRPA1.

Analysis of single-channel behavior revealed differences in the action of menthol and C16 on hTRPA1 and Δ1–688 hTRPA1 (Fig. 4 and Table S1). At +60 mV, G_s was larger and P_o was smaller for Δ1–688 hTRPA1 than hTRPA1 in the presence of menthol but not C16, whereas at −60 mV, P_o was larger for hTRPA1 than Δ1–688 hTRPA1 in the presence of C16 but not menthol (Fig. 4 *A* and *B* and Table S1). The rectification index (+60/−60 mV) for G_s and P_o showed clear differences in single-channel behavior between hTRPA1 and Δ1–688 hTRPA1 when exposed to nonelectrophilic compounds (Fig. 4*C*). Furthermore, C16 activated the menthol-insensitive chimera *Drosophila* transmembrane segment 5 (dTM5) -hTRPA1 between *D. melanogaster* (dTM5) and hTRPA1 (Fig. S8). Taken together, these findings are consistent with distinct binding sites for menthol and C16 and indicate that the N terminus modifies hTRPA1 channel responses to nonelectrophilic compounds in a voltage-dependent manner.

To further explore the influence of the N terminus on single-channel behavior, we used menthol as an hTRPA1 activator at room temperature. This ligand is assumed to bind to the transmembrane region of the channel protein and therefore, should not interfere with the integrity of the N terminus (35). As revealed by comparing single-channel currents and P_o between hTRPA1 and Δ1–688 hTRPA1 at different test potentials, the presence of the N-terminal ARD increased P_o at positive test potentials, while decreasing P_o at negative test potentials (Fig. 5). In contrast, the presence of the N-terminal ARD decreased G_s at positive test potentials, while leaving G_s unaffected at negative test potentials (Fig. 5).

Discussion

The ability to detect and avoid noxious temperatures is crucial for organism survival, but the underlying mechanisms of this beneficial property may also contribute to thermal allodynia or hypersensitivity, hallmarks of many chronic pain conditions in humans. Understanding the molecular mechanisms behind

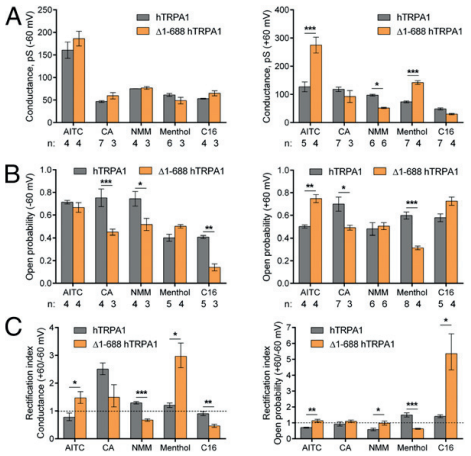

Fig. 4. The N-terminal ARD influences the channel behavior of the purified hTRPA1 when exposed to electrophilic and nonelectrophilic compounds. (*A* and *B*) Bar graphs summarize the mean G_s and P_o values for the TRPA1 activators AITC (100 μM), cinnamaldehyde (CA; 100 μM), NMM (100 μM), menthol (500 μM), and C16 (100 μM) at a test potential of either −60 or +60 mV. Multiple distinct open-channel levels were observed for AITC in Δ1–688 hTRPA1 (Fig. 3*A* and Fig. S5), of which the main levels (O_3 at +60 mV and O_1 at −60 mV) were used for calculations of G_s values. Single-channel currents of purified hTRPA1 and Δ1–688 hTRPA1 inserted into planar lipid bilayers were recorded with the patch-clamp technique in a symmetrical K^+ solution. (*C*) Analysis of the rectification index (+60/−60 mV) using the G_s and P_o data shown in *A* and *B* (Table S1). The dotted line indicates the level where no rectification would occur. Data are represented as means ± SEMs. $^*P < 0.05$, $^{**}P < 0.01$, and $^{***}P < 0.001$ indicate statistically significant differences between the hTRPA1 variants using (*A* and *B*) one-way ANOVA followed by Bonferroni's multiple comparison test or (*C*) a priori contrast analysis with adjustment for the degrees of freedom in the *F* test according to the Welch–Satterthwaite procedure.

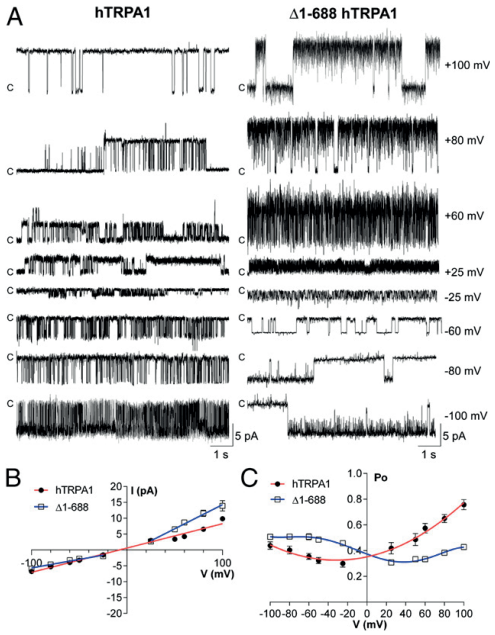

Fig. 5. The N-terminal ARD modifies hTRPA1 activity induced by menthol in a voltage-dependent manner. Purified hTRPA1 and Δ1–688 hTRPA1 were inserted into planar lipid bilayers. (*A*) As shown by representative traces, menthol (500 μM) evoked (*Left*) hTRPA1 and (*Right*) Δ1–688 hTRPA1 single-channel activity (upward deflection shows open-channel state at positive test potential, downward deflection shows open-channel state at negative test potential, and c shows closed-channel state). (*B*) Single-channel current–voltage (I–V) relationship and (*C*) single-channel P_o–voltage (P_o–V) relationship of the hTRPA1 and Δ1–688 hTRPA1 when activated by menthol (500 μM). The calculated mean slope G_s values were 77 ± 4 pS for hTRPA1 and 54 ± 6 pS (−100 to −25 mV) and 152 ± 7 pS (+25 to +100 mV) for Δ1–688 hTRPA1. These values are in good agreement with G_s values obtained at −60 and +60 mV in separate experiments (Fig. 4 and Table S1). Single-channel currents were recorded with the patch-clamp technique in a symmetrical K^+ solution at the various test potentials indicated on the right in *A*. Data are represented as means ± SEMs of four separate experiments. (*B*) $P < 0.01$ (+50 mV) and $P < 0.001$ (+60, +80, and +100 mV), and (*C*) $P < 0.05$ (+25 mV), $P < 0.01$ (−60 and +50 mV), and $P < 0.001$ (−50, −25, +60, +80, and +100 mV) indicate statistically significant differences at each test potential between the hTRPA1 channels using one-way ANOVA followed by Bonferroni's multiple comparison test.

thermosensation is, therefore, of importance from both biological and medical perspectives (1, 39). Several TRP channels have recently been proposed as thermosensors, of which the majority is involved in warm sensation (1–3, 39). However, to define a TRP channel as a thermosensor would require examination of the purified channel protein in a defined membrane environment, and to date, only rat TRPM8 and rat TRPV1 have been shown to be intrinsically thermosensitive proteins (4, 5). Here, we show for the first time, to our knowledge, that the purified hTRPA1 inserted into artificial lipid bilayers is an inherently cold-sensitive protein. Thus, the mammalian TRP channel family consists of an additional cold sensor—TRPA1—that, together with TRPM8, covers noxious to pleasant cold temperatures.

Mutational and chimeric strategies have been used to suggest specific thermosensitive regions and drug binding sites in TRP channels (8, 11, 13, 14, 16, 17, 19, 40). In this study, using the purified N-terminal ARD-deleted hTRPA1 to avoid potential artifacts in TRPA1 function caused by mutations or the creation of xenogeneic channels (7), we clearly show that the cold sensitivity and the binding site for HC030031, an inhibitor of rodent TRPA1 and hTRPA1 (7, 41), are located outside the N-terminal ARD. The search for a specific cold-sensitive region in mammalian TRPA1 channels should, thus, be directed toward the transmembrane and the C-terminal domains of TRPA1.

As shown for cold, electrophilic compounds also evoked robust hTRPA1 activity in the absence of the N-terminal ARD, providing a more complex picture of electrophile activation of hTRPA1 than generally believed. By comparing G_s and P_o values at +60 and −60 mV, we found voltage-dependent differences in channel behavior between the two hTRPA1 variants when exposed to electrophilic compounds. Interestingly, a triple cysteine mutation of the hTRPA1 N-terminal region (hTRPA1-3C) changed the voltage-dependent electrophilic activation of hTRPA1 by *p*-benzoquinone, an acetaminophen (paracetamol) metabolite (28, 29). Furthermore, the N-terminal region may suppress hTRPA1 channel gating, because the response to NMM was intact in the N-terminal ARD-deleted hTRPA1 (this study) but lost in the N-terminal triple cysteine mutant (22), having a greatly reduced capacity to form disulfide bonds (25). The response of hTRPA1 to the nonelectrophilic compounds menthol and C16 also did not require the presence of the N-terminal ARD, which however, modified hTRPA1 channel behavior in a voltage-dependent manner.

Although our data clearly show that electrophilic and nonelectrophilic compounds activate hTRPA1 outside the N-terminal ARD, random protein orientation in the artificial lipid bilayer and the existence of multiple levels of channel opening could complicate the analysis of the voltage-dependent channel behavior. A uniform protein insertion was not confirmed in each single experiment, but separate experiments showed the ability of the biotin derivatives of 2-((biotinoyl)amino)ethyl methanethiosulfonate and maleimide to activate hTRPA1 and the N-terminal ARD-deleted hTRPA1, respectively, only when applied to the bath solution, supporting a consistent asymmetric orientation of both proteins in the lipid bilayers. For comparison of G_s between the hTRPA1 variants at different voltages, we analyzed the current magnitude only for the main open-channel level. Because distinct multiple open-channel levels were frequently observed for AITC in the N-terminal ARD-deleted hTRPA1, G_s values and the rectification index obtained with AITC in hTRPA1 without the N terminus should be interpreted with caution. Interestingly, the hTRPA1 single-channel G_s values for electrophilic and nonelectrophilic compounds vary greatly, although within the wide range of values reported for mammalian TRPA1 (7). Whether this ligand-dependent variation in single-channel G_s is caused by pore dilation and modified by the N terminus warrant additional investigations. Based on our electrophysiological data, it is difficult to provide a simple biophysical fingerprint of hTRPA1, which may not be surprising considering the great variety of chemical interactions between ligands and TRPA1 (7). Nevertheless, our data raise the possibility that the N terminus modifies hTRPA1 channel behavior in a voltage-dependent manner.

The ability of TRPA1 to respond to nonelectrophilic compounds is intriguing but could indicate that endogenous TRPA1 modulators with similar chemical structures or properties exist (7). In this study, we show that menthol and the cannabinoids C16 and Δ^9-THC directly activate hTRPA1 without the need for cytoplasmic (e.g., Ca^{2+}) or cell membrane-associated factors. We found that the menthol-insensitive dTM5–hTRPA1 chimera (35) expressed in HEK293 cells was activated by C16, indicating that menthol and cannabinoids interact with distinct binding sites. Future studies identifying the binding sites for C16 and other cannabinoids may help us to understand nonelectrophilic regulation of TRPA1 and the potential of these binding sites as targets for

analgesics, including nontissue-damaging TRPA1 activators (29). Perhaps such TRPA1 activators can also be used to modulate aging in humans, because the TRPA1 activator AITC extended lifespan in transgenic *Caenorhabditis elegans* expressing hTRPA1 (42).

Although this study clearly shows that hTRPA1 is an inherently cold-activated ion channel, it does not resolve why studies of the expressed hTRPA1 have generated such conflicting findings regarding its cold sensitivity (8–15). However, we know that the regulation of TRPA1 is complex and that the channel sensitivity to ligands is dependent on the cellular context, including the redox state in the cell, the phosphoinositide composition of the cell membrane, and the intracellular activities of proline hydroxylase and protein kinase/phosphatase enzymes (7). Many of these factors are probably dependent on the cell expression system and the experimental conditions, and their future disclosure may pinpoint novel drug targets other than TRPA1 for treatment of clinical conditions characterized by TRPA1-dependent cold allodynia or hypersensitivity (7).

In conclusion, we show that hTRPA1 is an intrinsically cold-activated ion channel that constitutes a molecular thermosensor explaining TRPA1-dependent behavioral responses to noxious cold (7). The N-terminal ARD is not needed for activation of hTRPA1 by cold, electrophiles, and nonelectrophilic compounds or inhibition of hTRPA1 by HC030031. However, the N-terminal ARD may modify hTRPA1 channel behavior in a voltage-dependent manner. Targeting chemical interaction sites outside the TRPA1 N-terminal ARD may offer possibilities to fine tune TRPA1-based drug therapies [e.g., for treatment of pain associated with cold hypersensitivity (7) and cardiovascular disease (32)].

Materials and Methods

P. pastoris cell membranes, containing hTRPA1 or Δ1–688 hTRPA1, were collected and solubilized with fos-choline-14 detergent (Anatrace). Both proteins were purified using Ni-nitrilotriacetic acid affinity chromatography; Δ1–688 hTRPA1 was also subjected to size exclusion chromatography. Purified hTRPA1 (after Ni-nitrilotriacetic acid purification) and Δ1–688 hTRPA1 (tetrameric fraction from size exclusion chromatography) were reconstituted into preformed planar lipid bilayers or giant unilamellar vesicles. The vesicles were formed by electroformation using Vesicle Prep Pro Station (Nanion Technologies). Lipid stock was made by dissolving 10 mM 1,2-diphytanoyl-*sn*-glycero-3-phosphocholine:cholesterol (9:1) in trichloromethane. All lipid bilayer recordings were done on a Port-a-Patch planar patch-clamp system (Nanion Technologies) in a symmetrical K^+ solution at room temperature (22 °C) or below. Group data are expressed as means ± SEMs from *n* independent experiments (lipid bilayers or cell transfections). *SI Materials and Methods* has full details.

ACKNOWLEDGMENTS. We thank Brita Sundén-Andersson and Adine Karlsson for technical assistance and Dr. Ardem Patapoutian for providing us with the dTM5–hTRPA1 chimera. This work was supported by Swedish Research Council Grants 2010-5787 (to E.D.H. and P.M.Z.), 2010-3347 (to E.D.H. and P.M.Z.), 2007-6110 (to U.J.), and Formas 2007-718 (to P.K., E.D.H., U.J., and P.M.Z.), the Research School of Pharmaceutical Sciences at Lund University (U.J. and P.M.Z.), and the Medical Faculty at Lund University (E.D.H. and P.M.Z.).

1. Clapham DE, Miller C (2011) A thermodynamic framework for understanding temperature sensing by transient receptor potential (TRP) channels. *Proc Natl Acad Sci USA* 108(49):19492–19497.
2. Voets T, Talavera K, Owsianik G, Nilius B (2005) Sensing with TRP channels. *Nat Chem Biol* 1(2):85–92.
3. Panzano VC, Kang K, Garrity PA (2010) Infrared snake eyes: TRPA1 and the thermal sensitivity of the snake pit organ. *Sci Signal* 3(127):pe22.
4. Cao E, Cordero-Morales JF, Liu B, Qin F, Julius D (2013) TRPV1 channels are intrinsically heat sensitive and negatively regulated by phosphoinositide lipids. *Neuron* 77(4): 667–679.
5. Zakharian E, Cao C, Rohacs T (2010) Gating of transient receptor potential melastatin 8 (TRPM8) channels activated by cold and chemical agonists in planar lipid bilayers. *J Neurosci* 30(37):12526–12534.
6. Story GM, et al. (2003) ANKTM1, a TRP-like channel expressed in nociceptive neurons, is activated by cold temperatures. *Cell* 112(6):819–829.
7. Zygmunt PM, Högestätt ED (2014) TRPA1. *Handbook Exp Pharmacol* 222:583–630.
8. Kremeyer B, et al. (2010) A gain-of-function mutation in TRPA1 causes familial episodic pain syndrome. *Neuron* 66(5):671–680.
9. Bandell M, et al. (2004) Noxious cold ion channel TRPA1 is activated by pungent compounds and bradykinin. *Neuron* 41(6):849–857.
10. Jordt SE, et al. (2004) Mustard oils and cannabinoids excite sensory nerve fibres through the TRP channel ANKTM1. *Nature* 427(6971):260–265.
11. Wang H, Schupp M, Zurborg S, Heppenstall PA (2013) Residues in the pore region of Drosophila transient receptor potential A1 dictate sensitivity to thermal stimuli. *J Physiol* 591(Pt 1):185–201.
12. Zurborg S, Yurgionas B, Jira JA, Caspani O, Heppenstall PA (2007) Direct activation of the ion channel TRPA1 by Ca^{2+}. *Nat Neurosci* 10(3):277–279.
13. Chen J, et al. (2013) Species differences and molecular determinant of TRPA1 cold sensitivity. *Nat Commun* 4:2501.
14. Cordero-Morales JF, Gracheva EO, Julius D (2011) Cytoplasmic ankyrin repeats of transient receptor potential A1 (TRPA1) dictate sensitivity to thermal and chemical stimuli. *Proc Natl Acad Sci USA* 108(46):E1184–E1191.
15. May D, et al. (2012) Differential expression and functionality of TRPA1 protein genetic variants in conditions of thermal stimulation. *J Biol Chem* 287(32):27087–27094.
16. Gracheva EO, et al. (2010) Molecular basis of infrared detection by snakes. *Nature* 464(7291):1006–1011.
17. Kang K, et al. (2012) Modulation of TRPA1 thermal sensitivity enables sensory discrimination in Drosophila. *Nature* 481(7379):76–80.
18. Kang K, et al. (2010) Analysis of Drosophila TRPA1 reveals an ancient origin for human chemical nociception. *Nature* 464(7288):597–600.
19. Jabba S, et al. (2014) Directionality of temperature activation in mouse TRPA1 ion channel can be inverted by single-point mutations in ankyrin repeat six. *Neuron* 82(5): 1017–1031.
20. Bautista DM, et al. (2005) Pungent products from garlic activate the sensory ion channel TRPA1. *Proc Natl Acad Sci USA* 102(34):12248–12252.
21. Macpherson LJ, et al. (2005) The pungency of garlic: Activation of TRPA1 and TRPV1 in response to allicin. *Curr Biol* 15(10):929–934.
22. Hinman A, Chuang HH, Bautista DM, Julius D (2006) TRP channel activation by reversible covalent modification. *Proc Natl Acad Sci USA* 103(51):19564–19568.
23. Macpherson LJ, et al. (2007) Noxious compounds activate TRPA1 ion channels through covalent modification of cysteines. *Nature* 445(7127):541–545.
24. Cvetkov TL, Huynh KW, Cohen MR, Moiseenkova-Bell VY (2011) Molecular architecture and subunit organization of TRPA1 ion channel revealed by electron microscopy. *J Biol Chem* 286(44):38168–38176.
25. Eberhardt MJ, et al. (2012) Methylglyoxal activates nociceptors through transient receptor potential channel A1 (TRPA1): A possible mechanism of metabolic neuropathies. *J Biol Chem* 287(34):28291–28306.
26. Wang L, Cvetkov TL, Chance MR, Moiseenkova-Bell VY (2012) Identification of in vivo disulfide conformation of TRPA1 ion channel. *J Biol Chem* 287(9):6169–6176.
27. Escalera J, von Hehn CA, Bessac BF, Sivula M, Jordt SE (2008) TRPA1 mediates the noxious effects of natural sesquiterpene deterrents. *J Biol Chem* 283(35):24136–24144.
28. Ibarra Y, Blair NT (2013) Benzoquinone reveals a cysteine-dependent desensitization mechanism of TRPA1. *Mol Pharmacol* 83(5):1120–1132.
29. Andersson DA, et al. (2011) TRPA1 mediates spinal antinociception induced by acetaminophen and the cannabinoid Δ(9)-tetrahydrocannabiorcol. *Nat Commun* 2:551.
30. Weng Y, et al. (2012) Prostaglandin metabolite induces inhibition of TRPA1 and channel-dependent nociception. *Mol Pain* 8(1):75.
31. Nilius B, Prenen J, Owsianik G (2011) Irritating channels: The case of TRPA1. *J Physiol* 589(Pt 7):1543–1549.
32. Eberhardt M, et al. (2014) H_2S and NO cooperatively regulate vascular tone by activating a neuroendocrine HNO-TRPA1-CGRP signalling pathway. *Nat Commun* 5:4381.
33. Törnroth-Horsefield S, et al. (2006) Structural mechanism of plant aquaporin gating. *Nature* 439(7077):688–694.
34. Long SB, Tao X, Campbell EB, MacKinnon R (2007) Atomic structure of a voltage-dependent K^+ channel in a lipid membrane-like environment. *Nature* 450(7168): 376–382.
35. Xiao B, et al. (2008) Identification of transmembrane domain 5 as a critical molecular determinant of menthol sensitivity in mammalian TRPA1 channels. *J Neurosci* 28(39): 9640–9651.
36. Karashima Y, et al. (2009) TRPA1 acts as a cold sensor in vitro and in vivo. *Proc Natl Acad Sci USA* 106(4):1273–1278.
37. Sawada Y, Hosokawa H, Hori A, Matsumura K, Kobayashi S (2007) Cold sensitivity of recombinant TRPA1 channels. *Brain Res* 1160:39–46.
38. Kim D, Cavanaugh EJ, Simkin D (2008) Inhibition of transient receptor potential A1 channel by phosphatidylinositol-4,5-bisphosphate. *Am J Physiol Cell Physiol* 295(1): C92–C99.
39. Voets T (2012) Quantifying and modeling the temperature-dependent gating of TRP channels. *Rev Physiol Biochem Pharmacol* 162:91–119.
40. Brauchi S, Orta G, Salazar M, Rosenmann E, Latorre R (2006) A hot-sensing cold receptor: C-terminal domain determines thermosensation in transient receptor potential channels. *J Neurosci* 26(18):4835–4840.
41. Bianchi BR, et al. (2012) Species comparison and pharmacological characterization of human, monkey, rat, and mouse TRPA1 channels. *J Pharmacol Exp Ther* 341(2):360–368.
42. Xiao R, et al. (2013) A genetic program promotes C. elegans longevity at cold temperatures via a thermosensitive TRP channel. *Cell* 152(4):806–817.